A Neural Control Circuit for Cough- Like Defensive Behaviors in Mice

by

Noam Gannot

A dissertation submitted in partial fulfillment
of the requirements for the degree of
Doctor of Philosophy
(Oral Health Sciences)
in the University of Michigan
2024

Doctoral Committee:

Assistant Professor Peng Li, Chair
Professor Roger Cone
Professor Nisha J. D'Silva
Assistant Professor Joshua J. Emrick

Noam Gannot

ngannot@umich.edu

ORCID iD: 0000-0002-3617-5553

Dedication

To my village.

Acknowledgements

I could not have asked for a better hype team than the people that surrounded and supported me these last five years. These people have been by my side through all of graduate school's rollercoasters of ups and downs and I would not be where I am without them.

First and foremost, I would like to thank my mentors and advisors who shaped my graduate school to be unlike any other. Thank you, Dr. Peng Li for accepting me as the first graduate student in your lab and providing me with the opportunity to work on this research project. Thank you to my thesis committee – Dr. Roger Cone, Dr. Nisha D'Silva and Dr. Joshua Emrick for your consistent support and feedback. Thank you to Dr. Yuji Mishina for your unwavering support and to Dr. Wenjing Wang for allowing me to collaborate with your lab.

To my lab, who have not missed a single one of my talks, including the five-minute ones. You guys never missed an opportunity to support me in any way that you could. You all have been an integral part of my graduate school journey and made the lab environment the most positive, supportive and loving experience I could have asked for. Thank you, also, to all my mice.

To my wonderful Ann Arbor friends – from going on runs with me, to reluctantly agreeing to come to Crossfit, to having our dessert nights and for always dropping everything that you are doing when I needed you. I feel like the luckiest person alive that I got to spend my graduate school with you all and to know that I've made lifelong friends in you. To my non-

Michigan friends – while I didn't see you all as much as I would have liked in these last five years, I know that you are always a phone call away. They always say you are the company you keep, and I really hope that is true, because that means I get to be the most amazing, supportive, and loving human.

To my wonderful family. I have no idea where I would be without you. I know that your love and support is what keeps my head above water. Thank you for your technical and emotional support, for being by my side every step of the way and for truly being more than I ever thought I needed.

Finally, thank you to my boys. Ryan, you are my rock. Thor, you are my sunshine. Thank you for always telling me what I need to hear, not what I want to hear. Thank you for editing my thesis and questioning my comma usage. I love you so much.

Table of Contents

List of Figures

Abstract

Breathing is a vital and complex behavior that rapidly responds to the physiological states and stimuli in the body. Breathing patterns are controlled by the brainstem, which receives constant peripheral sensory information from the lungs and the airway. Respiratory defensive behaviors, such as coughs and expiratory reflexes, disrupt rhythmic respiration as a means of protecting the airway. The function of these reflexes is to remove inhaled particles, pathogens, irritants, or foreign bodies from the respiratory tract by generating a rapid expiratory airflow. A cough is generated by a complex and sequential motor pattern involving three phases: inspiration, compression, and expulsion. Meanwhile, an expiratory reflex lacks an initial inspiration. Often, both reflexes occur intermittently during clinically-defined episodes of coughing, hinting at a shared mechanism underlying these cough-like behaviors. Although these behaviors become excessive under pathological conditions, affecting quality of life, effective anti-tussive medications are lacking. Understanding how sensory stimuli within the body regulate coughs and expiratory reflexes may help to address this gap.

Here, we argue that tachykinin 1 (Tac1) neurons in the nucleus of the solitary tract (NTS) are a key component of the neural circuit that controls cough-like defensive behaviors in mice. First, we show that the NTS, a key hub in the brainstem for processing internal sensory signals and mediating interoceptive processes, contains heterogenous neuronal populations. Activating different neuronal populations via optogenetics within the NTS induced diverse breathing responses, including an ectopic inspiratory peak, apnea, and a sigh. Within these subtypes,

activation of Tac1 neurons triggers a specific respiratory behavior. Our detailed characterization of respiratory defensive behaviors, including electromyography (EMG), intrapleural pressure, box flow, video, and audio recordings, reveals that this respiratory behavior is cough-like. The NTS Tac1 neurons are activated during tussive challenges and play an essential role in cough-like behaviors. Optogenetic activation of Tac1 neurons is sufficient in inducing cough-like behaviors, while chronic ablation or acute silencing of these neurons diminishes the cough-like behaviors induced by tussive agents. Using neuronal tracing and optogenetics, we found that these NTS Tac1 neurons directly innervate and coordinate the medullary regions to control sequential phases of cough-like defensive behaviors. In summary, we argue that these Tac1 neurons act as central pattern generators for cough-like defensive behaviors in mice, and that they coordinate the downstream modular circuits to elicit the sequential motor pattern of forceful expiratory responses.

Chapter 1 Introduction

1.1 Respiration

Respiration is an example of an innate, involuntary, and vital activity that automatically modulates critical body functions on a continuous basis. An individual person takes about 20,000 breaths a day. Each eupneic, or normal, breath consists of an active inspiration, a post-inspiration, sometimes referred to as the first stage of expiration, followed by either an active or passive expiration (Dutschmann et al., 2014). An active inspiration consists of the contraction of the inspiratory muscles – the diaphragm and external intercostals. During the post-inspiratory phase, the diaphragm and laryngeal muscles contract, thereby slowing expiratory airflow. At rest, active inspiration is followed by a passive expiratory phase. An active expiration is produced when metabolism increases, or during everyday activities such as speech and laughing. During active expiration, the expiratory muscles (the abdominals and internal intercostals) are recruited (Del Negro et al., 2018). Breathing is one of the vital functions regulated by the internal conditions as it rapidly responds to physiological states and stimuli in the body (Chang et al., 2015; Prescott et al., 2020).

Breathing is constantly modulated by environmental, metabolic, or behavioral changes by responding to different sensory information, including afferent feedback from muscles. This includes short-term changes, such as exercise, disease, and injury, and long-term changes, such as growth and maturation (Shevtsova et al., 2019). Respiratory rhythm is adaptable due to the activity of neurons in the medulla that contain microcircuits that generate the inspiratory rhythm.

The breathing cycle consists of sighs, or large inspiratory efforts, that are necessary to reinflate collapsed alveoli. Alveoli are small air sacs at the end of the bronchioles where the lungs and the blood exchange oxygen and carbon dioxide during the process of respiration. At times, individual alveoli collapse, compromising the overall ability of the lungs to exchange oxygen and carbon dioxide. Sighing enables our brain and body to correct a physiological problem in our lungs, innately and subconsciously – i.e., collapsed alveoli.

1.2 Coughs and Expiratory Reflexes

Coughs and expiratory reflexes, which disrupt rhythmic respiration, act as defensive behaviors. These defensive expiratory reflexes are essential functions that clear the airways and protect the body against inhaled substances and invading pathogens (Banner, 1986; J. Widdicombe & Fontana, 2006; J. G. Widdicombe, 1998). These reflexes are crucial for maintaining the health of the respiratory system by expelling irritants, mucus, or foreign particles. Both the cough reflex and the expiratory reflex contain a sudden and forced expiration against a closed glottis, resulting in a characteristic sharp sound and body movement. Whereas coughing is distinguished primarily by a preceding inspiration (J. Widdicombe & Fontana, 2006; Zhuang et al., 2019). A coughing bout starts with a cough and continues with a series of expiratory efforts. Glottal closure may occur once or twice in a single cough effort (Chung & Widdicombe, 2004; J. Widdicombe & Fontana, 2006; Zhuang et al., 2019a). Although they are two distinct behaviors, this pattern indicates that there is likely to be a shared mechanism underlying coughs and expiratory reflexes.

1.2.1 Defining Coughs and Expiratory Reflexes

The cough reflex is an essential defensive respiratory function triggered by tussive (cough-evoking) stimuli in the airways to protect the body against inhaled substances and invading pathogens (Banner, 1986; J. G. Widdicombe, 1998). A cough is simply defined as an expulsion of air from the lungs with a characteristic sound and body movement, a description used frequently in clinical settings (Morice et al., 2006). However, the mechanisms underlying a cough are more complex.

Physiologically, a cough has three phases: inspiratory, compressive, and expiratory. In the inspiratory phase, the inhalation of air serves to lengthen the expiratory muscles. During the compressive phase, there is a brief closure of the glottis to maintain lung volume and a buildup of intrathoracic pressure due to the contraction of the expiratory muscles against a closed glottis. The expiratory phase starts with the opening of the glottis and concludes with the high velocity expulsion of gas that attempts to clear the airway of debris (Chang, 2006). Due to the rush of air out of the now opened glottis, a sound is produced during the expiratory phase.

The sound of a cough may vary but is due to vibration of the large airways and laryngeal structures during turbulent flow in expiration (Hashimoto et al., 2003; Korpas et al., 1987). Similar to a cough, an expiratory reflex produces a distinct sound due to the same mechanics. While some research has used sound to detect coughs and other respiratory events (Chen et al., 2013; F. Li et al., 2021), analysis of cough sounds has no clinical applications. It is also subjective and cannot be used as a diagnostic tool (Chang, 2006; Nemati et al., 2020).

An expiratory reflex is an additional defensive reflex of the respiratory tract that originates in the larynx and is meant to prevent aspiration. The expiratory reflex consists of a glottal closure and a forced expiration followed by a glottal opening and an expulsive airflow, in response to mechanical or chemical irritation of the vocal folds or trachea (Korpas & Jakus,

2000). This reflex was first described in 1841, using digital stimulation of an opened trachea of a dog, eliciting a series of convulsive expiratory efforts (Williams, 1841).

Ontogenetic studies revealed that the expiratory reflex occurs in infant cats and rats, even when sneezing and tracheobronchial cough are still absent. The expiratory reflex can be elicited days after birth while a respiratory response from the bronchi (i.e., cough) is not seen until at least two weeks after birth (Korpas & Kalocsayova, 1973; Korpáš & Tatar, 1975). This pattern suggests that the expiratory reflex is evolutionarily conserved and could be present as a defensive mechanism in other species, as well.

The expiratory reflex is distinct from a cough reflex in that its source is restricted to the larynx and vocal folds. The reflex also lacks the initial inspiratory phase of the cough and is defined as a forced expiratory effort against a closed glottis that subsequently opens to eject laryngeal debris and prevent aspiration of material (Tatar et al., 2008). The precise mechanism of action and implication of expiratory reflexes and whether they differ from coughs in clinical settings have not been clearly defined (Estis et al., 2014).

1.2.2 Types of Coughs

Reflexive coughing is primarily mediated by the brainstem, while a voluntary cough is cortically controlled (Mills et al., 2017). A reflexive cough is generally categorized into two main types: a wet (or productive) cough and a dry cough. A wet cough is a cough with mucus in the lung airways, which is an indicator of either a simple pulmonary infection, such as a cold, flu, or a more serious condition, such as pneumonia or chronic obstructive pulmonary disease (COPD) (Nemati et al., 2020). A dry cough typically does not expel mucus and can be caused by inflammation in the respiratory system. Dry cough may present as a predominant symptom in patients with asthma or COVID-19 (Pratter, 2006; Qu et al., 2021). An increased sensitivity of

the cough reflex can be observed in patients with dry cough. Although cough can be characterized into different types and arise from different causes, the motor output of the cough, including the muscles engaged and the three phases observed, is similar in each of these cases.

A paroxysmal cough is the term used to describe erratic attacks of uncontrollable and violent coughs that feel exhausting and painful (Singh, 2022). The most common type of paroxysmal cough is pertussis, also known as a whooping cough. A bacterial infection of the lower lungs caused by the Bordetella pertussis produces violent coughing fits. During a coughing episode, the release of all the air from the lungs will cause people to violently inhale with a whoop. Besides pertussis, asthma, chronic obstructive pulmonary disease, pneumonia, tuberculosis, and choking can also result in a paroxysmal cough (Geddes & Talbert, 2006).

A croup cough, which typically affects children under the age of five, is a viral infection that causes irritation and swelling in the upper airway. Croup is a common illness responsible for up to 15 percent of emergency department visits due to respiratory disease in children in the United States. It has a distinct sound and can cause a raspy voice and squeaky breathing. In most children, the symptoms subside quickly with resolution of the cough within two days (Zoorob et al., 2011).

Typically, a cough will be considered as either acute or chronic. The distinction between an acute cough and a chronic one is somewhat arbitrary and based on the duration of the symptom. An acute cough is common and lasts fewer than two weeks while a chronic cough lasts over three weeks. Patients generally self-medicate for acute cough and are more likely to seek medical attention when the cough becomes chronic (Mcgarvey & Nishino, 2004).

1.2.3 Treating Coughs

An occasional cough is a normal and healthy function of the body. However, coughing can become either excessive or insufficient, leading to devastating and potentially dire consequences. On the one hand, the cough reflex may be impaired, leading to the inability to cough effectively. When patients are unable to cough, they cannot clear airway secretions which frequently leads to lung congestion and respiratory infections (Byrd & Burns, 1975; DiMarco et al., 2006). On the other hand, the cough reflex can become excessive and inappropriately sensitive under pathological conditions. Chronic coughing is one of the most common reasons patients seek medical attention (Burt & Schappert, 2004), and is a common symptom for many diseases, including COVID-19 (Grant et al., 2020). Severe cases of chronic cough can cause vomiting, lightheadedness, airway irritation and rib fractures (J. A. Smith & Woodcock, 2016).

Despite chronic cough being one of the most frequent reasons for both primary care and specialty physician visits, its diagnosis and treatment remain challenging (Dicpinigaitis, 2020). The most common causes of chronic cough include asthma, post-nasal drip, or gastroesophageal reflux disease (GERD). People with asthma have sensitive airways which react to triggers, causing the muscles around the airways to contract, narrowing them and making it harder to breathe. Postnasal drip cough occurs when excess mucus collects and migrates into the back of the throat. Other chronic cough causes include respiratory conditions (e.g. bronchitis), sinus conditions, allergies, or certain infections. The treatments used for chronic cough depends on the associated health condition and may include decongestants, nasal sprays, or steroids.

Anti-tussive medications, such as cough syrup, are used to block the cough reflex. One of the main ingredients in cough syrup is dextromethorphan (DXM), the D isomer of the codeine analogue levorphanol. DXM acts centrally in the cough center in the medulla to suppress cough (Woo, 2008). In high doses, DXM can lead to fatal liver injury, cardiovascular effects, dizziness,

uncontrollable eye movement and over-sedation. More importantly, cough syrup was shown to be no more efficacious than placebo (Galli & Barbas, 2004; Schroeder & Fahey, 2002). Furthermore, cough syrup is not a targeted medication, instead, it blocks the cough reflex as opposed to treating the root cause of the cough. The lack of an effective anti-tussive medication is largely because the precise neuronal populations and molecular pathways involved in cough have not yet been identified.

1.2.4 Distinguishing Coughs from Sneezes

Sneezing and coughing are both important defensive reflex responses used to expel noxious xenobiotics, including infectious agents or irritants, and are also common symptoms of many allergies. A simple sneeze can travel up to 100 miles an hour and expel around 40,000 droplets, whereas a cough expels around 3,000 droplets (Dhand & Li, 2020). A sneeze is triggered by the stimulation of the upper respiratory tract and particularly the irritation of the mucous membranes of the nose and throat. Excessive sneezing may be a sign of rhinitis, an inflammatory disease characterized by the occurrence of nasal symptoms (Juniper et al., 2005). While sneezing is associated with various medical conditions, it can also arise due to bright light, during exercise or in response to a full stomach (Songu & Cingi, 2009). As is the case with coughs, the motor output and definition of a sneeze remains the same despite different causes for a sneeze.

A sneeze is defined as a deep inspiration followed by depression of the soft palate and palatine uvula with the elevation of the back of the tongue that partially closes the passage to the mouth. Initially, the abdominal and chest muscles activate, compressing the lungs, and producing a blast of air. Air bursts suddenly through the lungs with variable force, expelling mucus containing foreign particles or irritants from the nasal cavity. When the air is expelled during the

sneeze, the eyes are locked shut (Burke, 2012). On average, an individual may sneeze or blow their nose less than four times daily (Juniper et al., 2005), clearing their nose of bacteria and viruses.

Both coughs and sneezes help clear foreign particles or irritants from the respiratory system. However, a sneeze is an involuntary expulsion of air from the lungs through the throat or nose while a cough can be either a voluntary or involuntary forceful expulsion of air through the mouth. While the irritants for coughs and sneezes can be the same (e.g., bacteria, dirt, dust), the location of the irritation determines whether we cough or sneeze. A sneeze is related to the irritation of the upper nasal passages and the stimulation of the trigeminal nerve while a cough results from the irritation or inflammation to the respiratory tract and the stimulation of the vagus nerve (Baraniuk & Kim, 2007). Once these sensory nerves are stimulated, they send a signal to the brain, which then projects to the appropriate efferent musculature to produce either a cough or a sneeze. The neural pathways of these behaviors can be interrogated using animal models.

1.3 The current state of cough research

1.3.1 Animal models of cough

While a cough induced in a laboratory animal by mechanical or chemical stimuli does not perfectly mimic a spontaneous cough present in human disease, extensive experiments have increased the understanding of neural pathway regulating cough. The animals initially selected for cough research included anesthetized dogs, cats, and rabbits. In these models, coughing is provoked by a mechanical stimulus that is pushed against the trachea repeatedly. Cough induced in anaesthetized animals in this manner is a result of activation of mechanosensitive myelinated Aδ-fibres. It is important to note that general anesthesia decreases the conductivity of neural pathways and suppresses the activity of the central nervous system, as well as inhibits the

function of the higher brain circuits that modulate cough, which poses a disadvantage with the use of these animals (Belvisi & Hele, 2008). Furthermore, the use of these animals involves a high-cost element and a negative ethical perception, resulting in the more frequent use of smaller animal models (Plevkova et al., 2021).

Both anesthetized and conscious guinea pigs are often used in cough research. In a model of a urethane-anaesthetized guinea pig, mechanical stimulation is done similarly to the previously described models in larger animals – inducing a cough by the stimulation of Aδ fibres in the larynx and trachea by a nylon catheter (Canning et al., 2004). The use of the conscious guinea pig is widely recommended in cough research since they respond well to the majority of tussive aerosols. Furthermore, there is no observed anesthesia effect and their exposure to tussive agents causes similar reactions to those seen in humans (Belvisi & Bolser, 2002; Gatti et al., 2012; Hewitt et al., 2016; Laude et al., 1993; McGovern, Davis-Poynter, Rakoczy, et al., 2012). Although guinea pigs pose disadvantages since they lack the genetic tools available in other models, such as mice, this model is widely recommended for cough research (Plevkova et al., 2021).

Conscious mice are widely used across various research disciplines. However, there is general skepticism regarding the use of these animals in cough research. According to older data, mice lack airway afferent terminals that would be able to initiate a cough response and they are not able to produce a strong pressure gradient across their respiratory tracts that would be the optimal driving force for air expulsion (Belvisi & Bolser, 2002). However, more recent finding on neurophysiology concluded that mice possess a similar set of airway sensors and pulmonary reflexes as typically found in larger animals (Symanowicz et al., 2004; J. W. Zhang et al., 2006). The European Respiratory Society argues that sound monitoring is recommended as an essential

parameter to define, recognize, and analyze cough in laboratory animals (Morice et al., 2007), which is unreliable in the mouse model. Research that has used mice to study cough primarily used airflow and cough sound to detect coughing in response to chemical stimulation by exposure to capsaicin aerosol (Chen et al., 2013). However, the use of telemetry by the integration of an intrapleural pressure sensor, and the active expulsions recorded with box flow would enable for the detection of cough in mice (C. Zhang et al., 2017). Mice are small and inexpensive with readiness for genetic manipulation, which would allow us to better characterize the cough pathway. Therefore, there is a critical need to better characterize the cough behavior in mice.

1.3.2 Components of the cough pathway

The airways and lungs are densely innervated by sensory nerves that play a crucial role in both the normal physiological control of respiratory functions, as well as in pulmonary defense reflexes, such as cough. The afferent innervation responsible for mediating cough is derived from either the nodose (i.e., inferior) or jugular (i.e., superior) vagal ganglia (Monica et al., 2014). Previous studies in the guinea pig have identified two types of peripheral sensory fibers involved in triggering cough: thin myelinated Aδ-fibers arising from the nodose, and unmyelinated C-fibers arising from the jugular (Canning et al., 2004). Cough mediated by Aδ-fibers is triggered by aspirated pollutants, mechanical stimuli, and mucosal secretions. Meanwhile, cough mediated by C-fibers is induced by environmental chemicals, inflammation mediators, and tissue damage (Canning et al., 2004; Mazzone & Undem, 2016). In mice, the vagus nerve contains both fiber types with C-fibers originating from the jugular ganglia and innervating the upper and lower airways while Aδ-fibers originate from the nodose ganglia and innervate the upper airway (Chung et al., 2022; Mazzone & Undem, 2016). It should be noted

that the jugular and nodose ganglia in mice are not dissociated into two distinct structural units, but rather form small integrated structures called jugular-nodose ganglia (Han & de Araujo, 2021).

Cough requires primary afferent input to the brainstem leading to reflexive changes in respiration. Nodose and jugular neurons terminate in the nucleus of the solitary tract (NTS), discussed below, which has been reported as a subnuclei critical for coughing. This is because high expression of the neuronal activation marker (c-Fos) in the NTS has been associated with noxious airway challenges, electrical stimulations and microinjection studies (Canning, 2009; Canning & Mori, 2010; Davenport & Vovk, 2009; McGovern et al., 2012; Ohi et al., 2005). With respect to the basic cough reflex, neurons arising from the NTS project to the ventral respiratory column (VRC), described more in-depth below. The NTS's neurons that are in receipt of cough-specific airway sensory inputs have not been described (Monica et al., 2014). The cough-controlling neurons in the VRC and NTS then send signals to the larynx, trachea, and bronchi through vagal efferent nerves, which controls the contraction of inter-costal muscles and the diaphragm through spinal motor neurons and phrenic nerves, respectively (Lu & Cao, 2023).

Humans can voluntarily cough, choose to suppress their cough, and are acutely aware of an irritation that is present in their airways (i.e., the urge-to-cough). This indicates a significant level of behavioral and conscious control over the basic cough reflex pathway. Therefore, the cough reflex has inputs from higher cortical and subcortical regions, as well. Unfortunately, very little is known about the neural basis for higher brain regulation of coughing (Chung et al., 2022; Hegland et al., 2012; Mazzone et al., 2011).

1.3.2.1 The Nucleus of the Solitary Tract

The NTS (**Figure 1-1**) is a major heterogeneous brain center that receives afferent inputs from visceral organs and relays visceral information to medullary effector nuclei, the rostral brainstem, forebrain areas, and the spinal cord (Cutsforth-Gregory & Benarroch, 2017). The NTS therefore plays diverse functions in various interoceptive responses and plays a critical role in the control of cardiovascular, respiratory, and gastrointestinal functions. (Mazzone & Undem, 2016).

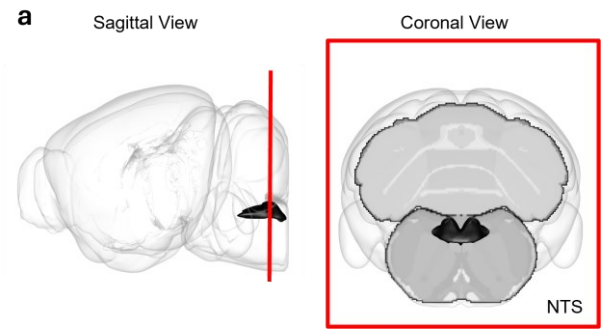

Figure 1-1 **The nucleus of the solitary tract**. **a**, A sagittal and coronal view of the NTS (black).

The NTS is in the dorsolateral medulla and extends from the level of the caudal portion of the facial nucleus to the caudal portion of the pyramidal decussation (Dampney, 1994). It can be subdivided into rostral, intermediate, and caudal regions, each including different subnuclei defined based on their position relative to the solitary tract (McRitchie et al., 1994). Each of these regions receive different afferent inputs.

The NTS receives visceral afferent inputs primarily via the cranial nerves. The rostral NTS (rNTS) receives taste inputs and signals via the facial, glossopharyngeal, and vagus nerves. The intermediate NTS (iNTS) receives gastrointestinal afferents from the vagus nerve. The caudal NTS (cNTS) receives cardiorespiratory afferents that convey information from baroreceptors and chemoreceptors via the glossopharyngeal nerve. All other afferents, including those from the heart, lung, and gastrointestinal tract, are transmitted to the NTS via the vagus

nerve (Benarroch et al., 2007). Our research focuses on the caudal NTS and its role in respiration.

With respect to the cardiovascular and respiratory systems, most of the afferents converge preferentially in the iNTS and the cNTS (Kumada et al., 1990). The neurons in these regions are organized according to the afferent sensory information they receive. The iNTS receives information from the arterial baroreceptors and from the slow-adapting pulmonary stretch receptors (SARs) while the cNTS receives afferents from peripheral chemoreceptors and rapid-adapting pulmonary stretch receptors (RARs) (Kubin et al., 2006; Machado, 2001; Mifflin, 1992; Mifflin et al., 1988). Therefore, distinct groups of NTS neurons may respond to different stimuli and recruit specific neural pathways to generate patterns of responses due to the recruitment of downstream sympathetic and respiratory pathways depending on the sensory information (Zoccal et al., 2014).

1.3.2.2 The Ventral Respiratory Column

The kernel of respiratory rhythm and pattern generation is due to neuronal activity in the ventral respiratory column (VRC). The VRC, which contains both inspiratory and expiratory neurons, is housed in the ventral surface of the medulla oblongata (Zoccal et al., 2014). Here, various voluntary and involuntary demands on respiratory activity are coordinated. The inspiratory neurons fire action potentials during the inspiratory phase of the respiratory cycle, while the expiratory neurons fire action potentials during the expiratory phase. These neurons, which are found in discreate locations throughout the VRC, either project to other brainstem neurons or function as premotor neurons with projections to the respiratory motor neurons (Neubauer, 2006).

The VRC extends from the caudal pole of the facial motor nucleus to the spino-medullary junction (Bautista et al., 2014). The VRC is composed of four distinct sub-nuclei: Bötzinger complex (BötC), pre-Bötzinger complex (preBötC), rostral ventral respiratory group (rVRG) caudal ventral respiratory group (cVRG) (Bianchi et al., 1995) (**Figure 1-2**). The roles of each are discussed below.

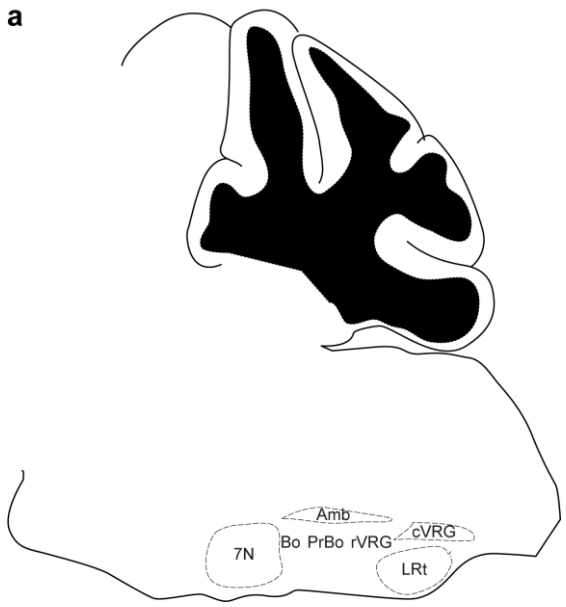

Figure 1-2 **The ventral respiratory column**. a, The ventral column (VRC) extends from the rostral to the caudal end of the medulla and includes the caudal ventral respiratory group (cVRG), the rostral ventral respiratory group (rVRG), the Pre-Bötzinger (PrBo) and Bötzinger (Bo) complexes. The VRC lies ventrolateral to the nucleus ambiguous (Amb). LRt: lateral reticular nucleus 7N: facial nucleus.

The Bötzinger complex (BötC), which contains mostly expiratory neurons, has widespread expiratory functions and plays a critical role in determining the length of post inspiration and expiration during eupnea (Smith et al., 2007). The BötC also integrates reflexes that elicit a temporary arrest of breathing, or apnea by either initiating or prolonging the duration of post inspiration and expiration (Smith et al., 2007). The neurons in the complex are inhibitory in nature and have widespread axonal projections to ensure inspiratory neuronal silencing during expiration (Song et al., 2001).

The preBötC is the anatomical location of the inspiratory rhythm generator (Smith et al., 1991). The underlying rhythm of inspiratory muscle contraction is due to neuronal activity in this region and many breathing-related neurons in this region have pacemaker-like qualities that show activity in phase with inspiration (Del Negro et al., 2018). Ablation of neurokinin 1–expressing (NK1R) neurons in the pre-Bötzinger complex severely disrupts inspiration and abolishes rhythmic activity (Gray et al., 2001), highlighting the importance of this region in inspiratory rhythm generation.

The rVRG contain inspiratory neurons that excite phrenic motoneurons using glutamate as a neurotransmitter. The phrenic pre-motoneurons are mostly concentrated in the most caudal portion of the rVRG and exciting these neurons has no effect on the respiratory rhythm (Feldman et al., 1984; Monnier et al., 2003). However, stimulating the rostral and dorsal portions of the rVRG, where the respiratory interneurons are located, causes changes in respiratory rhythm (Alheid et al., 2002).

On the other hand, the cVRG contains expiratory-modulated neurons that activate motoneurons in the thoracic and lumbar spinal cord, innervating the muscles of expiration (i.e. the abdominal and internal intercostal muscles) during forced breathing (Saji & Miura, 1990). Neurons in the cVRG do not seem to be involved in respiratory rhythm during eupnea, including inspiratory and expiratory duration and respiratory frequency (Bianchi et al., 1995; Bongianni et al., 2005). However, the cVRG is involved in behaviors that involve expiratory prolongation, such as during coughs, emesis, and vocalization (Holstege, 1989; Poliacek et al., 2007; Umezaki et al., 1997).

The VRC lies ventrolateral to the nucleus ambiguus (NA), which plays a significant role in various physiological processes that are essential for human function. The NA contains the

cell bodies of motor nerves that are related to respiration (e.g. laryngeal motoneurons), digestion (e.g. esophageal motoneurons), and control of the heart (e.g. cardiac vagal motoneurons) (Petko & Tadi, 2023). The motor neurons of the NA provide efferent motor innervation to the ipsilateral muscles of the soft palate, pharynx, larynx, and upper esophagus. These include the intrinsic muscles of the larynx, such as the vocal cords and the cricothyroid muscle, as well as extrinsic muscles like the stylopharyngeus and the muscles of the soft palate. The NTS relays sensory input to the NA, which then coordinates the motor responses required for functions like swallowing, respiration, speech, and reflexive responses such as reflex coughing or clearing the airway (Godson Akunna & Ed, 2023).

1.3.3 Addressing the gaps

An estimated $12 billion was spent on cough and cold medications in 2022 (Terlep & Abbott, 2022). Despite the prevalence of these medications, it appears that the currently used antitussives are largely ineffective, even though the efficacy of antitussive compounds is extensively studied in currently used animal models (Morice, 2015). Numerous achievements have been made in the understanding of cough in both the peripheral and central neural mechanisms, which is tremendous progress in the course of finding targeted therapeutic options. A roadblock in finding further targeted therapeutic options is the lack of information on the molecular identities of the neurons mediating coughing in the brainstem and related synaptic pathway.

The mouse is the foremost mammalian model for studying human disease and human health. Mice have anatomical, physiological, and genetic similarity to humans. Furthermore, mice are small, easy to maintain, and their genome can be easily manipulated (Medicine & Bryda, 2013; The Jackson Laboratory, n.d.). Therefore, the use of mice in the context of cough research is

appealing. Before any progress can be made to fill the research gaps described here, the cough behavior in mice must be initially characterized and described in detail to allow for further investigation and build on the work that was previously done in other animal models used in cough.

1.4 Dissertation Overview

Coughing is an important respiratory function that protects the airways and the lungs against accumulated secretions. The cough reflex can be activated by inhaled particles, pathogens, irritants, or having a lung disease, such as asthma or COVID-19. When the brain detects these triggers, it activates the expiratory musculature to control coughing by expelling air from the respiratory system to clear these accumulated secretions. Coughing could become excessive with severe consequences under pathological conditions, leading people to seek medical attention. Effective anti-tussive medications are lacking due to the limited knowledge on the neural circuit controlling coughing.

In this thesis, we develop a mouse model to study the neural pathways of coughing with the genetic and neurogenetic tools available in mice. We demonstrate that molecularly distinct NTS neurons trigger diverse breathing patterns upon optogenetic activation. Then, we identify a sub-population of neurons within the NTS that express the neuropeptide gene tachykinin 1 (Tac1) that are activated during tussive challenges. Photoactivation of these neurons is sufficient in inducing cough-like behaviors in mice while genetic ablation or chemogenetic silencing of these neurons diminishes the coughs induced by tussive agents. These results reveal the first genetically defined neurons in the brain that mediate coughing induced by tussive agents. We then identify regions within the VRC that play a role in the downstream cough circuit of the NTS Tac1 neurons. We show that the NTS Tac1 neurons integrate these downstream targets to induce

cough-like behaviors in mice. Based on these results, we show that the NTS Tac1 neurons are the key cough control center.

This thesis advances the knowledge of the endogenous central neural circuit underlying cough-like behaviors in mice. Furthermore, it may lead to the potential identification of drug targets for manipulating cough, thereby providing new opportunities for the development of novel therapeutics and better treatments for those suffering from excessive coughing.

Chapter 1 was largely adapted from the following manuscript in review:
Gannot N., Li X., Phillips C., Ozel A., Uchima Koecklin K., Lloyd J., Zhang L., Emery K., Stern T., Li J., Li. P. A vagal- brainstem interoceptive circuit for cough- like defensive behaviors in mice. Nature Neuroscience.

Chapter 2 The Heterogenous Functions of the Nucleus of the Solitary Tract Neurons in Breathing Control

Breathing is regulated by the internal conditions since breathing rapidly responds and is continuously regulated by the physiological states and stimuli in the body (R. B. Chang et al., 2015; Prescott et al., 2020). The internal stimuli from the visceral organs are largely sensed by the sensory neurons in the vagus nerve, and then transmitted to the brain through relay regions like the NTS (Canning et al., 2014; Mazzone & Undem, 2016). How distinct respiratory behaviors are mediated by the NTS are largely unknown. Although the molecular heterogeneity of the NTS neurons started to be revealed recently (Dowsett et al., 2021; Ludwig et al., 2021; Reiner et al., 2022), their precise functions in the control of respiration has not been studied. In this chapter, we demonstrate that the NTS is made of molecularly distinct neurons that trigger diverse breathing patterns upon optogenetic activation.

2.1 Single cell RNA sequencing study of the NTS

To dissect the heterogeneity of NTS cells, we first carried out a single cell RNA sequencing study of the mouse cNTS using the 10X Genomics Chromium platform. Single cell RNA sequencing allows us to understand cellular differences in expression. Hence, it is directly applicable to the study of cell heterogeneity (Andrews et al., 2020). In total, we sequenced 9,578 cells. After removing the low-quality cells, the first-round analysis produced 8 clusters of 5,523 cells, which correlated to different cell types in the mouse central nervous system (**Figures 2-1 a-b**). We next investigated the cellular heterogeneity of the putative neuron cluster of 1,939 cells.

the analysis produced 19 molecularly distinct cell clusters, identifiable with unique markers (**Figure 2-1 c**). Since we have identified the different neuronal populations that make up the NTS, we can take advantage of mouse genetics and neuroscience tools to characterize whether these different neuronal subtypes play a role in respiration.

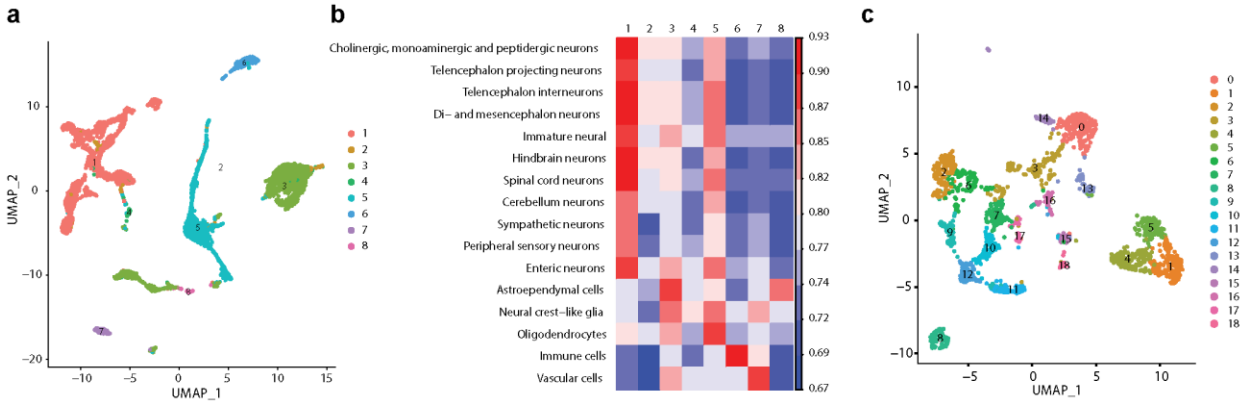

Figure 2-1 **The cNTS is made of molecularly heterogenous neurons**. **a**, UMAP plot of 5,523 high-quality NTS cells showing 8 different cell populations. **b**, 8 clusters of the NTS cells are annotated based on published dataset of the nervous system. **c**, UMAP plot of the putative neurons showing 19 molecularly distinct subclusters.

2.2 Optogenetic manipulation of different neuronal population in the NTS induces diverse breathing responses

To examine the role of the neuronal subsets in controlling breathing, we carried out a functional screen using optogenetic activation of different neuronal subsets in the NTS in transgenic mouse lines. Optogenetics allows for the precise control of the activity of neurons with the use of light. In optogenetics, neurons are modified to express light-sensitive ion channels, or opsins enabling either their activation or deactivation with pulses of light with high temporal resolution. Limiting the genetic modification to a specific cell type allows for the study of functions associated with only those cells (Boyden et al., 2005). One of the commonly used microbial opsins is channelrhodopsin, which allows for the fast depolarization of neurons upon exposure to light through direct stimulation of ion channels. Channelrhodopsin-2 (ChR2) is a blue light activated cation channel with high conductance at physiological pH and traffics well to

the membrane. Shining a blue light on neurons that express ChR2 results in excitation or depolarization of the neuron (Deisseroth & Hegemann, 2017). We can express ChR2 specifically in a desired region and neuronal population utilizing conditional gene expression in the mouse.

We can take advantage of the Cre-loxP system to express ChR2 in Cre positive neurons using FLEx switches, sometimes also referred to as a DIO switch, or Double-floxed Inverse Orientation (Cronin, 2016). Our gene of interest, ChR2, is initially inversed or in the antisense "off" position and flanked by two pairs of lox-P sites. Only in the presence of Cre, the gene of interest is flipped to the "on" orientation and is expressed. The inverted version of a gene will not be expressed so DIO can be used to control gene expression (**Figure 2-2**).

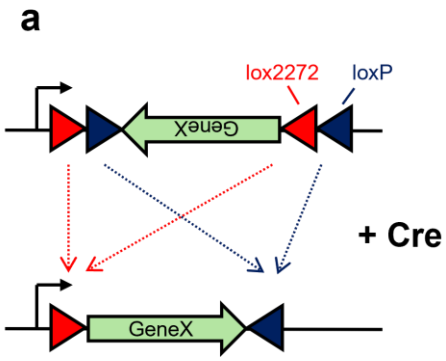

Figure 2-2 **A DIO vector**. **a**, Inversion occurs via either loxP or lox2272, followed by the excision of the two lox-P sites. The DIO vector turns on gene expression only in the presence of Cre.

The adenoassociated viral vector (AAV) encoding the Cre-dependent expression of channelrhodopsin-2 (AAV-DIO-ChR2-eYFP) was stereotactically injected into the NTS of various mouse Cre lines. Three weeks later, the Cre-positive neurons were activated by a blue laser in freely moving mice. The animal's breathing responses were recorded in a whole-body plethysmograph (WBP) chamber.

The WBP allows for the measurement of respiratory function using a sensitive pressure transducer that measures pressure changes inside the chamber. The chamber is fitted with screen pneumotaches, allowing air to pass outside the chamber. Therefore, the small pressure changes in

the chamber are related to respiratory flow (*Whole Body Plethysmography - PrimeBioscience*, 2017). The unrestrained WBP measures air expansions and contractions that take place within the chamber, which are indicative of the animals breathing. During inspiration, the air is heated and humidified as it is transferred from the outside to the inside of the lungs. The diaphragm and intercostal muscles contract, causing a slight negative pressure in the lungs. This decrease in pressure forces air out of the plethysmograph through the pneumotach located in the side of the WBP. During expiration, the diaphragm relaxes to return to its resting position, and the external intercostal muscles relax to depress the ribs and sternum. Both the reclaiming of heat and humidity in the expired air and the possible compression cause air to be drawn back into the plethysmograph and the flow of air drawn into the plethysmograph through the pneumotach is measured (Data Sciences International, 2021).

When different NTS neuronal populations were activated, animals exhibited diverse breathing responses, including an ectopic inspiratory peak (**Figures 2-3 a-f**), apnea (**Figures 2-3g- h**), and a sigh (**Figures 2-3 k-l**). The activation of the Vglut2, Gal and Oprm1 neuronal populations all produced similar inspiratory responses while the activation of the Grp neuronal population was more reminiscent of a sigh observed in freely moving mice (Yao et al., 2023).

Interestingly, among these different breathing responses, the activation of tachykinin 1 (Tac1) neurons induced a breathing pattern with a stereotypic breathing trace shown on the WBP bow flow recording. (**Figures 2-3 i-j**). Although this stereotyped breathing pattern was not observed in the resting state, it resembles the respiratory defensive reflexes of humans and other species (Iwata et al., 2015; Xiang et al., 1998) and will be discussed further in the next chapters.

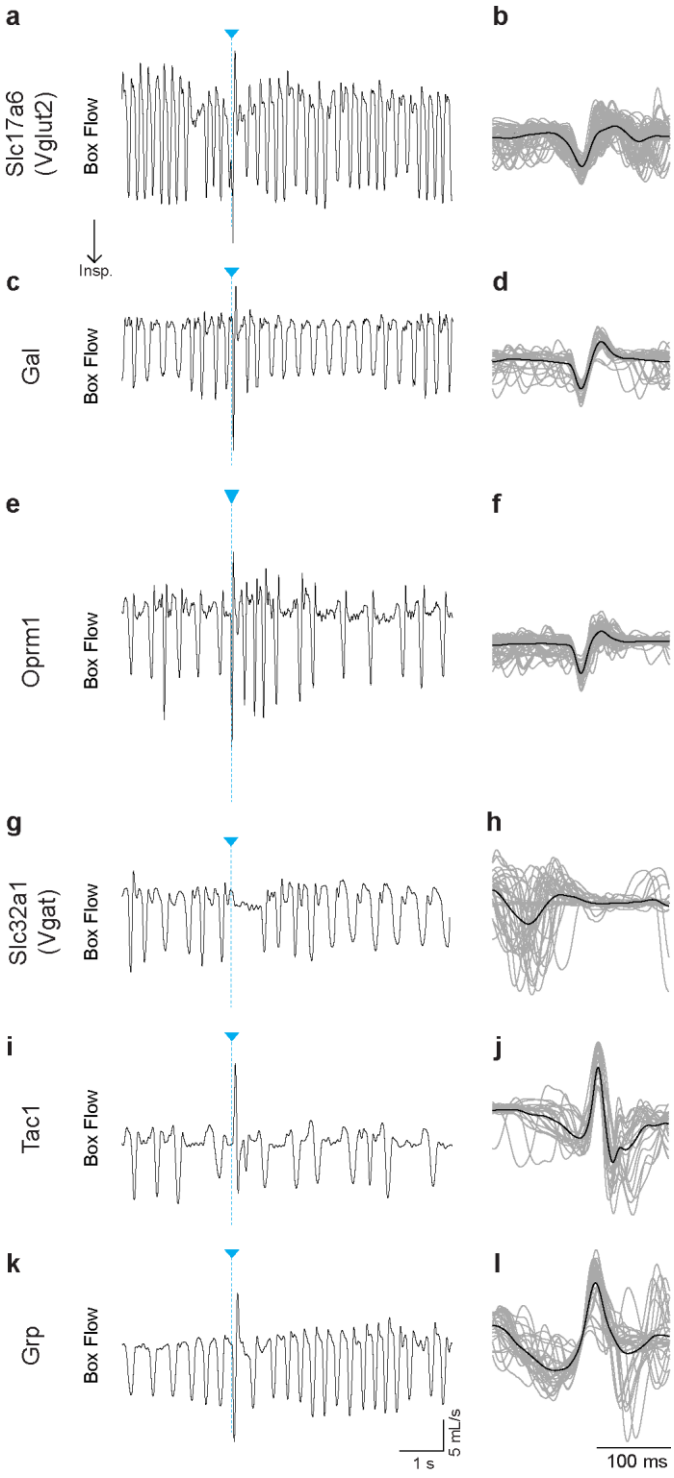

Figure 2-3 **Optogenetic activation of NTS neuronal subsets elicits diverse breathing responses in freely moving mice. a,** 15ms laser activation of Vglut2-Cre neurons induces an ectopic inspiratory peak **b**, Individual (gray) and average (black) traces for ectopic inspiratory peaks induced by optogenetics of Vglut2 neurons (n=30 events, 3 mice). Traces aligned by inspiratory peak. **c,** 15ms laser activation of Gal-Cre neurons induces an ectopic inspiratory peak. **d**, Individual (gray) and average (black) traces for ectopic inspiratory peaks induced by optogenetics of Gal neurons (n=30 events, 3 mice). Traces aligned by inspiratory peak. **e,** 15ms laser activation of Oprm1-Cre neurons induces an ectopic inspiratory peak. **f**, Individual (gray) and average (black) traces for ectopic inspiratory peaks

induced by optogenetics of Oprm1 neurons (n=30 events, 3 mice). Traces aligned by inspiratory peak. **g**, 15ms laser activation of Vgat-Cre neurons induces apnea. **h**, Individual (gray) and average (black) traces for apnea induced by optogenetics of Vgat neurons (n = 30 events, 3 mice). Traces aligned by start of laser. **i**, Activation of Tac1-Cre neurons induces a stereotyped breathing pattern. **j**, Individual (gray) and average (black) traces for the stereotyped breathing pattern induced by optogenetics of Tac1 neurons (n = 30 events, 3 mice). Traces aligned by the compressive peak. **k**, 15ms laser activation of Grp-Cre neurons elicits a sigh. **l**, Individual (gray) and average (black) traces for sighs induced by optogenetics of Grp neurons (n = 30 events, 3 mice). Traces aligned by when they cross the baseline.

2.3 Discussion

Breathing is a vital and complex neuronal behavior. Breathing patterns are controlled by our brain which receives constant peripheral sensory information from the lungs and the airway. The NTS, which receives this input via the cranial nerves, plays an important role in cardiorespiratory activity. Recent work has revealed the role of different neuronal populations within the NTS that modulate respiration differently (Do et al., 2020; Fu et al., 2019; Yu et al., 2022), highlighting the importance of the NTS in diverse respiratory responses and respiratory-related activity.

In this chapter, we aimed to understand the heterogeneity of NTS cells. To this end, we carried out a functional and molecular screen using various transgenic mouse lines to optogenetically activate different neuronal subsets in the NTS and examine their functions in controlling breathing. Our results showed that activating different neuronal populations within the NTS induced an array of breathing responses, including inspiratory, expiratory and apnea behaviors. It should be noted that effects on other respiratory related activity, such as breathing frequency, tidal volume and minute ventilation, were not analyzed. This is because only short 15ms laser pulses were given to activate these neurons. Activating a subpopulation of neurons expressing the neuropeptide gene Tac1 induced a stereotypic response. In future chapters, we will further dissect and characterize this respiratory behavior.

NTS is the major portal through which visceral afferent information concerning cardiovascular, respiratory, and gastrointestinal systems enters the brain. In this chapter, we

demonstrated the diverse role the NTS plays specifically in regulating diverse respiratory responses. Here, only the effects of respiration were measured when different neuronal populations were activated. Due to the diverse role of the NTS in other behaviors, it would be interesting to observe the effects these optogenetic activations have on other behaviors. Furthermore, it would be interesting to trace their downstream targets throughout the brain and the spinal cord and compare whether or not they converge on similar efferent pathways since different neuronal populations within the NTS modulate respiration differently.

Chapter 2 was largely adapted from the following manuscript in review:
Gannot N., Li X., Phillips C., Ozel A., Uchima Koecklin K., Lloyd J., Zhang L., Emery K., Stern T., Li J., Li. P. A vagal- brainstem interoceptive circuit for cough- like defensive behaviors in mice. Nature Neuroscience.

Dr. Ayse Blige Ozel and Dr. John P. Lloyd performed the experiments in 2-1. Noam Gannot performed the experiments in 2-3.

Chapter 3 Characterizing Respiratory Defensive Behaviors in Freely Moving Mice

The average person who is moderately active during the daytime breathes about 20,000 liters of air every 24 hours. Inevitably, this air contains potentially harmful particles and gases, such as dust, soot, mold, fungi, and bacteria. Fortunately, the respiratory system is equipped with defensive mechanisms that help clean and protect it. These defensive mechanisms, including coughs, sneezes, and expiratory reflexes, are generated by a common muscular system, which is also used in breathing. However, these behaviors differ significantly in their mechanical features and regulation. For example, stimulation of the larynx can evoke the expiration reflex, a prompt expiration without preceding inspiration. The stimulation of the oropharynx and lower airways provokes the cough reflex. The stimulation of the nasal passage triggers sneezing (Tomori et al., 2012). These actions also engage different muscle recruitment. For instance, the styloglossus muscle plays a specific role in elevating the back of the tongue during sneezing, but not during coughing, leading to the expiratory nasal airflow (Satoh et al., 1998; Simera et al., 2015). It is likely that the respiratory pattern generator undergoes reconfiguration to produce these distinct expiratory defensive behaviors. This information is most readily obtained from in vivo experimental models in which multiple airway defensive behaviors can be produced.

In the previous chapter, we showed that activating a subpopulation of neurons expressing the Tac1 gene induced a stereotypic expiratory response. As mentioned previously, there is skepticism regarding the use of mice to study these expiratory behaviors (Belvisi & Bolser,

2002), partly because these behaviors have not been fully characterized in mice. In this chapter, we seek to characterize and differentiate between these respiratory defensive behaviors in mice.

3.1 Mimicking the activation of NTS Tac1 neurons using a tussive agent

The most used animal model in cough research is the guinea pig. Despite its usage, this model lacks the genetic tools to precisely define cough controlling neurons and circuits (Canning & Chou, 2008). Unfortunately, this barrier limits the discovery of endogenous cough pathways, as well as the development of a targeted anti-tussive medication. In contrast, the mouse is a premier mammalian model for the study of the genetic and molecular bases of physiology and behavior. The ability to manipulate the mouse genome makes them an attractive candidate for cough research. Despite this, mice have not been used to study coughing due to the scholarly debate about their ability to cough (Belvisi & Bolser, 2002).

To investigate whether mice exhibit respiratory defensive behaviors, we started with the nebulization of capsaicin, a tussive agent extracted from chili peppers, as it consistently induces coughing in humans and other species (Daller et al., 2012; Iwata et al., 2015; Midgren, et al., 1992; Xiang et al., 1998), and perhaps other respiratory defensive reflexes. When mice are placed in the WBP and exposed to capsaicin, breathing events characterized by an upward peak were observed (**Figure 3-1 a-c**), resembling the breathing response elicited by NTS Tac1-Cre activation (**Figure 2-5 i-j**). This upward peak is attributed to increased pressure in the respiratory system against a closed airway. Compression of the muscles in the body and the chest wall during this phase draws air into the WBP chamber, resulting in an upward airflow trace in the box flow, characteristic of a compressive phase (Chen et al., 2013; C. Zhang et al., 2017). Therefore, mice exhibit respiratory defensive behaviors in response to a capsaicin challenge.

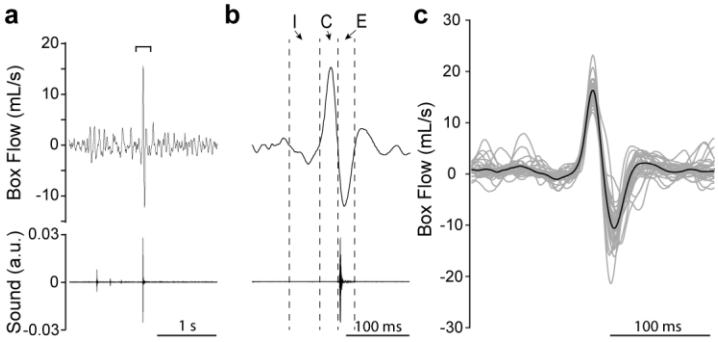

Figure 3-1 **Respiratory response to the nebulization of capsaicin**. **a**, Stereotyped respiratory trace (top) and corresponding audio (bottom) of a capsaicin-evoked respiratory response. Bar, 1 s. **b**, Magnified depiction of panel a showing the division of the inspiratory phase (I), the compressive phase (C), and the expulsive phase (E). Bar, 100ms. **c**, Individual (gray) and average (black) traces for respiratory responses induced by tussive challenges (n=30, three mice). Bar, 100ms.

3.2 Distinguishing cough-like behaviors from sneeze-like behaviors in mice

While distinguishing between coughs and sneezes is straightforward in humans, the differentiation of these respiratory behaviors in animals has not been characterized. Furthermore, nebulization of capsaicin has been suggested to induce respiratory defensive behaviors resembling both coughs and sneezes in mice (Chen et al., 2013; Iwata et al., 2015; Kamei et al., 1993; F. Li et al., 2021). To distinguish between these defensive behaviors, we hypothesized that cough-like and sneeze-like behaviors would manifest with distinct breathing waveforms in mice given the distinct sensory afferent pathways and motor outputs.

To explore this hypothesis, we utilized an intranasal administration of compound 48/80, to induce histamine release and trigger a respiratory response in addition to the nebulization of capsaicin (Rothschild, 1970). To eliminate sneeze-like behaviors mediated by the trigeminal pathway innervating the nasal passage, we conducted anterior ethmoidal nerve (AEN) denervation to destroy the sensory afferent for sneeze-like behaviors. Utilizing a hierarchical clustering method, we categorized respiratory patterns from both stimuli before and after AEN denervation by focusing on the characteristic compressive phase. The respiratory patterns were classified into 8 clusters based on the morphology of the respiratory trace (**Figure 3-2 a**).

Subsequently, we reasoned that post-AEN denervation animals, lacking the afferent from the nasal passage, should exhibit minimal sneeze-like behaviors. Based on the occurrence of each cluster in pre- vs. post-AEN conditions and the similarity of breathing patterns, we classified all respiratory defensive events into two classes (**Figure 3-2 b-c**). As the majority of class 2 events (83%) were observed in animals with an intact AEN, they are designated as sneeze-like behaviors (**Figure 3-2 c**). In contrast, class 1 events occur in both pre- and post-AEN conditions (40% and 60%, respectively), representing cough-like behaviors, since these events were not impacted by the AEN denervation (**Figure 3-2 b**).

To facilitate automated and unbiased categorization of respiratory responses in future analyses, we employed training on a linear support vector machine (SVM) for breath pattern classification and achieved a significant accuracy rate of 98.08% compared to the hierarchical clustering method (**Figure 3-2 d-e**). This high accuracy not only underscores the confidence in our clustering outcomes, but also emphasizes that the separated signal geometries are indicative of distinct physiological functionalities. Thus, we developed a straightforward linear SVM classifier that establishes a robust and dependable technique for future sample analysis, reinforcing the idea that distinct signal geometries correlate with unique physiological functionalities.

Applying the linear SVM classifier to an extended dataset, we observed that compound 48/80 induces both cough-like and sneeze-like behaviors (**Figure 3-2 h**) while the vast majority (>92%) of behaviors induced by capsaicin were characterized as cough-like behaviors (**Figure 3-2 i-j**). The occurrence of sneeze-like behaviors in the compound 48/80 assay significantly decreased after AEN denervation, from 17 ± 5.2 to 2.8 ± 1.0, representing an 84% reduction (**Figure 3-2 h**). In contrast, the cough-like behaviors induced in both the compound 48/80 assay

and the capsaicin assay remained unaffected by AEN denervation (**Figure 3-2 h-i**). The cough-like behaviors demonstrated a significantly shorter duration and larger amplitude in the compressive phase (**Figure 3-2 f-g**) compared to sneeze-like behaviors. This behavior is consistent with the previous reports in other species (Daller et al., 2012; Iwata et al., 2015; Korpas J, 1979; Venkatasamy et al., 2010; Xiang et al., 1998). Therefore, the linear SVM classifier will be used for analyzing the respiratory defensive behaviors in the subsequent experiments and chapters.

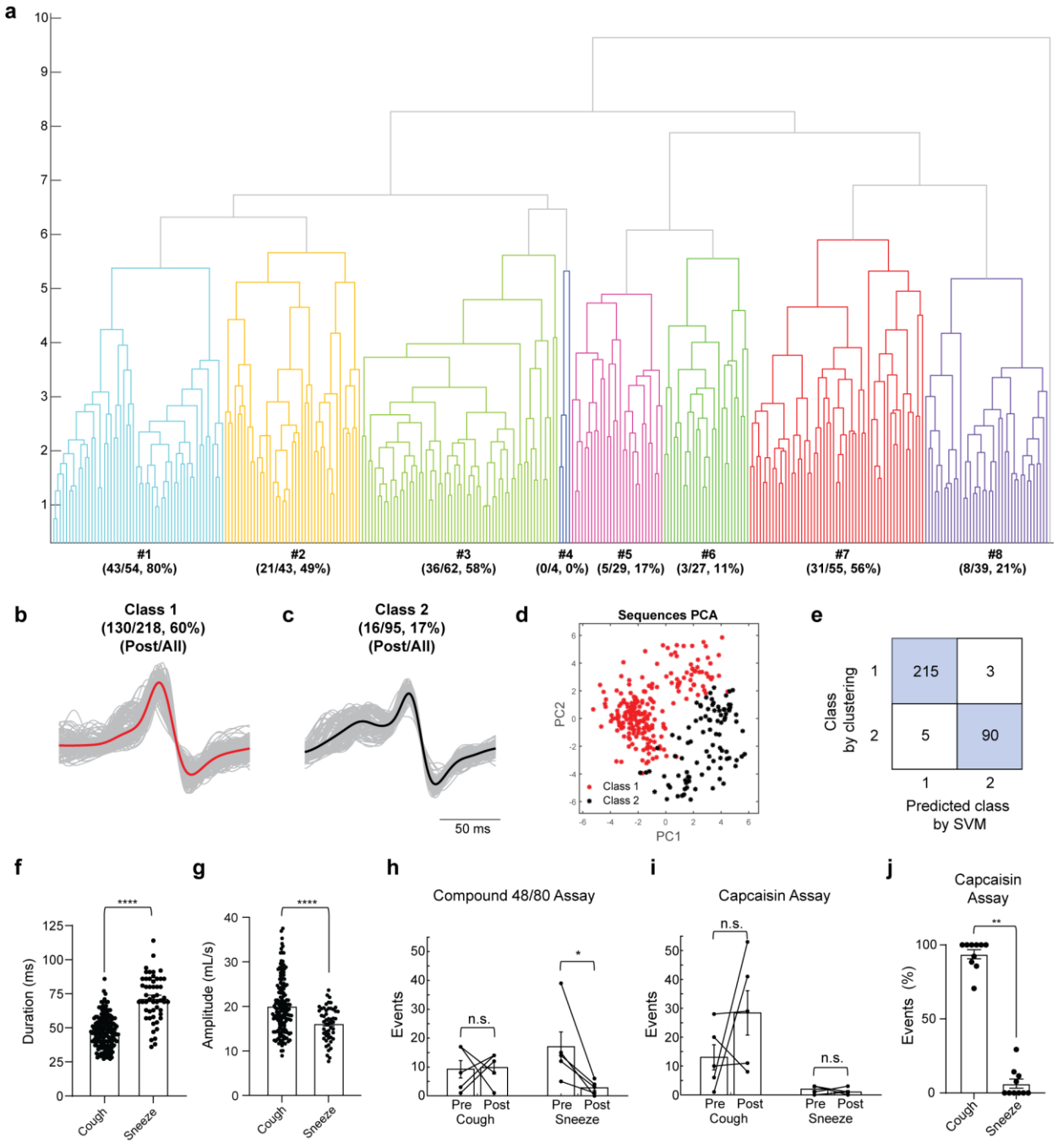

Figure 3-2 **Characterization of respiratory defensive behaviors before and after AEN denervation**. **a**, Hierarchical clustering separates all expiratory events (n = 313 breathing traces, 4 mice) induced by either a capsaicin assay or a compound 48/80 assay into 8 clusters. Each cluster was assessed for the percentage of events occurring after the AEN denervation over the total number in the cluster. Clusters with a ~20% or lower percentage indicate that the breathing patterns predominantly occur in mice with intact AEN and diminish after AEN denervation, designating it as sneeze-like. Clusters with a ~50% or higher percentage indicate that the breathing patterns are not dependent on intact AEN and are designated as cough-like. Based on this assessment and the similarity between clusters, breathing patterns were classified into two classes. **b**, Individual (gray) and average (red) traces characterized as class one (n = 218 events, 4 mice). Note that 60% of the respiratory events classified in class 1 occurred prior to AEN denervation. **c**, Individual (gray) and average (black) traces characterized as class two (n = 95 events, 4 mice). Note that 17% of the respiratory events classified in class 1 occurred after AEN denervation.

d, PCA plot of all events in b and c. **e**, the confusion matrix of the linear SVM method that is used to distinguish between the two clusters moving forward. Please note that linear support vector machine (linear SVM) demonstrates an accuracy of 98.08% for these two classes. **f**, Duration difference between cluster one (i.e., cough-like) (n = 218 events, 4mice) and cluster two (i.e. sneeze-like) (n = 95 events, 4 mice) of the compressive phase ($p<0.0001$, Mann-Whitney test). **g**, Amplitude difference between cluster one (i.e., coughs) (n = 218 events, 4 mice) and cluster two (i.e. sneeze-like) (n = 95 events, 4 mice) of the compressive phase ($p<0.0001$, Mann-Whitney test). **h**, Cough-like (class 1) ($p = 0.92$, paired t-test) and sneeze-like behaviors (class 2) ($p = 0.04$, paired t-test) in a 10-minute compound 48/80 assay in mice (n = 5 mice) before (pre) and after (post) an anterior ethmoidal nerve (AEN) denervation. **i**, Cough-like (class 1) ($p = 0.26$, paired t-test) and sneeze-like behaviors (class 2) ($p = 0.375$, Wilcoxon matched-pairs signed rank test) in a 6-minute capsaicin assay in mice (n = 5 mice) before (pre) and after (post) an anterior ethmoidal nerve (AEN) denervation. **j**, Quantification of the occurrence of cough-like and sneeze-like responses in 6-minute capsaicin assay. n = 93 events, 10 mice, $p=0.0039$ Mann Whitney test.

3.3 Comparing coughs to expiratory reflexes

Given that the vast majority of the respiratory defensive behaviors induced by the nebulization of capsaicin were identified as coughs, we proceed to use this stimulus to further characterize the cough-like defensive responses in mice. Exposure of nebulized 30 μM capsaicin to mice triggered behavior responses that resembled the cough reflex and the expiratory reflex (**Figure 3-1**) in human and other species (Iwata et al., 2015; C. Zhang et al., 2017).

As discussed previously, there are three main phases of the cough reflex: (1) the inspiratory phase, (2) the compressive phase and (3) the expulsive phase. The expiratory reflex is composed of only the compressive and the expulsive phases of the cough reflex. Each of these phases are described in-depth below.

The cough begins with a deep inspiratory phase with the aim of attaining a high lung volume. During this phase, the glottis opens widely because of the contraction of the abductor muscles, allowing for the rapid entry of large amounts of air into the lungs (Irwin et al., 1977). When air is taken into the lung, it is heated and humidified, as it is transferred from outside the lung. Therefore, the intrapleural pressure decreases while the flow trace shows a downward peak (**Figure 3-3, blue**). The air taken into the lungs during the inspiratory phase of the cough is referred to as the 'operating' volume, which significantly affects the mechanical changes during coughs. Specifically, the operating volume is an important determinant of both the peak flow

achieved and volume expelled but has little influence on the pressures generated in the chest and abdomen. Therefore, an operating volume larger than the proceeding eupneic inspiration leads to a more productive cough. Although coughs can occur with smaller operating volumes, some coughs may be ineffective (J. A. Smith et al., 2012).

The following two phases, the compressive and expulsive phases, are shared with the expiratory reflex. The compressive phase begins with the closure of the glottis and continues with the contraction of the expiratory muscles. During this phase, the intrapleural pressure rapidly increases to produce the flow rates necessary for a productive expulsion due to the closure of the glottis and compression of the muscles in the chest wall. The flow trace (box flow) exhibits an upward peak as air flows into the chamber (**Figure 3-3, purple**). It is important to note that the compressed air in the lung causes air to be drawn into the chamber during this phase, even though no air flows in or out of the animal. Therefore, the change of flow shown on the trace indicates flow into and out of the chamber, not the animal (Data Sciences International, 2021).

The third and final phase begins with the sudden opening of the glottis, releasing the pressure in the lungs. It is during the expulsive phase that the function of the cough or expiratory reflex is carried out – the removal of the undesired material from the lungs and airways. During this phase, the intrapleural pressure is suddenly reduced as the pressure in the lungs is released. The cough sound is produced in this phase due to air rushing past the opened glottis. As a result, the box flow is negative as air rushes out of the chamber (**Figure 3-3, red**).

While a cough can simply be referred to as a single three-phase event, in practice, it often occurs as an epoch, bout, or attack (Fontana & Widdicombe, 2007). Cough bouts often consist of a combination of both a cough reflex and an expiratory reflex. During a cough epoch, an initial

inspiration is followed by a series of glottal closures and expiratory efforts sometimes with interspersed inspirations (Korpas J, 1979; J. Widdicombe & Fontana, 2006). Isolated coughs and expiratory reflexes are easy to distinguish, but they are usually grouped together during a cough epoch (Fontana & Widdicombe, 2007). Moreover, the cough literature does not distinguish between the two reflexes or whether the coughs are single events or epochs. Instead, the two reflexes are grouped together and measured as frequency of expiratory efforts (J. Widdicombe & Fontana, 2006). During the capsaicin challenge in our study, the majority of the stereotyped respiratory responses observed (83 ± 3.2%, n = 20 mice) were attributed to the cough reflex, which starts with an inspiratory phase. Therefore, both coughs and expiratory reflexes were analyzed together as cough-like behaviors in mice in this study.

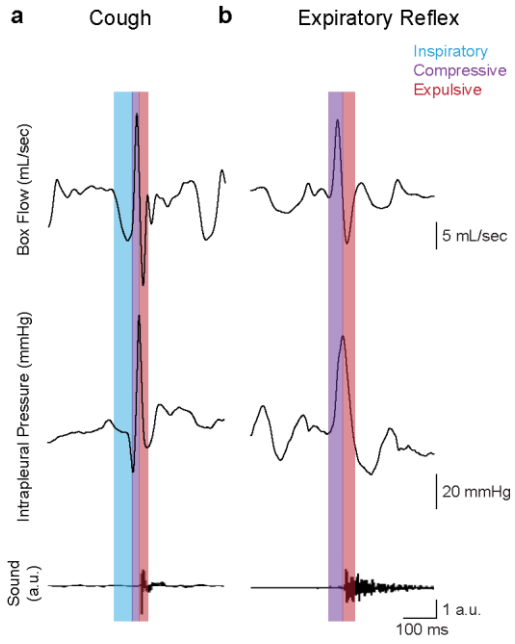

Figure 3-3 **Distinguishing coughs from expiratory reflexes in freely moving mice**. **a**, Simultaneous recordings of a cough-like response with the box flow by whole body plethysmograph (WBP), intrapleural pressure by telemetry, and sound recording. Please note that a cough is composed of three distinct phases: (1) the inspiratory phase (blue), (2) the compressive phase (purple) and (3) the expulsive phase (red). In the inspiratory phase, the intrapleural pressure decreases and air is inhaled into the lungs. The box flow is negative (flow out of the chamber) due to the increased temperature and humidity of the inhaled air in the animal body. In the compressive phase, which occurs immediately following the inspiratory phase, the glottis is closed and the muscles compress air in the lungs, which results in a rapid increase of the intrapleural pressure. Because of the compression of the body, the pressure in the chamber decreases and air flows into the chamber (a positive box flow). In the expulsive phase, the glottis is opened and the intrapleural pressure is released. The cough sound is produced as air rushes past the glottis. Because the air

with high pressure is released from the lungs to the chamber, the air flows out of the chamber (a negative box flow). **b**, Simultaneous recordings of an expiratory reflex with the box flow by whole body plethysmograph (WBP), intrapleural pressure by telemetry, and sound recording. Please note that the expiratory reflex is made up of the last two phases of the cough: the compressive phase (purple) and the expulsive phase (red).

3.4 Characterizing the cough- like behaviors in mice

We developed a platform to simultaneously record a panel of physiological parameters, including respiratory airflow, intrapleural pressure, audio, and video, in response to the tussive challenge (**Figure 3-4 a**). Other than the use of capsaicin as a tussive agent, we also utilized citric acid and polyvinyl alcohol. Both capsaicin and citric acid are used as nebulized tussive agents (**Figure 3-4 c-d**) while polyvinyl alcohol is delivered intranasally to model postnasal drip coughs (Iwata et al., 2015) (**Figure 3-4 e-f**). In postnasal drip, excessive mucus drains down the back of the throat and triggers a forced expiration through mechanical stimulation of the larynx (Morice, 2004). This evokes mechanostimulation and induces cough-like reflexes (Lee & Eccles, 2004) (**Figure 3-4 f**). The inhalation of capsaicin and citric acid predominantly activates airway C fibers (Tanaka & Maruyama, 2005; Taylor-Clark, 2015) whereas Aδ-fibers are triggered by mechanical stimuli (Canning et al., 2004; Mazzone & Undem, 2016). The cough-like events evoked by these different stimuli all followed the same three-phase pattern observed and the events observed here were all characterized using the SVM model described earlier.

The frequency of cough-like events is dependent on the concentration of the tussive agent (**Figure 3-4 g-i**) and only sparse cough-like responses were observed in the nebulization of the vehicle (**Figure 3-4 b**). From the concentration curves (**Figure 3-4 g-i**), the optimal concentration of each tussive agent was determined and we have demonstrated that different tussive agents can induce both mechanically and chemically induced cough-like behaviors in mice.

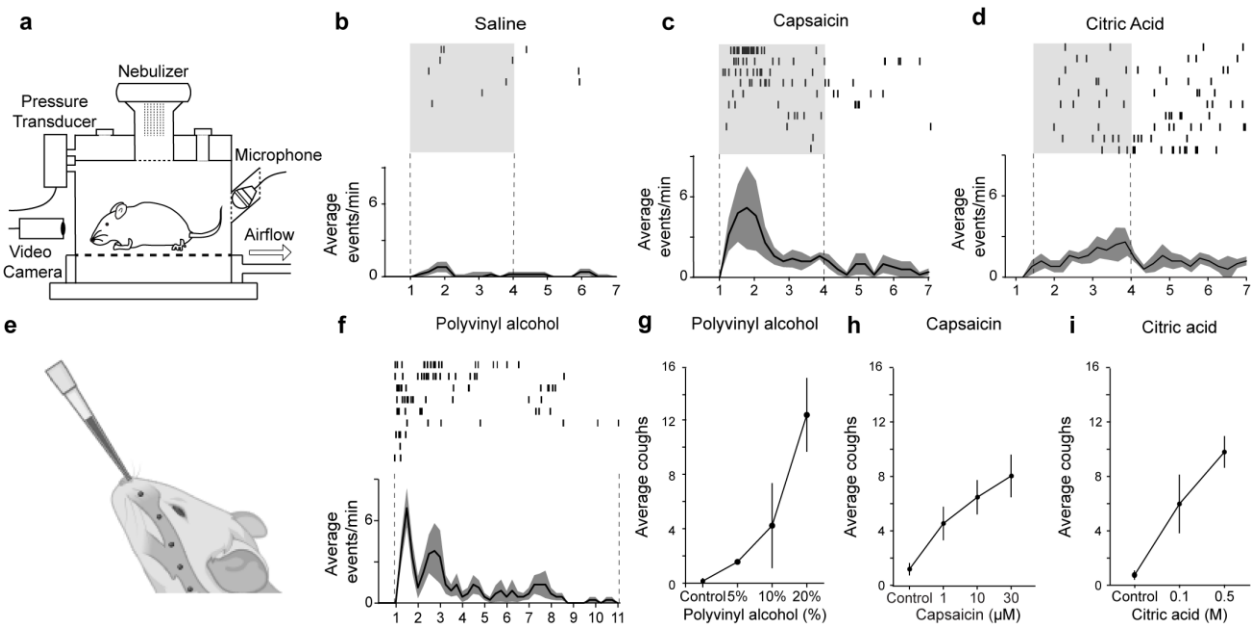

Figure 3-4 **Tussive agents used to induce cough- like behaviors in mice**. **a**, A schematic showing the modified WBP chamber utilized for the tussive challenge. The intrapleural pressure catheter and telemetry sensor are not shown. **b**, Top: raster plots of cough-like behaviors across ten naïve mice during 3-minute nebulization of saline (gray) and 3-minute following nebulization where the mouse remained in the chamber. Bottom: average events rate of all raster plots; shaded area, SEM. **c**, Top: raster plots of cough-like behaviors across ten naïve mice during 3-minute nebulization of 30μM capsaicin (gray) and 3-minute following nebulization where the mouse remains in the chamber; Bottom: cough-like response rate of all raster plots; shaded area, SEM. n=10 mice. **d**, Top: raster plots of cough-like behaviors across ten naïve mice during 3-minute nebulization of 0.5M citric acid (gray) and 3-minute following nebulization where the mouse remains in the chamber. Bottom: cough-like response rate of all raster plots; shaded area, SEM. n=10 mice. **e**, A schematic showing the intranasal administration of polyvinyl alcohol. Created in Biorender. **f**, Top: raster plots of cough-like behaviors across ten naïve mice during a 10-minute recording after a 20% polyvinyl alcohol intranasal injection. Bottom: cough-like response rate of all raster plots; shaded area, SEM. n=10 mice. **g**, Cough-like behaviors in a 10-minute cough assay with different concentrations of polyvinyl alcohol (n=15 mice). **h**, Cough-like behaviors in a 6-minute cough assay with different concentrations of capsaicin (n=15 mice). **i**, Cough-like behaviors in a 6-minute assay with different concentrations of citric acid (n=15 mice).

Occasionally, repetitive cough-like behaviors were observed in the tussive challenge (**Figure 3-5 b**). The cough-like behaviors induced by capsaicin require the intact vagus nerves (**Figure 3-5 c**), but not the AEN (**Figure 3-5 d**). Furthermore, these respiratory behaviors are distinct from other respiratory patterns and audio events (**Figure 3-6**) observed during the tussive challenge of capsaicin (Iwata et al., 2015; F. Li et al., 2021; P. Li et al., 2016; Xiang et al., 1998). Therefore, consistent with the studies that have likewise described coughs in mouse models (Chen et al., 2013; Iwata et al., 2015; Kamei et al., 1993; Zhang et al., 2017), our results

demonstrate that mice exhibit cough-like behaviors following the exposure to tussive agents, which is dependent on the vagus nerve.

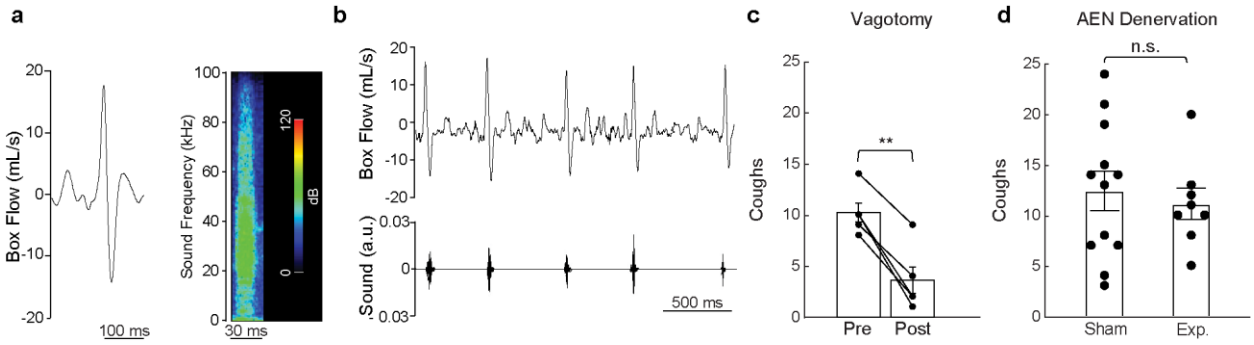

Figure 3-5 **Characterization and validation of the cough-like behavior**. **a**, Stereotyped breathing waveform (left) and sound spectrum (right) of a cough-like response evoked by capsaicin. Bars, 100ms (left) and 30ms (right). **b**, Repetitive cough-like behaviors evoked by a tussive challenge. Bar, 500ms. **c**, Cough-like behaviors in a 6-minute capsaicin assay before (pre) and after (post) unilateral vagotomy (n=5 mice, p=0.001, paired t-test). **d**, Cough-like behaviors in a 6-minute cough assay in mice with an anterior ethmoidal nerve (AEN) denervation (n=8 mice) compared to mice with a sham surgery (n=12 mice), p=0.63, unpaired t-test.

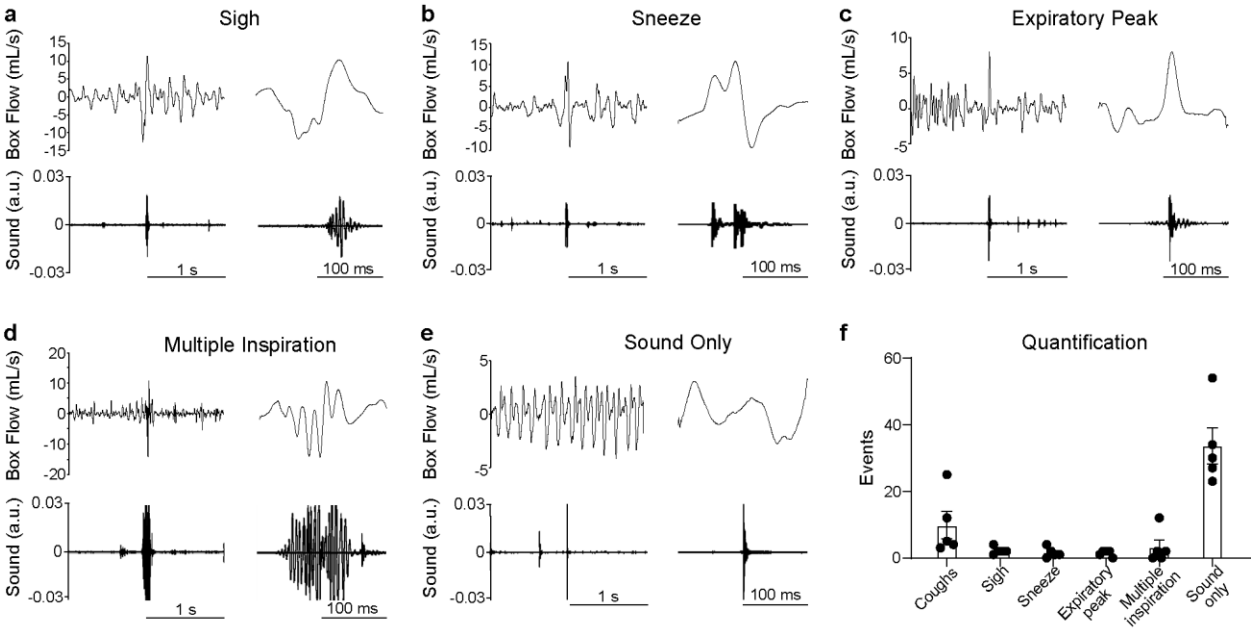

Figure 3-6 **Characterization of other behavioral events during a tussive challenge**. **a**, A sigh is characterized by a biphasic and augmented inspiration. **b**, A sneeze is defined using the linear SVM model. **c**, An expiratory peak is defined as an expiratory peak with no obvious inspiratory phase. **d**, Multiple inspiration event is characterized by multiple inspiratory peaks with continuous and loud sound signal. Note that the sound trace is cropped at 0.03. **e**, A sound only event is a regular breathing pattern with an audio signal that is greater than or equal to 0.03. Note that all these events in a-e are correlated to audio peaks comparable or greater than that of a cough-like response. **f**, Quantification of various respiratory and audio events in a 6-minute tussive challenge assay. n=5 mice. Data is presented as mean ± SEM. Please note that the vertical scale on the audio graphs displays the amplitude. a.u., arbitrary unit.

3.5 Discussion

The most used animal model in cough research is the guinea pig, and previously the cat, which have led to the advancement of cough research in both the peripheral and central neural mechanisms (Canning & Chou, 2008). Since these animal models lack the tools to precisely define the cough controlling neurons and circuits, the use of the mouse in this context is appealing due to the vast genetic tools available. Although the mouse serves as a widely used mammalian model for the study of the genetic and molecular bases of physiology and behavior, the evolutionary conservation of various respiratory defensive behaviors in mice remains inconclusive (F. Li et al., 2021; Mackenzie et al., 2004).

In this chapter, we have demonstrated that mice exhibit a cough-like behavior in response to different tussive agents and we have characterized this behavior using box flow, intrapleural pressure, video, and audio. The box flow trace observed is comparable to traces characterized as coughs in guinea pigs (Chou et al., 2018; Zhuang et al., 2019) and aligns with previously reported research that have similarly used the mouse model to elicit a cough (Chen et al., 2013; Iwata et al., 2015; Kamei, Iwamoto, Kawashima et al., 1993; C. Zhang et al., 2017). The use of mice is a departure from the status quo of currently used animal models. Such a shift will enable the characterization of the neuronal motor output and the endogenous neural cough circuit, which was previously unattainable in the guinea pig model.

The European Respiratory Society argues that sound monitoring is recommended as an essential parameter to define, recognize, and analyze cough in laboratory animals (Morice et al., 2007). While sound has been incorporated in these results, further characterization of the cough sound, and how it differs from a sneeze, will be an important addition to this work. However, sound is unreliable as it is detected in other respiratory behaviors as we show in Figure 3-6.

Therefore, we have incorporated multiple parameters, including detailed breathing traces and physiological evidence, to delineate cough and sneeze behaviors. Furthermore, we integrated hierarchical clustering and machine learning to unbiasedly differentiate between coughs and sneezes.

Depending on the stimulus, different respiratory behaviors are triggered such that each motor task is executed in a temporally and mechanically discrete manner. Since these behaviors disrupt rhythm respiration, it is likely that inhibitory neurons in the BötC are recruited to prolong post inspiration. Now that we have validated and characterized these behaviors in mice, we can utilize the tools available in them to further dissect how distinct respiratory behaviors are triggered and how neurons in the ventral respiratory column are recruited.

Chapter 3 was largely adapted from the following manuscript in review:
Gannot N., Li X., Phillips C., Ozel A., Uchima Koecklin K., Lloyd J., Zhang L., Emery K., Stern T., Li J., Li. P. A vagal- brainstem interoceptive circuit for cough- like defensive behaviors in mice. *Nature Neuroscience*.

Noam Gannot and Chrystian Phillips performed the experiments in 3-1 and 3-5. Dr. Xingyu Li, Dr. Tomer Stern and Noam Gannot performed the experiments in 3-2. Noam Gannot performed the experiments in 3-3, 3-4 and 3-6.

Chapter 4 The Role of NTS Tac1 Neurons in Cough-Like Defensive Behaviors in Mice

Since we have characterized cough-like behaviors in mice, we can now take advantage of the mouse model to identify the neurons that play a role in this behavior in mice. Although the NTS has been implicated in mediating coughing, the cellular identity of NTS neurons and how these neurons control cough remains largely unknown (Canning et al., 2006, 2014). Previously, we have shown that activating the NTS Tac1 neurons induces a cough-like response (**Figure 2-5 i-j**). In this chapter, we identify the role of these NTS Tac1 neurons in cough-like behavior in mice.

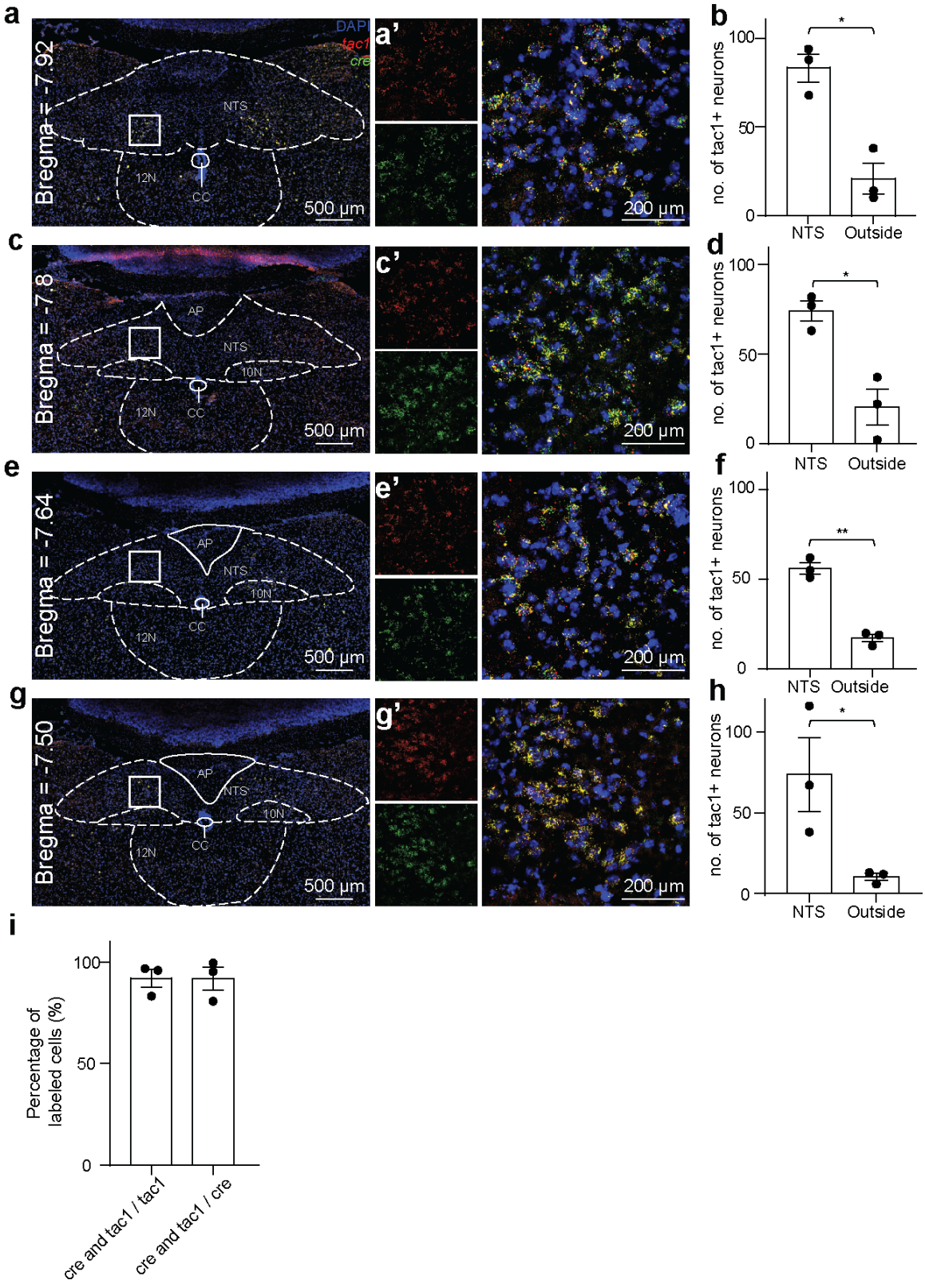

Figure 4-1 **Distribution of Tac1 neurons in the brainstem. a, c, e, g,** Multiplex single molecule in situ hybridization (RNAscope) of the NTS brain region from Tac1-Cre mice probed for *Tac1* (green) and *Cre* (red)

transcripts across different bregma levels. The box regions are enlarged and shown in a', c', e' and g'. Blue, DAPI. Bars, 500µm in a, c, e, g; 200µm in a', c', e' and g'. CC, central canal; 10N, the dorsal motor nucleus of vagus; 12N, hypoglossal nucleus; NTS, nucleus of the solitary tract. **b, d, f, h,** Quantification of the number of *Tac1* positive neurons in the NTS compared to the immediate surrounding areas (area postrema, cuneate nucleus and dorsal motor nucleus of the vagus nerve). p = 0.005, unpaired t-test (b), 0.009, unpaired t-test (d), 0.0005, unpaired t-test (f), 0.05, unpaired t-test (h); n=3 mice. **i**, The percentage of *Tac1* positive neurons that are positive for *Cre* (left), and the percentage of *Cre* positive neurons that are positive for *Tac1* (right) (n=3 mice).

Given the importance of Tac1 neurons and of Tac1-Cre recombination for interventional strategies, we first produced a map of Tac1 positive cells in the medulla including regions surrounding the NTS and show the proportion of Tac1 positive cells recapitulated by Tac1-Cre. Multiplex single molecule in situ hybridization results showed that Tac1-Cre is both specific and efficient in targeting the Tac1 neurons in the NTS (**Figure 4-1**), allowing us to use this mouse line for our characterization studies.

4.1 Optogenetically activating NTS Tac1 neurons induces a cough-like response in mice

To examine whether the behavioral response to the activation of NTS Tac1 neurons is a cough-like behavior, we combined optogenetic activation with a detailed behavioral characterization. We stereotactically injected AAV-DIO-ChR2-eYFP into the NTS of Tac1-Cre mice and implanted an optic fiber 200 microns above the injection site (**Figure 4-2 a**), allowing for cell body activation. Four weeks later, the AAV construct was specifically expressed in the NTS Tac1 neurons (**Figure 4-2 b-c**), allowing us to control them optogenetically.

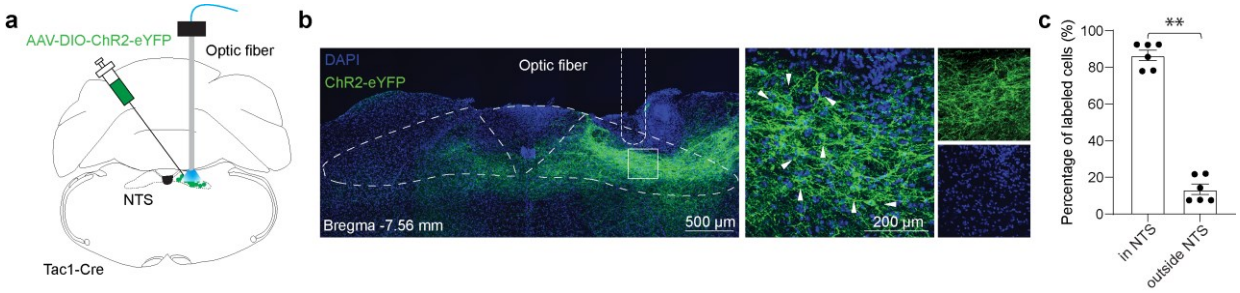

Figure 4-2 **ChR2 injection into the NTS of Tac1- Cre mice. a**, Schematic for optogenetic activation of NTS Tac1 neurons. AAV-DIO-ChR2-eYFP was stereotactically injected in the NTS of Tac1-Cre mice, and an optic fiber was implanted above the injection site. Laser was connected to activate the neurons. **b**, Brain slice showing the expression of ChR2-eYFP and optic fiber implantation in the NTS of a Tac1-Cre mouse. Bar, 500µm and 200µm (inset). **c**, Quantification of the number of ChR2-eYFP+ cells in the NTS compared to the immediate surrounding

areas (area postrema, cuneate nucleus and dorsal motor nucleus of the vagus nerve) (n=6 mice; p=0.002, Mann Whitney test).

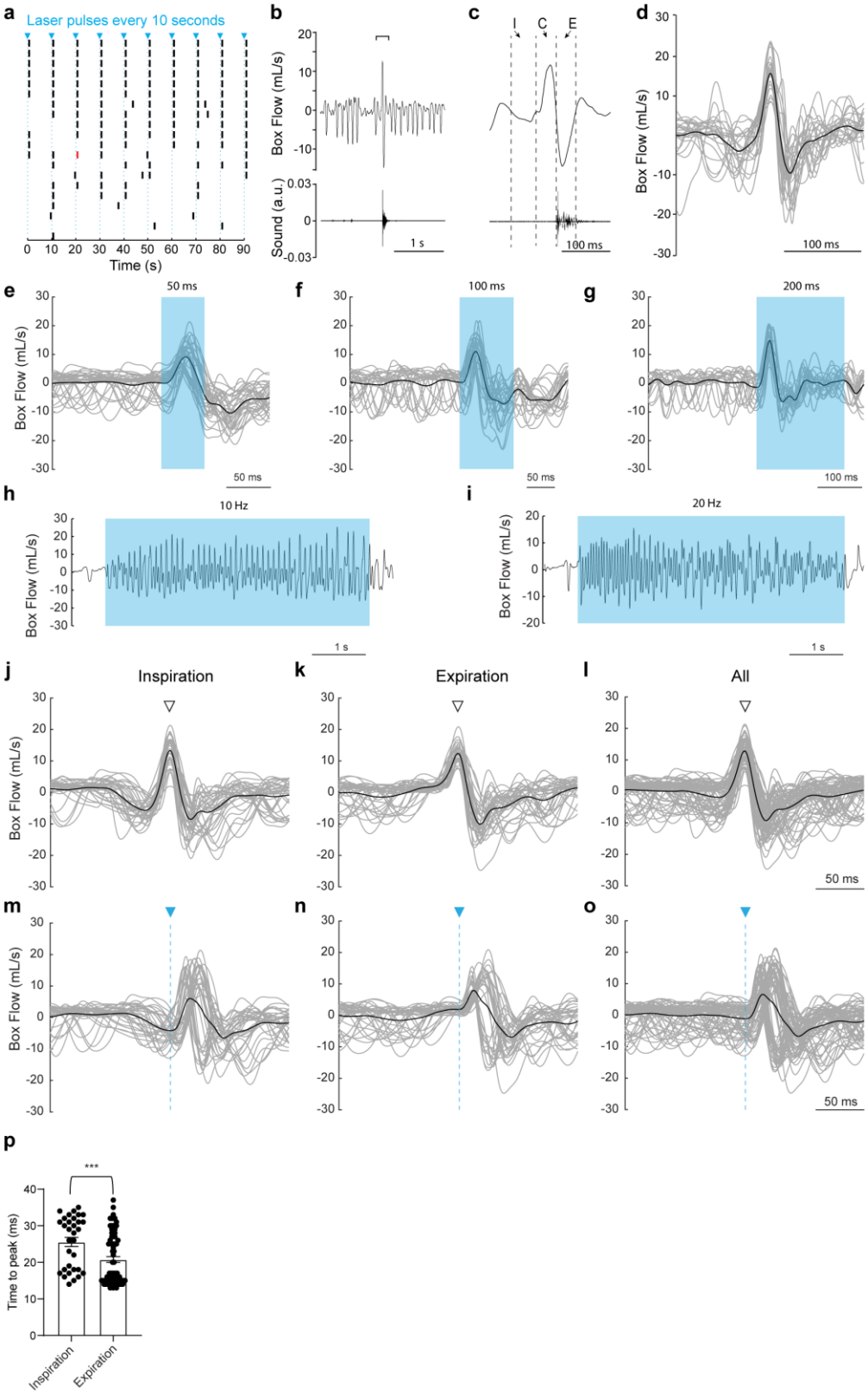

Figure 4-3 **Optogenetically activating NTS Tac1 neurons indues cough-like responses. a**, Raster plot of cough-like behaviors (tick marks) following photostimulation (blue triangle, 15ms duration per activation); respiratory trace (red tick mark) depicted in panels b and c (n=20 trials, 5 mice). **b**, Stereotyped respiratory trace (top) and corresponding audio (bottom) of a cough-like behavior upon photostimulation that phenocopy a capsaicin-evoked cough. Bar, 1 s. **c**, Magnified depiction of panel b. Bar, 100ms. **d**, Individual (gray) and average (black) traces for cough-like behaviors induced by optogenetics and aligned by the compressive peak. (n=30 events, 3 mice). Bar, 100ms. **e**, Individual (gray) and average (black) traces for cough-like behaviors induced by a 50ms laser pulse (n = 30 events, 3 mice). Bar, 50ms. Traces aligned by laser onset. Blue, laser on. **f**, Individual (gray) and average (black) traces for cough-like behaviors induced by a 100ms laser pulse (n = 30 events, 3 mice). Bar, 50ms. Traces aligned by laser onset. Blue, laser on. **g**, Individual (gray) and average (black) traces for cough-like behaviors induced by a 200ms laser pulse (n = 30 events, 3 mice). Bar, 100ms. Traces aligned by laser onset. Blue, laser on. **h**, Respiratory trace for an event induced by a 10Hz optogenetic cell body activation. Bar, 1s. Blue, laser on. **i**, Respiratory trace for an event induced by a 20Hz optogenetic cell body activation. Bar, 1s. Blue, laser on. **j**, Individual (gray) and average (black) traces for cough-like behaviors induced by a 15ms laser pulse (n = 33 events, 3 mice). Bar, 50ms. Traces aligned by compressive peaks. Laser hit during eupneic inspiration. **k**, Individual (gray) and average (black) traces for cough-like behaviors induced by a 15ms laser pulse (n = 33 events, 3 mice). Bar, 50ms. Traces aligned by compressive peaks. Laser hit during eupneic expiration. **l**, Individual (gray) and average (black) traces for all events in j and k. Traces aligned by compressive peaks. **m**, respiratory events in j, now aligned by laser onset. (n = 33 events, 3 mice). Bar, 50ms. **n**, respiratory events in k, now aligned by laser onset. (n = 33 events, 3 mice). Bar, 50ms. **o**, respiratory events in l, now aligned by laser onset. (n = 33 events, 3 mice). Bar, 50ms. **p**, Quantification of the time between laser onset to the compressive peak, when laser hits during eupneic inspiration (n = 32 events, 3 mice) or eupneic expiration (n = 79 events, 3 mice; p = 0.0002, Mann Whitney test).

Optogenetically activating these neurons using 15ms laser pulses every 10 seconds induced a behavioral response in mice reminiscent of the tussive challenge induced cough-like responses observed in chapter two, including the three distinct cough phases (**Figure 4-3 b-d**). The stereotyped responses were induced in most of the photoactivation events and occurred immediately after the laser stimulation (**Figure 4-3 a**). Similar responses were observed under various laser stimulation conditions, where a longer laser pulse induces a single event and a 10 or 20Hz frequency stimulation induces repetitive responses (**Figure 4-3 e-i**). Interestingly, a typical three phase cough-like response was triggered when the laser hit during the eupneic inspiratory phase (**Figure 4-3 j, m**). Meanwhile laser activation during eupneic expiration induced the compressive phase and expulsive phase directly (**Figure 4-3 k, n**). In summary, our findings indicate that activation during inspiration does not halt the ongoing inspiration. Conversely, activation in the eupneic expiration phase triggers the compression and expulsive phases immediately. We posit that this discrepancy may account for the differences observed in coughs

and expiratory reflexes. Furthermore, it suggests that Tac1 neurons and their downstream circuits undergo regulation influenced by the ongoing breathing cycle.

As a control for the surgery and the laser light, Tac1-Cre mice were injected with the construct AAV-Ef1a-DIO-eYFP and a fiber was implanted above the injection site. When the optic fiber was connected to a laser, there was neither a behavioral nor respiratory response (**Figure 4-4**). This is significant as it indicates that activating the NTS Tac1 neurons induces a cough-like response, not the laser.

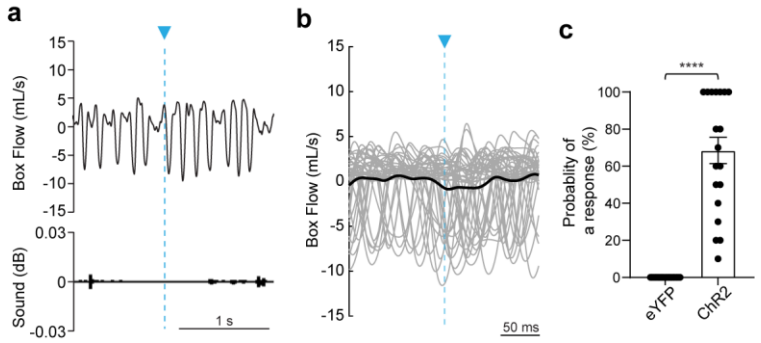

Figure 4-4 **Tac1- Cre mice injected with a control virus don't exhibit cough-like behaviors. a,** A control mouse injected with AAV-Ef1a-DIO-EYFP and implanted with an optogenetic fiber shows no respiratory nor sound response to laser stimulation. Bar, 1s. **b**, Individual (gray) and average (black) traces for behaviors induced by a 15ms pulse in control mice (n = 30 events, 3 mice). Bar, 50ms. Traces aligned by onset of laser. **c**, The probability of inducing a respiratory response in ChR2 injected mice (20 trials, 5 mice) compared to control mice (Tac1-Cre mice injected with a control eYFP AAV, 20 trials, 3 mice). $p < 0.0005$, unpaired t-test.

Next, we wanted to validate that the responses induced by optogenetic activation of Tac1 neurons are cough-like behaviors as opposed to sneezes. While both reflexes cause explosive airflow, the nasal airflow in sneezing is much greater than that in coughing. Cough can be induced by the stimulation of the superior laryngeal nerve (SLN) while a sneeze can be induced by stimulating the anterior ethmoidal nerve (AEN). The upper airway muscles were compared when fictive coughs and fictive sneezes were induced in decerebrated cats. The main difference was observed in the increased activity of the styloglossus muscle during sneezing whereas it was virtually silent during coughing (Satoh et al., 1998). The styloglossus muscle is a paired extrinsic

muscle of the tongue that causes the lateral margins of the tongue to curve upwards, as well as to retract and elevate the tongue in a posterior and superior direction (Dotiwala & Samra, 2023). The activity of the styloglossus muscle might account for the nasal airflow difference observed in sneezing in cats.

Other than the lack of activity of the styloglossus muscle, coughing is characterized by vocal cord closure due to its essential role in the cough reflex. During the inspiratory phase, the vocal cords open widely allowing additional air to pass through into the lungs. Then, the epiglottis closes off the windpipe during the compressive phase, and, simultaneously, the abdominal and rib muscles contract, thereby increasing the pressure behind the epiglottis. With the increased pressure induced by the vocal cord closure, the air is forcefully expelled once the vocal cords open, which creates a rushing sound as it moves very quickly past the now opened vocal cords during the expulsive phase of the cough (Sandhu & Kuchai, 2013).

Due to the role of the vocal cords in cough and the styloglossus muscle in sneeze, we examined vocal cord movement and muscle activity in the anesthetized mouse. When the SLN of the mouse was stimulated, the vocal cord closure was significantly increased in comparison to basal breathing (**Figure 4-5 h**), but the activity of the styloglossus muscle was unaffected as shown in the electromyograph (EMG) recording (**Figures 4-5 b-e**). In contrast, when the AEN was stimulated inducing a fictive sneeze, the styloglossus muscle activity was dramatically induced (**Figures 4-5 c-f**) with no significant change in vocal cord closure (**Figure 4-5 i**), which is reminiscent to sneezing in other species (Satoh et al., 1998; Simera et al., 2015). More importantly, the activation of Tac1 neurons induced vocal cord closure, not activation of the styloglossus muscle (**Figure 4-5a, d,** and **g**), suggesting that the induced behaviors are distinct from a sneeze. Therefore, the optogenetic activation of the NTS Tac1 neurons induces a cough-

like behavior with the three phases shown in a tussive challenge evoked cough, and similar muscle movement and vocal cord closure.

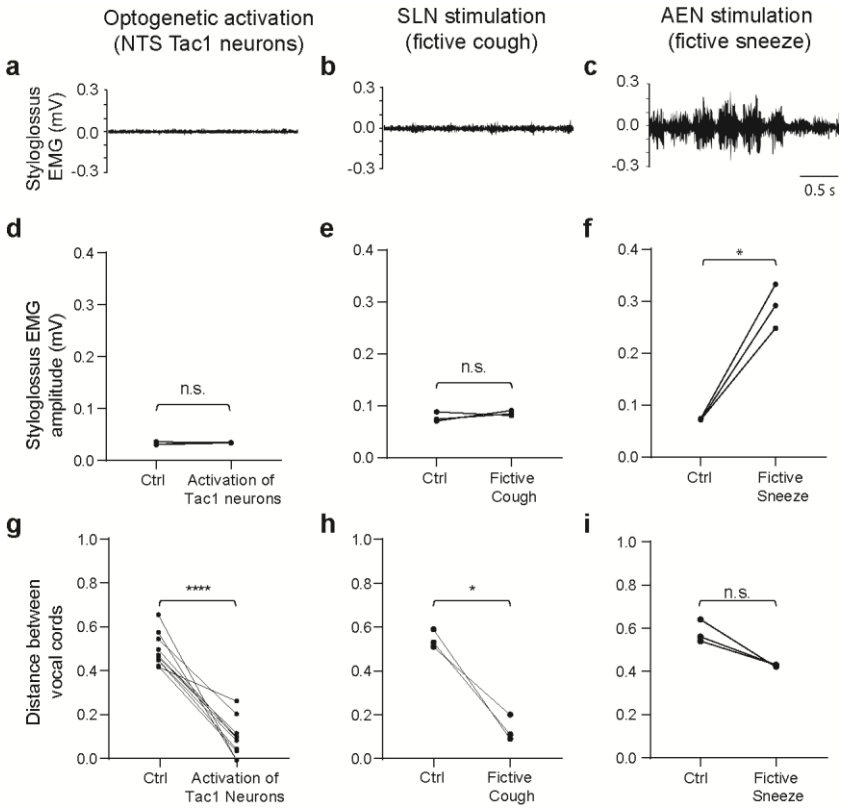

Figure 4-5 **Characterization of respiratory defensive behaviors in anesthetized mice. a**, An EMG recording of the styloglossus muscle during optogenetic activation of a cell body activation of NTS Tac1 neurons. **b**, An EMG recording of the styloglossus muscle during a stimulation of the superior laryngeal nerve (SLN), which induces a fictive cough. **c**, An EMG recording of the styloglossus muscle during a stimulation of the anterior ethmoidal nerve (AEN), which induces a fictive sneeze. **d**, Quantification of panel a of the amplitude of the styloglossus muscle EMG ($p = 0.28$, paired t-test, $n = 3$ events). **e**, Quantification of panel b of the amplitude of the styloglossus muscle EMG ($p = 0.54$, paired t-test. $n = 3$ events). **f**, Quantification of panel c of the amplitude of the styloglossus muscle EMG ($p = 0.012$, paired t-test, $n = 3$ events). **g**, Distance between vocal cords (normalized) during optogenetic stimulation of NTS Tac1 neurons compared to basal breathing (Ctrl) in the same mouse. ($n = 11$ trials; $p < 0.0001$, paired t-test). **h**, Distance between vocal cords (normalized) during SLN stimulation compared to basal breathing (Ctrl) in the same mouse. ($n = 3$ trials; $p = 0.0176$, paired t-test). **i**, Distance between vocal cords (normalized) during AEN stimulation compared to basal breathing (Ctrl) in the same mouse. ($n = 3$ trials; $p=0.25$, Wilcoxon matched-pairs signed rank test).

4.2 NTS Tac1 neurons are activated by a tussive challenge of capsaicin

While the optogenetics results are striking, they don't necessarily mimic what happens to these neurons in vivo in response to a tussive challenge. Therefore, we examined whether these neurons are naturally activated by a tussive challenge by staining the brainstem sections for the

immediate early gene c-Fos. Immediate early genes are activated transiently and rapidly in response to a wide variety of cellular stimuli. Therefore, the expression of c-Fos by individual neurons is widely used to relate cell activation to behavior (Hoffman et al., 1993).

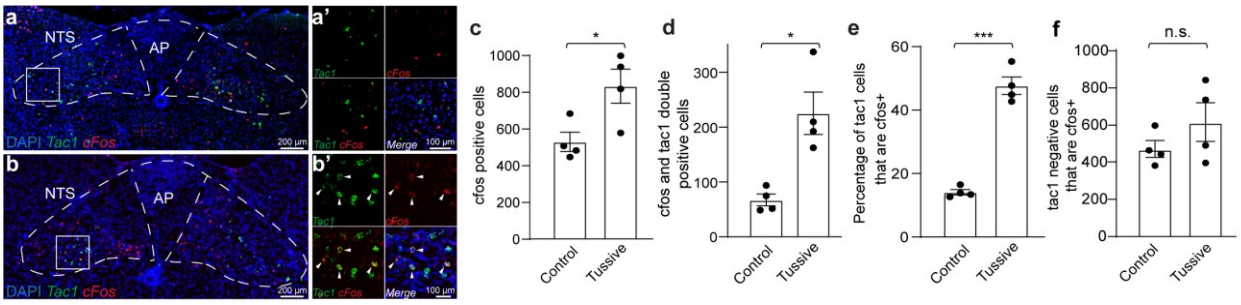

Figure 4-6 **NTS Tac1 neurons are activated by a tussive challenge**. **a**, **b**, Multiplex single molecule in situ hybridization (RNAscope) of the NTS brain region from mice under control in panel a and tussive challenge in panel b probed for *Tac1* (green) and *c-Fos* (red). The box regions are enlarged and shown in a' and b'. Blue, DAPI. Arrows, cells positive for *Tac1* and *c-Fos*. AP: area postrema. Bars, 200 µm in a and b. 100 µm in a' and b'. **c**, Quantification of the *c-Fos* positive neurons in control (n=4 mice) vs experimental (n=4 mice) mice, (p = 0.02, unpaired t-test). **d**, Quantification of *c-Fos* and *Tac1* double positive neurons in control (n=4 mice) vs experimental (n=4 mice) mice (p = 0.02, unpaired t-test). **e**, Percentage of Tac1 neurons that are c-Fos positive in control (n=4 mice) vs experimental (n=4 mice) mice (p = 0.0003, unpaired t-test). Compared to controls, experimental mice had a statistically significant increase in *c-Fos* and *Tac1* double positive cells. **f**, Quantification of *Tac1*-negative cells that are *c-Fos* positive. Please note that there is no difference between control (n=4 mice) and experimental (n=4 mice) mice (p = 0.07, unpaired t-test).

Multiplex single molecule fluorescent in situ hybridization results showed that *c-Fos* positive neurons in the NTS significantly increased after a 10-minute tussive challenge of capsaicin (**Figures 4-6 a-c**), indicating that the NTS plays a role in the tussive challenge. More importantly, our results show that the *c-Fos* and *Tac1* double positive neurons increased three-fold compared to the control (**Figure 4-6 d**), indicating that NTS Tac1 neurons were activated by the tussive challenge of capsaicin. Nearly half of the *Tac1*-positive NTS neurons are labeled by *c-Fos* (**Figure 4-6 e**). In contrast, *c-Fos* positive neurons in the *Tac1* negative NTS population did not significantly increase (**Figure 4-6 f**). Taken together, these results suggest that the NTS Tac1 neurons are preferentially activated in the NTS by a tussive challenge of capsaicin.

4.3 Loss of function studies

4.3.1 Ablation of NTS Tac1 neurons reduces the number of tussive challenge evoked cough-like behaviors in mice

To examine whether the NTS Tac1 neurons are required in mediating cough-like responses, we ablated these neurons and observed this effect on the cough-like response in mice. AAV-DIO-taCasp3 (Yang et al., 2013) was stereotactically injected into the NTS of Tac1-Cre mice. Caspase-3 is a cysteine–aspartic acid protease that cleaves cellular targets and executes apoptosis, or cell death (Ponder & Boise, 2019). Injecting Caspase-3 in a Cre dependent manner genetically ablates the Tac1 neurons (**Figure 4-7 a**). After 4 weeks, Tac1 neurons were significantly ablated in the NTS, compared to mice injected with a control virus (**Figure 4-7 b-c**). Importantly, the injection did not affect the number of Tac1 neurons in regions immediately surrounding the NTS (**Figure 4-7 d**), indicating the targeting specificity to the NTS.

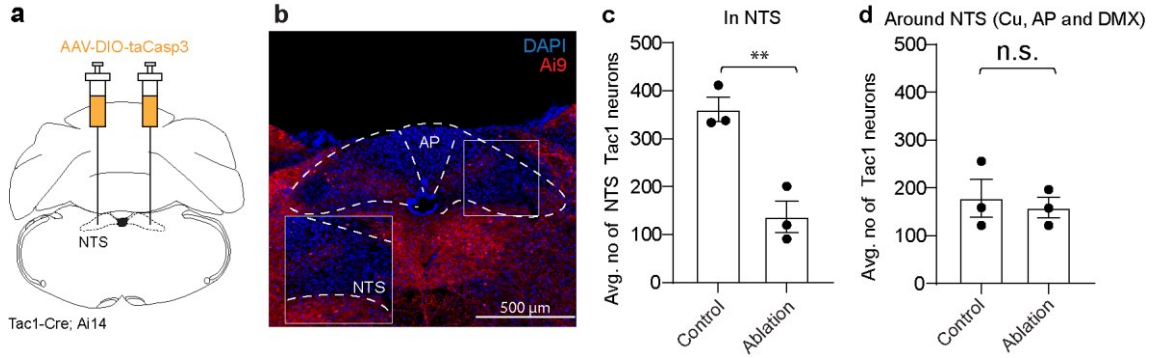

Figure 4-7 **taCasp3 injection into the NTS of Tac1- Cre mice. a**, Schematic showing the genetic ablation of Tac1 neurons by bilateral stereotactic injection of AAV-DIO-taCasp3 in the NTS of a Tac1-Cre mouse. **b**, Mouse NTS brain slice shows the absence of Ai9 neurons in the Tac1-Cre mouse after the genetic ablation. Bar, 500µm. Please note that the labeling of neurons ventral to the NTS is a result of the developmental expression of Tac1-Cre. **c**, Quantification of the number of NTS Tac1 neurons (labeled by Tac1-Cre, Ai14) in mice with (control, n=3 mice) and without (ablation, n=3 mice) ablation ($p = 0.005$, unpaired t-test). **d**, Quantification of the number of Tac1 neurons immediately around the NTS in mice with (control, n=3 mice) and without (ablation, n=3 mice) ablation ($p = 0.68$, unpaired t-test).

After ablation, mice were placed in the WBP chamber and exposed to the nebulization of the tussive agents. The cough-like responses to the aerosols of capsaicin or citric acid were

dramatically reduced in the mice after the Tac1 neurons were genetically ablated, compared to before these neurons were ablated. This trend suggests that Tac1 neurons are necessary in mediating the cough-like responses induced by tussive challenge. Mice injected with a control virus showed no significant difference in their cough-like responses to the tussive challenges (**Figure 4-8,** "Control").

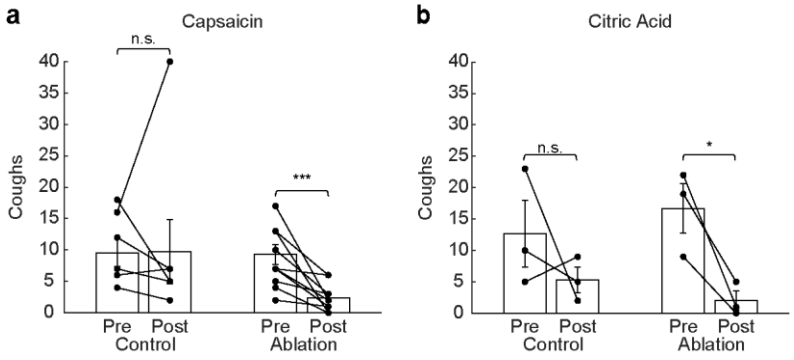

Figure 4-8 **Chronically ablating NTS Tac1 neurons reduces the number of cough-like behaviors in mice. a**, Quantification of cough-like behaviors in a 6-minute tussive challenge of capsaicin in Tac1-Cre; Ai9 fl mice with (Ablation, n=11 mice) and without (Control, n=7 mice, mice injected with a control virus) taCasp3 injection before (pre) and after (post) surgery. For control mice, p=0.3594, Wilcoxon matched-pairs signed rank test. For experimental mice, p = 0.0002, paired t-test. **b**, Quantification of cough-like behaviors in a 6-minute tussive challenge of citric acid in Tac1-Cre; Ai9 fl mice with (Ablation, n=3 mice) and without (Control, n=3 mice, mice injected with a control virus) taCasp3 injection before (pre) and after (post) surgery. For control mice, p=0.4215, paired t-test. For experimental mice, p = 0.049, paired t-test.

Importantly, the eupneic breathing and sighing in normoxia and hypoxia were not affected (**Figure 4-9**) by the ablation of the NTS Tac1 neurons. These results demonstrate that the NTS Tac1 neurons are specifically required for cough-like behaviors in mice and not other respiratory behaviors.

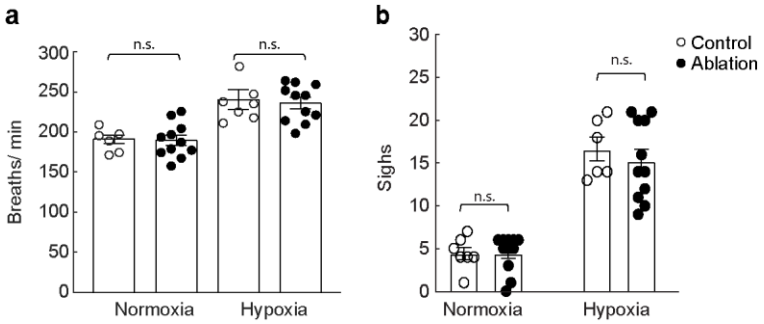

Figure 4-9 **Chronically ablating NTS Tac1 neurons has no effect on other respiratory behaviors. a**, Respiratory rate of animals with the ablation of NTS Tac1 neurons (Ablation, n=11 mice) and control animals (Control, n=7 mice) in normoxia (21% O2 balanced by N2) and hypoxia (10% O2 balanced by N2). For normoxia, p=0.86, unpaired t-test. For hypoxia, p=0.92, Mann Whitney test. **b**, Sigh rate in normoxia (p = 0.75, Mann Whitney test) and hypoxia (p = 0.31, Mann Whitney test) conditions in mice with (Ablation, n=11 mice) and without (Control, n=6 mice) ablation of Tac1 neurons.

4.3.2 Chemogenetic silencing of NTS Tac1 neurons reduces the number of tussive challenge evoked cough-like behaviors in mice

Next, we acutely silenced these NTS Tac1 neurons using chemogenetics. Chemogenetics allows for the reversible modulation of cell populations and neural circuitry by systemically injecting an activating ligand. Here, we used Designer Receptors Exclusively Activated by Designer Drugs (DREADD)-based chemogenetics. DREADDs are muscarinic receptors that have been genetically engineered to be activated by clozapine N-oxide (CNO), a synthetic drug, which acts as a chemical actuator, that was not previously recognized by these proteins (Manvich et al., 2018; Roth, 2016). Here, we used hM4Di, a genetically engineered human M4 muscarinic receptor that signals through the Gαi/o G-protein pathways and inhibits neuronal signaling. Gi signaling in neurons opens potassium channels resulting in an influx of potassium ions that decreases the resting membrane potential of neurons and their capacity to depolarize (Armbruster et al., 2007). Therefore, neurons expressing hM4Di treated with CNO are observed to have dramatically decreased firing rates and therefore acutely silenced.

The AAV vector AAV-DIO-hM4Di-mCherry (Krashes et al., 2011) was stereotactically injected into the NTS of Tac1-Cre mice. Following Cre-mediated recombination, the hM4Di receptor is expressed in Tac1 neurons (**Figure 4-10 a-b**), with approximately 80 % located in the NTS (**Figure 4-10 c-d**). Importantly, no labeling was observed in the vagal ganglia (**Figure 4-10 e**).

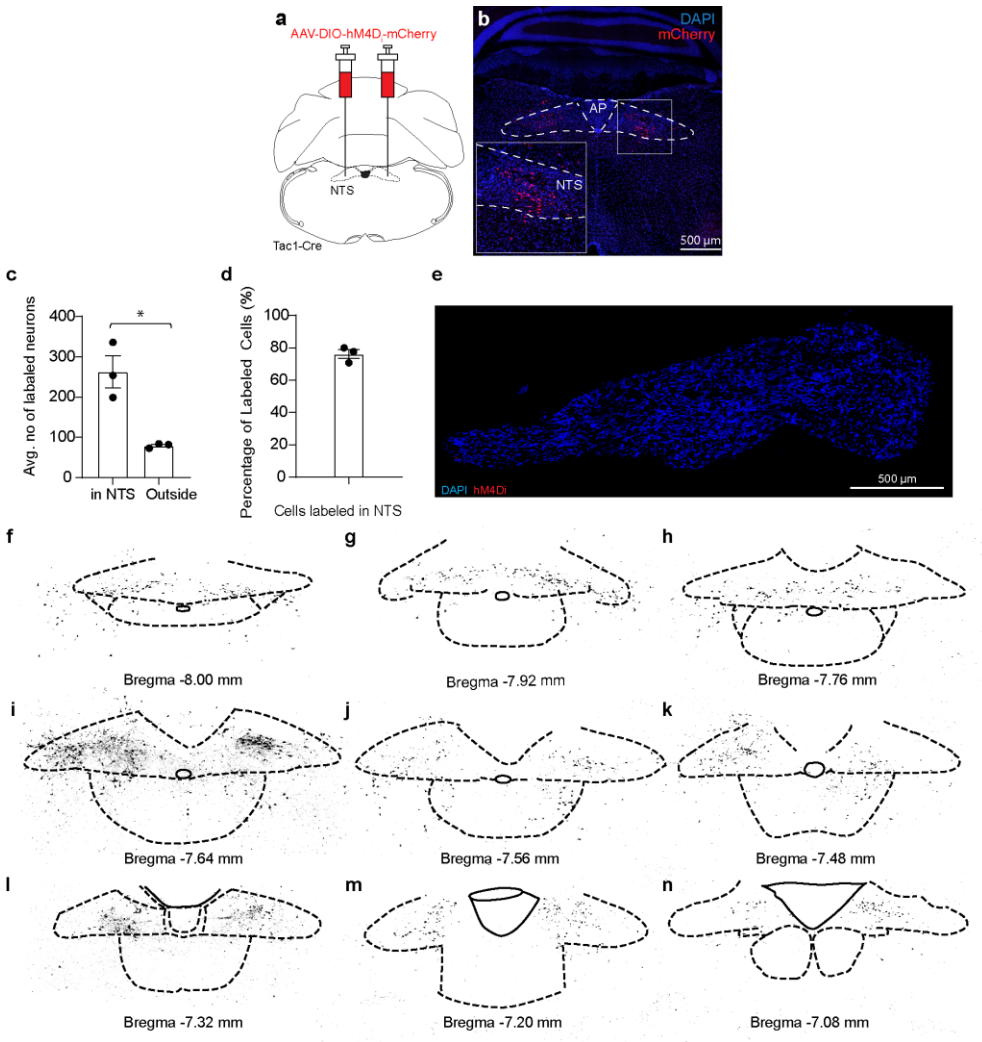

Figure 4-10 **hM4di injection into the NTS of Tac1- Cre mice. a**, Schematic showing the hM4Di expression in Tac1 neurons by bilateral stereotactic injection of AAV-DIO-hM4Di-mCherry in the NTS of a Tac1-Cre mouse. **b**, Mouse NTS brain slice shows the expression of hM4Di-mCherry in the Tac1-Cre mouse. Bar, 500µm. **c**, Quantification of the labeled neurons inside (in NTS) and outside (Outside) of the NTS in mice injected with hM4Di into the NTS (n=3 mice; p = 0.01, unpaired t-test). **d**, The percentage of all labeled cells that are in the NTS of Tac1-Cre mice injected with hM4Di (n=3 mice). **e**, Confocal image of the vagal ganglia of Tac1-Cre mice that was injected with hM4Di into the NTS. Injection into the NTS does not lead to cell labeling in the ganglia. Bar, 500µm. **f-n**, Distribution of hM4Di labeled neurons (black) of a Tac1-Cre mouse throughout different bregma levels. Please note that these images were all taken from the same mouse, while the quantifications in panels c and d were done in three mice.

Upon systemic administration of CNO (1 mg/kg body weight), Tac1-Cre mice exhibited a significant reduction in their cough-like behavior induced by tussive challenges of different reagents compared to a saline injection (**Figure 4-11**). On the other hand, no effect of CNO was observed in animals injected with a control vector AAV-DIO-mCherry. These findings indicate

that NTS Tac1 neurons are necessary for chemically and mechanically induced cough-like responses in mice and that a CNO injection has no effect on the cough-like behavior in mice.

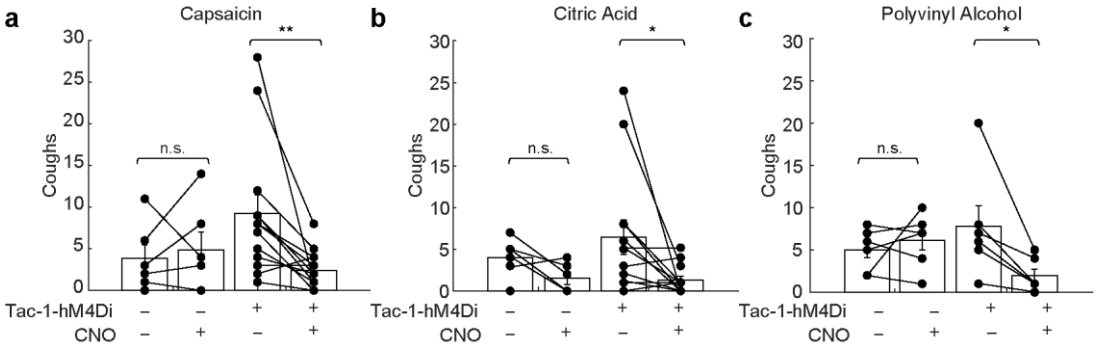

Figure 4-11 **Acutely silencing NTS Tac1 neurons reduces the number of cough-like behaviors in mice**. **a**, Quantification of cough-like behaviors in a 6-minute tussive challenge of capsaicin in mice with (+, n=13 mice) and without (-, n=6 mice, Tac1-Cre mice injected with AAV-DIO-mCherry) hM4Di expression in Tac-1 neurons (Tac1-hM4Di) treated with (+) and without (-, vehicle only) CNO injection. For control mice, p=0.65, paired t-test. For experimental mice, p=0.002, Wilcoxon matched pairs signed rank test. **b**, Quantification of cough-like behaviors in a 6-minute tussive challenge of citric acid in mice with (+, n=13 mice) and without (-, n=6 mice, Tac1-Cre mice injected with AAV-DIO-mCherry) hM4Di expression in Tac-1 neurons (Tac1-hM4Di) treated with (+) and without (-, vehicle only) CNO injection. For control mice, p=0.06, paired t-test. For experimental mice, p=0.015, Wilcoxon matched pairs signed rank test. **c**, Quantification of cough-like behaviors in a 10-minute tussive challenge of polyvinyl alcohol in mice with (+, n=6 mice) and without (-, n=6 mice, Tac1-Cre mice injected with AAV-DIO-mCherry) hM4Di expression in Tac-1 neurons (Tac1-hM4Di) treated with (+) and without (-, vehicle only) CNO injection. For control mice, p=0.47, paired t-test. For experimental mice, p=0.03, paired t-test.

In contrast, other breathing phenotypes, including eupneic breathing, sneezing, sighing, and hypoxia respiratory responses, were not affected by the silencing of NTS Tac1 neurons (**Figure 4-12**). As demonstrated in the chronic ablation condition, acute silencing of NTS Tac1 neurons significantly reduces the number of tussive agent induced cough-like events and did not affect other respiratory responses.

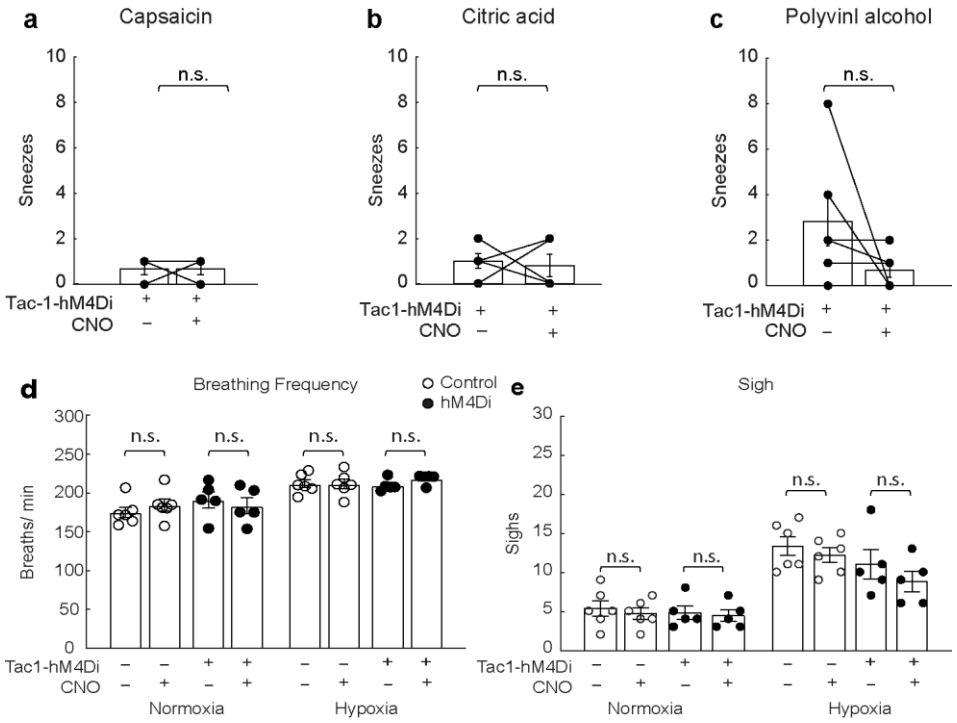

Figure 4-12 **Acutely silencing NTS Tac1 neurons has no effect on other respiratory behaviors. a**, Quantification of sneeze-like behaviors in a 6-minute tussive challenge of capsaicin in mice with hM4Di expression in Tac1 neurons (Tac1-hM4Di) treated with (+) and without (-, vehicle only) CNO injection (n=5 mice, p>0.9999, Wilcoxon matched-pairs signed rank test). **b**, Sneeze-like behaviors in a 6-minute tussive challenge of citric acid in mice with hM4Di expressed in NTS Tac1 neurons treated with (+) and without (-, vehicle only) CNO injection (n=4 mice; p>0.9999, Wilcoxon matched-pairs signed rank test). **c**, Sneeze-like behaviors in a 10-minute challenge of an intranasal injection of 20% polyvinyl alcohol in mice with hM4Di expressed in NTS Tac1 neurons treated with (+) and without (-, vehicle only) CNO injection (n=6 mice; p = 0.16, paired t-test). **d**, Breathing frequency in normoxia and hypoxia conditions in mice with (+, n=5 mice, not significant) and without (-, n = 6, Tac1-Cre mice injected with AAV-DIO-mCherry) hM4Di expression in Tac1 neurons (Tac1-hM4Di) treated with (+) and without (-, vehicle only) CNO injection. For control mice, p = 0.39, paired t-test (normoxia) and p = 0.80, paired t-test (hypoxia); for experimental mice, p = 0.60, paired t-test (normoxia) and p = 0.12, Wilcoxon matched-pairs signed rank test (hypoxia). **e**, Sigh rate in normoxia and hypoxia conditions in mice with (+, n=5 mice) and without (-, n=6 mice, Tac1-Cre mice injected with AAV-DIO-mCherry) hM4Di expression in Tac1 neurons (Tac1-hM4Di) treated with (+) and without (-, vehicle only) CNO injection. For control mice, p = 0.50, paired t-test in normoxia and p = 0.42 in hypoxia, paired t-test; for experimental mice, p = 0.54 in normoxia, paired t-test, and p = 0.13, paired t-test in hypoxia.

4.4 Glutamate release by Tac1 neurons is required for cough-like responses

The tachykinin 1 gene encodes several neuropeptides, including substance P (SP) and neurokinin A (NKA), as well as the NH_2-terminally extended forms of NKA, neuropeptide K (NPK) and neuropeptide γ (NPγ) (Steinhoff et al., 2014). Of these neuropeptides, SP and its receptor NK1R have been implicated in controlling cough with contradicting results. The exposure of guinea pigs to SP prior to a citric acid tussive challenge did not result in a significant

increase in citric acid-induced coughs (El-Hashim & Amine, 2005). In humans, aerosols of SP did not cause cough in normal subjects whereas it did in patients with common colds (Sekizawa et al., 1996). Increased levels of SP in plasma are associated with persistent cough in humans and might be related to airway sensitivity in asthmatic cough (Otsuka et al., 2011). SP was shown to be an endogenous substance causing cough in awake guinea pigs and the SP antagonist is a useful tool for treatment of cough in respiratory disease (Ujie et al., 1993). Furthermore, SP has been implicated in influencing coughing through central or peripheral pathways (Mazzone et al., 2005; Mutolo et al., 2007). Therefore, the contribution of these neuropeptides and fast neurotransmitters in cough remains inconclusive. With the cough-like behavior established here, we utilized mouse genetics to address this question.

We first conditionally deleted the vesicular glutamate transporter 2 (Vglut2), an essential gene for glutamate transportation, in all Tac1 neurons, by crossing Tac1-Cre to Vglut2 flox allele. We found that Tac1-Cre, Vglut2 fl/fl mice do not cough in response to the nebulized capsaicin (0 ± 0 times per 6 minutes), compared to their littermate controls that coughed 12.79 ± 9.6 times per 6 minutes (**Figure 4-13 a**). These results suggest that the release of glutamate is essential for mediating cough-like behaviors in mice.

To test the role of tachykinin neuropeptides in mediating cough-like behaviors, we exposed the Tac1-/- mice to the tussive challenge. In these mice the Tac1 gene and its encoded neuropeptides are genetically deleted (Cao et al., 1998). Surprisingly, these mice do not exhibit a significant attenuation in their cough-like responses to capsaicin, and they cough 6.9 ± 3.4 times per 6 minutes in comparison to their littermates that coughed 9.2 ± 7.8 per 6 minutes (**Figure 4-13 b**). We thus conclude that glutamate, not tachykinin 1 neuropeptides, is required for cough-like behaviors in mice.

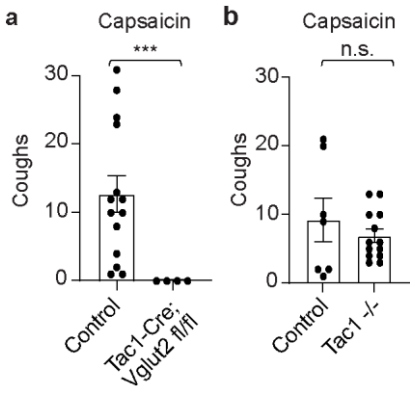

Figure 4-13 **Glutamate release mediates cough-like behaviors in mice. a**, Quantification of cough-like behaviors in a 6-minute capsaicin challenge of Tac1-Cre, Vglut2 fl/fl mice (n = 4 mice) and their littermate controls (n=14 mice) (p = 0.0007, Mann Whitney test). **b**, Quantification of cough-like behaviors in a 6-minute capsaicin challenge of Tac1 -/- (n=13 mice) and their littermate controls (n=7 mice; p = 0.50, unpaired t-test).

4.5 Discussion

The peptides of the tachykinin family are widely distributed within the mammalian peripheral and central nervous systems and play as excitatory neurotransmitters in diverse contexts (Pennefather et al., 2004). In the nucleus accumbens, Tac1 neurons regulate avoidance responses to aversive stimuli (He et al., 2023). Tac1 neurons in the parabrachial nucleus are activated by noxious stimuli and trigger robust escape responses to heat via connections to the reticular formation (Barik et al., 2018). Tac1 neurons have also been linked to respiratory behaviors. For example, preBötC Tac1 neurons play a role in the generation of rhythmic breathing and parabrachial Tac1 expressing neurons are involved in state-dependent breathing control (Arthurs et al., 2023; Rousseau et al., 2023). The role of NTS Tac1 neurons in defensive respiratory behaviors, such as cough, has not been identified.

The NTS has been reported as a subnuclei critical for coughing (Canning, 2009; Canning & Mori, 2010; Davenport & Vovk, 2009; McGovern et al., 2012; Ohi et al., 2005). However, the NTS neurons that are in receipt of cough-specific airway sensory inputs have not been described (Monica et al., 2014) since doing so was unattainable in the previously used animal models in

cough research. In the previous chapter, we characterized and validated the cough-like behavior in mice. Therefore, we can utilize the genetic tools available in mice to identify cough-controlling neurons.

In this chapter, we have demonstrated that NTS Tac1 neurons play an essential role in cough-like behaviors in mice. Specifically, these neurons are activated by a tussive challenge, as shown by the multiplex single molecule fluorescent in situ hybridization results. Furthermore, optogentic activation of these neurons is sufficient in inducing cough-like behaviors in mice and we have shown that this behavior is distinct from that of a sneeze-like behavior. These neurons are also necessary for the cough-like response in mice. The genetic ablation or chemogenetic silencing of the NTS Tac1 neurons attenuates the cough-like response. Importantly, the ablation and silencing of these neurons has no effect on other respiratory responses. Finally, our results in this chapter also show that these cough-like behaviors are mediated by glutamate release and not the Tac1 neuropeptides. By doing so, we have identified the first genetically defined neurons that play a role in cough-like defensive behaviors in mice.

Chapter 4 was largely adapted from the following manuscript in review:
Gannot N., Li X., Phillips C., Ozel A., Uchima Koecklin K., Lloyd J., Zhang L., Emery K., Stern T., Li J., Li. P. A vagal- brainstem interoceptive circuit for cough-like defensive behaviors in mice. *Nature Neuroscience*.

Noam Gannot performed the experiments in 4-1, 4-2, 4-4, 4-6, 4-7, 4-10 and 4-13. Noam Gannot and Chrystian Phillips performed the experiments in 4-3. Dr. Karin Harumi Uchima Koecklin performed the experiments in 4-5. Noam Gannot, Katie Emery and Chrystian Phillips performed the experiments in 4-8, 4-11 and 4-12. Katie Emery and Chrystian Phillips performed the experiments in 4-9.

Chapter 5 NTS Tac1 Neurons Directly Innervate Downstream Regions to Control Cough-Like Behaviors in Mice

In the previous chapter, we showed that the NTS Tac1 neurons play an essential role in cough-like behaviors in mice. Therefore, we want to trace their downstream targets to figure out how they control this cough-like behavior. Because activation of NTS Tac1 neurons is sufficient in inducing cough-like responses, these neurons could function as a relay node, transmitting tussive sensory inputs to the brain, or a part of the cough central pattern generator, thereby controlling the phases and timing of a cough.

5.1 The projection patterns of NTS Tac1 neurons

Initially, we mapped the projection pattern of the NTS Tac1 neurons by injecting an AAV vector encoding a membrane GFP and a synaptophysin-mRuby to label the presynaptic terminals (AAV-hsyn-FLEX-mGFP-2A-Synaptophysin-mRuby) into the NTS of Tac1-Cre mice (**Figure 5-1 a-c**). Four weeks later, we observed the projections and presynaptic terminals of Tac1 neurons in the ventral respiratory column where the key cough-controlling neurons are located (Bolser & Davenport, 2002; Canning et al., 2014) (**Figure 5-1 d**). Our results further validated that these NTS Tac1 neurons play a role in the cough-like behavior in mice.

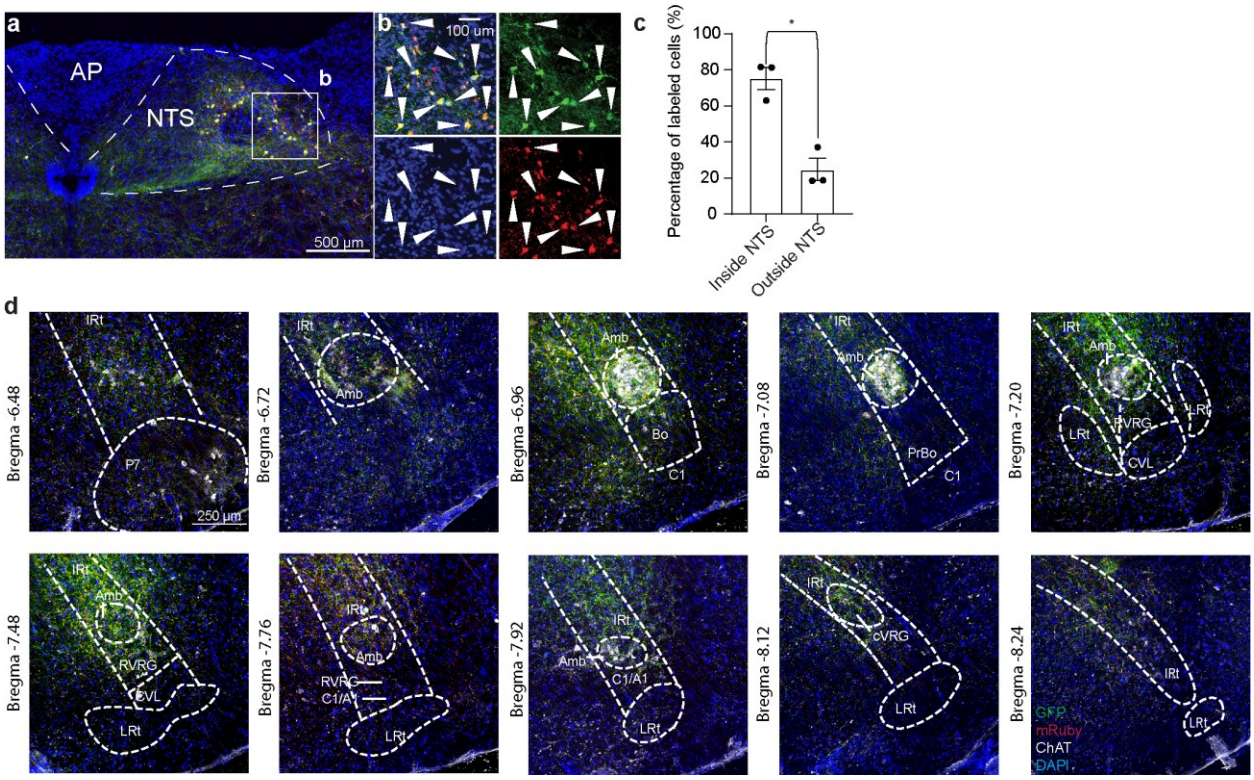

Figure 5-1 **Anterograde tracing of NTS Tac1 neurons in the ventral respiratory column**. **a**, Confocal image of a mouse NTS that was unilaterally injected with AAV-hSyn-FLEX-MGFP-2A-Synaptophysin-mRuby. Bar, 500µm. **b**, Enlarged image of NTS from a showing the labeling of NTS neurons. Arrow heads, the labeled cell bodies of NTS neurons. Bar, 100µm. **c**, Quantification of the percentage of labeled cells inside the NTS compared to those outside the NTS. (n = 3 mice; p = 0.04, Mann Whitney test). **d**, Anterograde tracing of NTS Tac1 neuron processes (green) and presynaptic terminals (red) across different bregma levels of the ventral respiratory column Bar, 250µm. ChAT (gray) labels the motor neurons.

Particularly, robust innervation was seen in and around the nucleus ambiguus (NA) (**Figure 5-2 a-b**; referred to as para-NA thereafter), where the motor nucleus controls the glottis and the respiratory control neurons are located. During the compressive phase of the cough and expiratory reflex, there is a brief closure of the glottis to maintain lung volume (A. B. Chang, 2006). The motor neurons of the NA provide efferent motor innervation to the ipsilateral muscles of the larynx. The larynx is a cartilaginous segment of the respiratory tract located in the anterior aspect of the neck that contains the vocal cords (Suárez-Quintanilla et al., 2023).

Robust innervation was also observed in the caudal ventral respiratory group (cVRG) (**Figure 5-2 c-d**), where the premotor neurons to the expiratory muscles are located. The cVRG

contains expiratory-modulated neurons that activate motoneurons in the thoracic and lumbar spinal cord, innervating the muscles of expiration (Saji & Miura, 1990). During both the expulsive phase of the cough and expiratory reflex, the expiratory muscles are activated (Bolser et al., 2000; Rhee et al., 2016; Schreiber et al., 2021).

The results in this section indicate that the NTS Tac1 neurons project to regions that play a crucial role in multiple phases of the cough and expiratory reflexes. While these results are promising, it does not indicate whether these projections are functional.

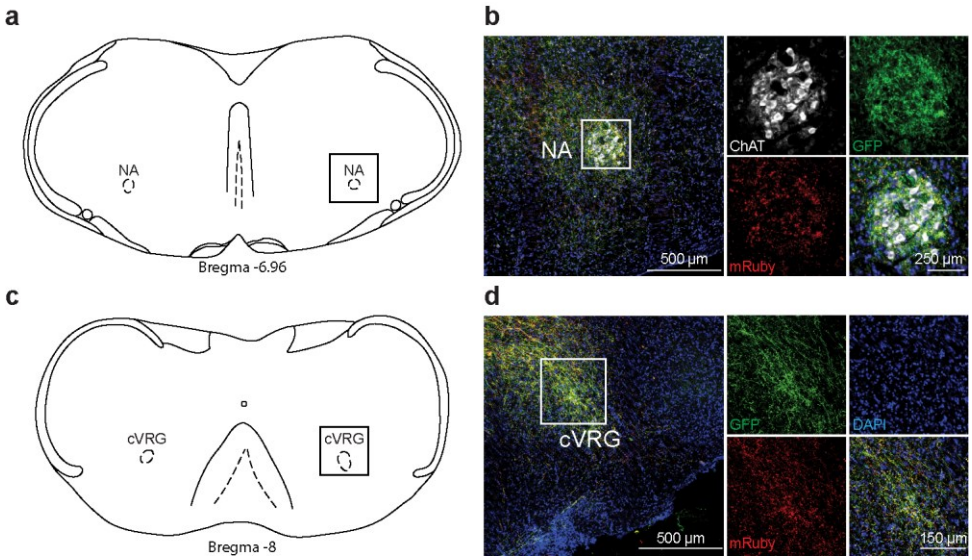

Figure 5-2 **NTS Tac1 neurons project to regions important in coughing**. **a**, Schematic showing the location of the nucleus ambiguous (NA) in the bregma level -6.96. The boxed region is shown in panel b. **b**, Mouse brainstem slice showing innervation of Tac1 neuron processes (green) and presynaptic terminals (red) in the ipsilateral NA region. ChAT labels the motor neurons in the NA. Bars, 500µm and 250µm. **c**, Schematic showing the location of the caudal ventral respiratory group (cVRG) in the bregma level -8. The boxed region is shown in panel d. **d**, Mouse brainstem slice showing innervation of Tac1 neuron processes (green) and presynaptic terminals (red) in the ipsilateral cVRG region. Bars, 500µm and 150µm.

5.2 Optogenetically activating NTS Tac1 neuronal projections induced diverse breathing patterns

To assess the functions of these NTS Tac1 projections, we again used optogenetics. The AAV vector encoding ChR2 was injected into the NTS of Tac1-Cre mice. Contrary to the cell

body activation, an optic fiber was implanted above either the para-NA or the cVRG to activate these terminals, respectively (**Figures 5-3 a-b, 5-4 a-b**).

We optogenetically activated the NTS Tac1 terminals into the para-NA using a 15ms laser pulse -- the same condition used for the cell body activations. Doing so, induced a respiratory pattern with a compressive phase found in both coughs and expiratory reflexes, but with a reduced expulsive phase (**Figures 5-3 c-f**). Similar responses were observed under various laser stimulation conditions (**Figures 5-3 g-i**).

The NA coordinates the motor responses required for functions like swallowing, respiration, speech, and reflexive responses (Godson Akunna & Ed, 2023). These results indicate that the NTS Tac1 neurons send sensory input to the NA to coordinate the cough response. However, the induced respiratory trace observed here differs from that of a cell body activated cough observed in the previous chapter and a tussive challenge evoked cough, observed in chapter three. These results indicate that the terminal projections into the para-NA are only responsible for a partial cough response and other regions seem to be necessary for the integrated cough response.

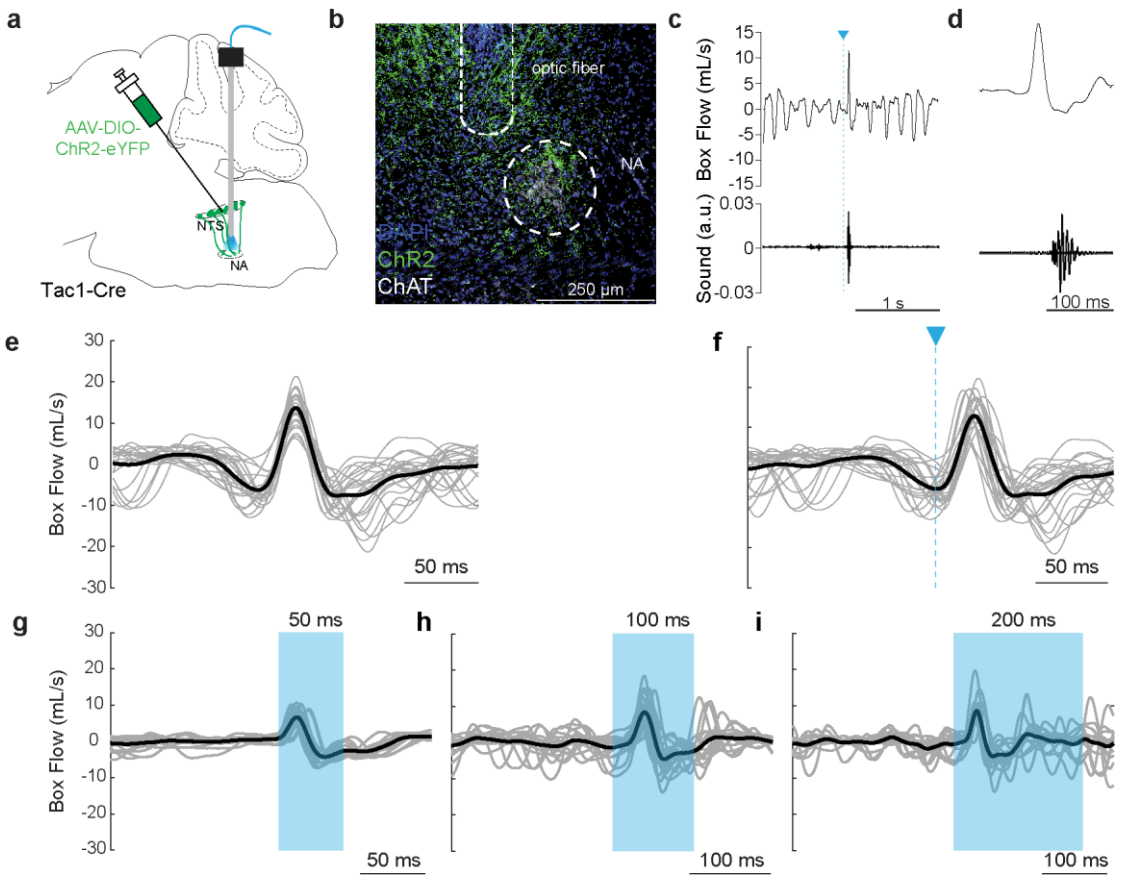

Figure 5-3 **Optogenetically activating the NTS Tac1 projections into NA induces a distinct respiratory response**. **a**, Schematic for optogenetic activation of NTS Tac1 neuronal projection into the para-NA region. AAV-DIO-ChR2-eYFP was stereotactically injected in the NTS of Tac1-Cre mice, and an optic fiber was implanted above the ipsilateral para-NA. Laser was connected to activate the projections. **b,** Brain slice showing the expression of ChR2-eYFP and optic fiber implantation in the NA of a Tac1-Cre mouse for NA terminal optogenetics activation. Bar, 250μm **c**, Stereotyped respiratory trace (top) of a breathing trace upon a 15ms photostimulation of Tac1 neuron processes to the para-NA region. Bar, 1s. **d**, Magnified depiction of panel c. Bar, 100ms. **e**, Individual (gray) and average (black) traces for 15ms NA terminal activations (n=25 trials, 3 mice). Traces aligned by compressive peak. Bar, 50ms. **f**, Respiratory traces from e, now aligned by laser onset. Bar, 50ms. **g**, Individual (gray) and average (black) traces for 50ms NA terminal activations (n=30 events, 3 mice). Bar, 5 ms. Traces aligned by laser onset. Blue, laser on. **h**, Individual (gray) and average (black) traces for 100ms NA terminal activations (n=30 events, 3 mice). Bar, 100ms. Traces aligned by laser onset. Blue, laser on. **i**, Individual (gray) and average (black) traces for 200ms NA terminal activations (n=30 events, 3 mice). Bar, 100ms. Traces aligned by laser onset. Blue, laser on.

In contrast, a 15ms photoactivation of cVRG terminals induced only an expiratory peak, which was not observed in the para-NA terminal activation (**Figure 5-4 c-d**). The observed behavior has a longer latency and higher probability than para-NA activation (**Figure 5-4 j-k**). Similar responses were observed under various laser stimulation conditions (**Figure 5-4 g-i**).

The cVRG is involved in behaviors that involve expiratory prolongation (Holstege, 1989; Poliacek et al., 2007; Umezaki et al., 1997). The results observed here indicate that the NTS Tac1 neurons coordinate the recruitment of cVRG neurons for the cough-like response. As observed in the para-NA terminal results, the induced respiratory trace observed here differs from that of a cell body activated cough-like response observed in the previous chapter and a tussive challenge evoked cough, observed in chapter three. Furthermore, this response differs from the response observed in the activation of the para-NA terminals. These results highlight that the terminal projections into the cVRG are only responsible for a partial cough response and this response differs from the projections into the para-NA region.

As a control for the fiber implantation surgery and to ensure that the fiber implantation in the cVRG region did not cause any circuit damage, mice underwent a capsaicin tussive challenge prior to the implantation and four weeks after surgery -- enough time for the virus to express. There was no significant difference in the respiratory responses of these mice. This result rules out the potential circuit damage caused by fiber implantation (**Figure 5-4 l**) and suggests the observed result was not due to the fiber implantation.

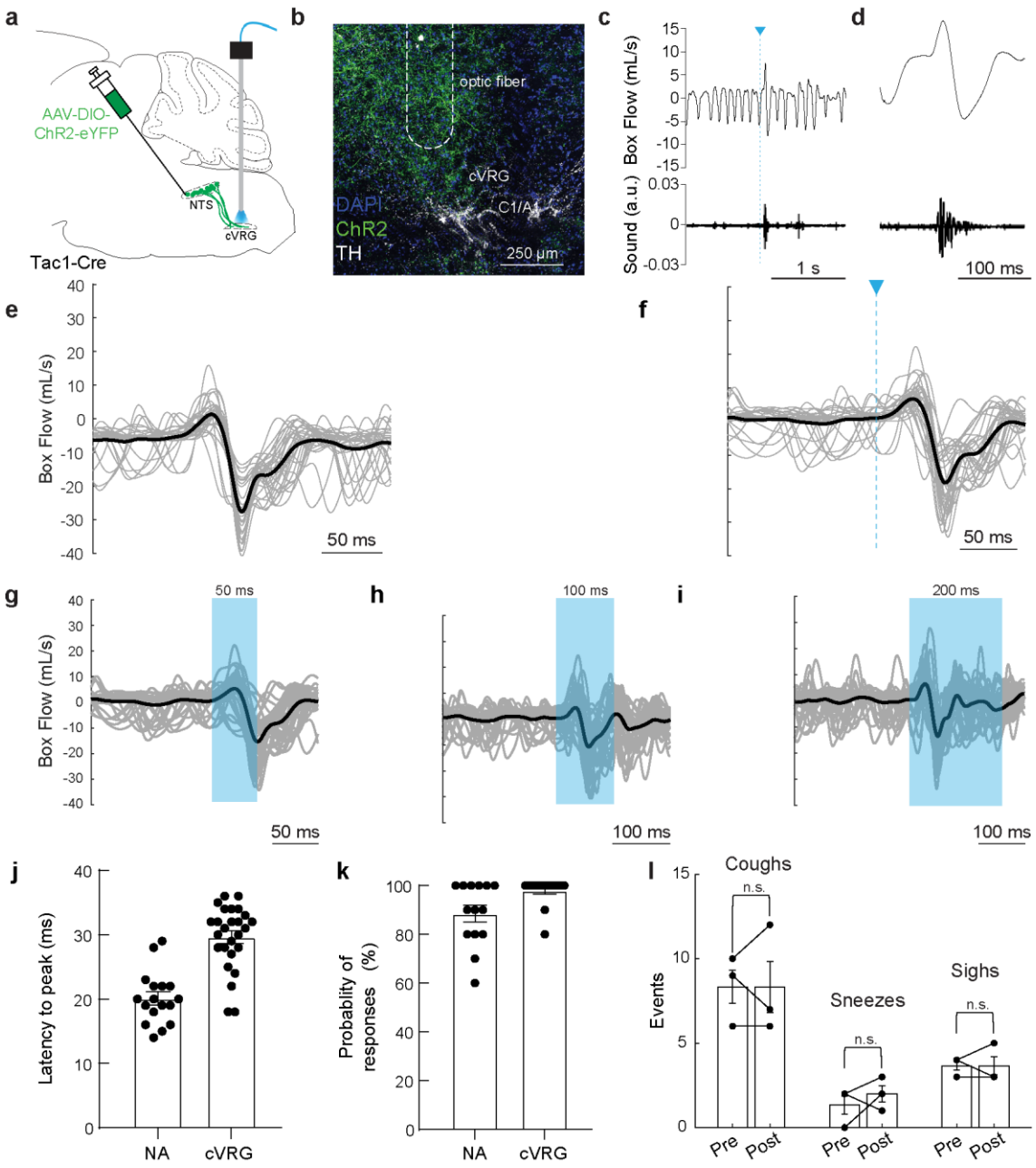

Figure 5-4 **Optogenetically activating the NTS Tac1 projections into NA induces a distinct respiratory response**. **a**, Schematic for optogenetic activation of NTS Tac1 neuronal projection into the ipsilateral cVRG region. AAV-DIO-ChR2-eYFP was stereotactically injected in the NTS of Tac1-Cre mice, and an optic fiber was implanted above the ipsilateral cVRG. Laser was connected to activate the projections. **b**, Brain slice showing the expression of ChR2-eYFP and optic fiber implantation in the cVRG of a Tac1-Cre mouse for cVRG terminal optogenetics activation. Bar, 250 µm. **c**, Stereotyped respiratory trace (top) of a breathing trace upon a 15ms photostimulation of Tac1 neuron processes to the cVRG region. Bar, 1s. **d**, Magnified depiction of panel c. Bar, 100ms. Please note that the upwards peak here is an expiration without compression. **e**, Individual (gray) and average (black) traces for cVRG terminal activations (n=25 trials, 3 mice). Traces aligned by downards peak. Bar, 50ms. **f**, Respiratory traces from e, now aligned by laser onset. Bar, 50ms. **g**, Individual (gray) and average (black) traces for 50ms cVRG terminal activations (n=40 events, 3 mice). Bar, 50ms. Traces aligned by laser onset. Blue, laser on. **h**, Individual (gray) and average (black) traces for 100ms cVRG terminal activations (n=40 events, 3 mice). Bar, 100ms. Traces aligned by laser onset. Blue, laser on. **i**, Individual (gray) and average (black) traces for 200ms cVRG terminal

activations (n=40 events, 3 mice). Bar, 100ms. Traces aligned by laser onset. Blue, laser on. **j**, Quantification of the time between laser onset to the initial upward peak, for NA terminal activations (n=17 events, 3 mice) and cVRG terminal activations (n=26 events, 3 mice). **k**, the probability of inducing a respiratory response in ChR2 injected mice for NA terminal activations (n=14 events, 3 mice) and cVRG terminal activations (n = 15 events, 3 mice). **l**, Quantification of the number of cough-like events ($p = 1$, paired t-test), sneeze-like events ($p = 0.75$, Wilcoxon matched-pairs signed rank test) and sighs ($p>0.9999$, Wilcoxon matched-pairs signed rank test) of mice injected with AAV-DIO-ChR2-eYFP in the cVRG region and implanted with a fiber optic above the cVRG region (n=3 mice) in a 6-minute tussive challenge of capsaicin before (Pre) and five weeks after (Post) surgery.

5.3 The role of the vocal cords

As previously noted, closure of the vocal cords is an integral part of coughing. The vocal cord closure during coughing helps generate a high subglottic pressure. Their subsequent opening is associated with an accelerated expiratory flow (Loudon & Shaw, 1967). We observed airway closure, as measured by the distance between the vocal cords, while activating NTS Tac1 neurons (**Figure 4-5 g**) and inducing a fictive cough by SLN stimulation (**Figure 4-5 h**). Therefore, we visualized the effect of vocal cord closure when activating these NTS Tac1 terminals.

Vocal cord visualization of the Tac1 terminals into the para-NA regions confirmed that the activation triggered airway closure (**Figure 5-5 b-d**). In contrast, cVRG terminal activation did not induce vocal cord closure (**Figure 5-5 e-g**). The vocal cords play a role only during the compressive phase of the cough and expiratory reflex. Once the vocal cords open, the expulsive phase begins. These results strengthen the optogenetic results observed in the previous section, specifically, that these two terminal projections seem to play a role in different phases of the integrated cough-like response.

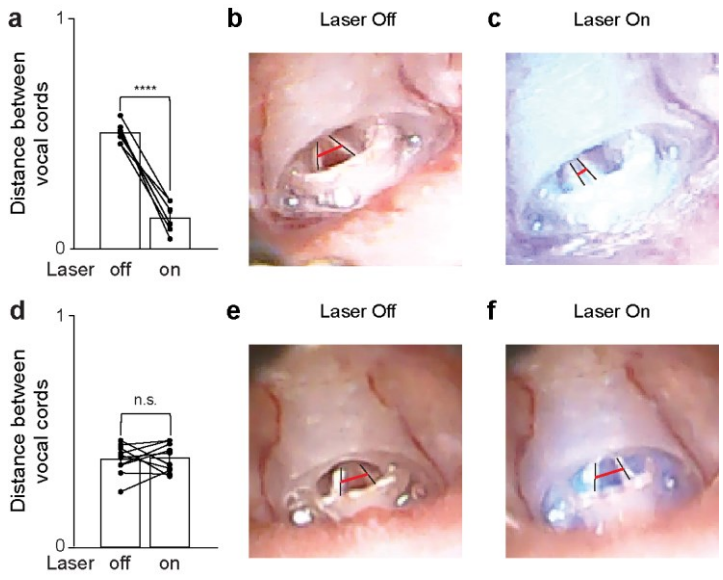

Figure 5-5 **Vocal cord closure during optogenetic activation. a**, The distance between vocal cords before (off) and during (on) laser activation of the NA terminals. (n=7 trials, 3 mice; $p<0.0001$, paired t-test). **b**, Snapshot of vocal cords before NA terminal laser activation. Red line measured distance. **c**, Snapshot of vocal cords during NA terminal laser activation. Red line measured distance. **d**, The distance between vocal cords before (off) and during (on) laser activation of the cVRG terminals. (n=10 trials, 3 mice; $p = 0.82$, paired t-test). **e**, Snapshot of vocal cords before cVRG laser activation. Red line measured distance. **f**, Snapshot of vocal cords during cVRG laser activation. Red line, the measured distance.

5.4 NTS Tac1 neurons send collateral projections to both the NA and cVRG

There are two plausible scenarios: (1) that individual NTS Tac1 neurons send collateral projections to both para-NA and cVRG regions, or (2) that the NTS Tac1 neurons are heterogenous and distinct NTS Tac1 neurons project to these regions, respectively. To distinguish between these two possibilities, we injected AAVretro-DIO-eGFP and AAVretro-DIO-mCherry to the NA and cVRG regions of Tac1-Cre mice, respectively (**Figure 5-6 a**). These virus vectors are delivered at the axonal terminals and can be retrogradely transported toward neuronal cell bodies throughout the axons, allowing for retrograde tracing (Surdyka & Figiel, 2021). Four weeks later, we observed that about half of neurons were labeled and expressed by both markers (**Figure 5-6 b-c**), suggesting that NTS Tac1 neurons send collateral projections to para-NA and cVRG regions, coordinating the downstream circuits.

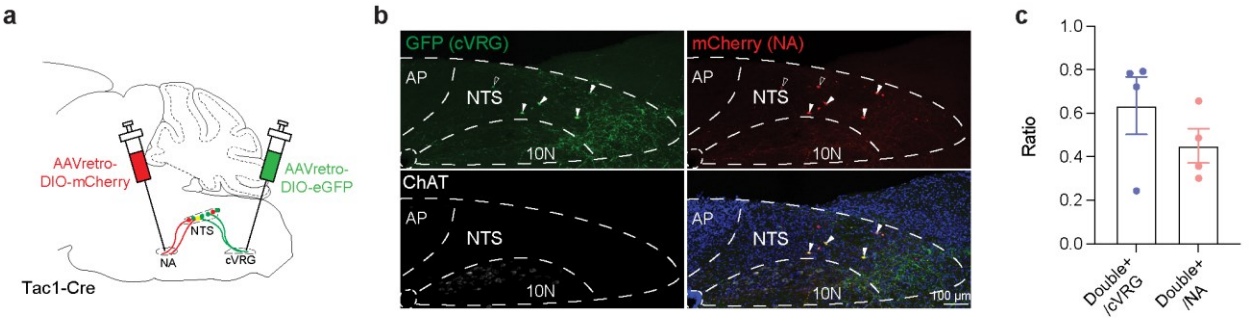

Figure 5-6 **NTS Tac1 neurons send collateral projections to both para-NA and cVRG regions. a,** Schematic for retrograde circuit tracing of NTS Tac1 neurons. Retrograde AAVretro-DIO-GFP and AAVretro-DIO-mCherry were injected in the cVRG and NA regions of Tac1-Cre mice, respectively. Neuronal labeling in the NTS was subsequently analyzed. **b,** Representative mouse brainstem slice of the NTS displaying Tac1-Cre neurons by retrograde AAV injected into the cVRG (green) and para-NA (red) regions. ChAT (gray) is used to label the 10N ventral to the NTS. Filled arrowheads, neurons labeled by both retroAAVs; open arrowheads, neurons labeled by only one retroAAV. Bar, 100 µm. **c,** Quantification of the ratios of double labeled neurons over total neurons labeled by either AAV.

5.5 Discussion

Here, we show that NTS Tac1 neurons send projections to distinct medullary areas (1) in the vicinity of the nucleus ambiguus (para-NA), and (2) in the vicinity of the caudal ventral respiratory group (cVRG). Both the NA and the cVRG play roles in coughs and expiratory reflexes, which are defined as forced expirations against a closed glottis. Optogenetically activating these projections evoke different respiratory responses. Upon imaging the effect of vocal cord closure on these activations, we observed vocal cord closure in the para-NA terminal activation, but not in the cVRG terminal activation. As stated previously, a cough is composed of three distinct phases: the inspiratory phase, the compressive phase and the expulsive phase. In contrast, the expiratory reflex is composed of only two: the compressive and expulsive phases. The vocal cord closure during the compressive phase of a cough increases the intrapleural pressure. We show that activation of Tac1+ NTS terminals in the para-NA and cVRG regions evoke respectively partial but complementary elements of the integrated cough response. The NTS to para-NA circuit plays a role in the compressive phase of coughs and expiratory reflexes

while the NTS to cVRG circuit plays a role in the expulsive phase of coughs and expiratory reflexes as indicated by the vocal cord recordings. Instead of a simple sensory relay node, these results of distinct effects in terminal activations suggest that NTS Tac1 neurons are a critical component of the central pattern generator for cough-like behaviors.

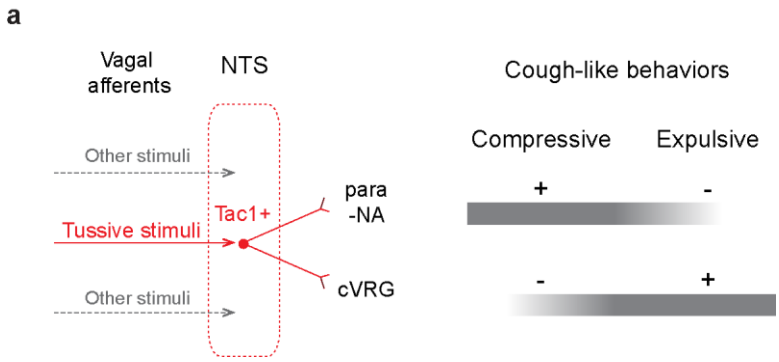

Figure 5-7 **Photoactivation of Tac1+ NTS terminals evoke respectively partial but complementary elements of the integrated cough-like response**. **a**, NTS receives different interoceptive stimuli through the vagal afferents. Tac1 neurons in the NTS are activated by tussive stimuli, and integrate different medullary circuit modules (i.e., para-NA and cVRG) to control the sequential motor phases of a forced expiration. An expiratory reflex contains two phases: the compressive phase, and the expulsive phase while a cough also contains an initial inspiratory phase. The Tac1 neurons – para-NA circuit controls the compressive phase, while the Tac1 neurons – cVRG circuit controls the expulsive phase. cVRG, caudal ventral respiratory group; NA, the nucleus ambiguus; NTS, the nucleus of the solitary tract.

Chapter 5 was largely adapted from the following manuscript in review:

Gannot N., Li X., Phillips C., Ozel A., Uchima Koecklin K., Lloyd J., Zhang L., Emery K., Stern T., Li J., Li. P. A vagal- brainstem interoceptive circuit for cough-like defensive behaviors in mice. *Nature Neuroscience*.

Noam Gannot performed the experiments in 5-1, 5-2, 5-3, 5-4 and 5-5. Dr. Xingyu Li performed the experiments in 5-6.

Chapter 6 MSPOTIT2 Application in Mouse

Coughing often becomes excessive with severe consequences under pathological conditions resorting people to seek medical attention. Chronic cough, which has a debilitating effect on quality of life, is one of the main reasons people seek medical attention (French et al., 1998). Opioids, such as morphine, codeine or pholcodeine, have been used as antitussives for centuries (Mudge, 1778). Codeine, a mu-opioid receptor (MOR) agonist, is a popular antitussive. The exact central targets of codeine in the cough circuit are unknown. Its antitussive efficacy appears to be largely dependent on the cough model and the species being tested, though (Adcock et al., 2003; Davenport et al., 2007; Dicpinigaitis et al., 2014; Smith et al., 2006). Conversely, fentanyl, another MOR agonist and a commonly used analgesic for severe pain, is known to induce cough (Generali & Cada, 2014; Pandey et al., 2005; Zhou et al., 2019). Although these opioids may act as an effective indirect antitussive, their use can produce side effects, such as drowsiness, nausea, constipation, and physical dependence (Chung, 2005). The mechanisms for how these opiates suppress cough is poorly understood (Dickinson et al., 2014). Thus, unveiling these mechanisms will be an important step towards developing better, more targeted, antitussive medications.

Despite the prevalence of cough, the current treatments are as effective as a placebo. When there are no other underlying health conditions, patients often seek over-the-counter anti-tussive medications, such as cough syrup. One of the main ingredients in cough syrup is dextromethorphan (DXM), a synthetic opioid (Dickinson et al., 2014). In high doses, DXM can

lead to fatal liver injury, cardiovascular effects, dizziness, uncontrollable eye movement and over-sedation. More importantly, cough syrup was shown to be no more efficacious than placebo (Galli & Barbas, 2004; Smith, S. M., Schroeder, K., & Fahey, 2014). Therefore, patients are using and abusing cough syrup while its efficacy remains questionable. The lack of an effective anti-tussive medication is largely due to the neuronal populations and molecular pathways involved in cough not being identified.

Now that we have characterized a genetically defined central cough circuit that is both necessary and sufficient in producing cough, we have identified possible target sites for these opioids. Within this circuit, the NTS Tac1 neurons are necessary for cough production and send a glutamatergic signal to activate the motor neurons in the NA, which closes the larynx. The NTS Tac1 neurons and the NA motor neurons are key nodes in this cough circuit. Interestingly, high expression level of opioid receptor mu 1 (Oprm1) gene has been shown in both the NA and the NTS, indicating possible overlap between the cough circuit and the opioid system. It would be informative to develop a tool that would allow for the study of opioids in the cough circuit in mice. To this end, we optimized the in vivo use of a genetic tool developed by the Wang Lab.

6.1 The effects of opioids on the tussive challenge

Since we have characterized the cough-like behavior in mice, we can use them to further study the mechanisms through which opioids act to either suppress or enhance coughing. Initially, we sought to characterize the effect of opioids on the cough-like behaviors in mice. Thirty minutes prior to a six-minute tussive challenge of capsaicin, mice received an intraperitoneal injection of either morphine, fentanyl, or a vehicle. The frequency of cough-like events was significantly reduced after a 30mg/kg injection of morphine, compared to an injection of saline. In contrast, a 1mg/kg injection of fentanyl significantly increased the number of

capsaicin-evoked cough-like events (**Figure 6-1**). The opposing effects of codeine and fentanyl indicate that there are multiple mechanisms that regulate coughing.

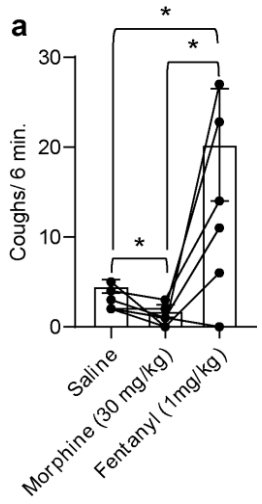

Figure 6-1 **The effects of morphine and fentanyl on coughs**. **a**, Compared to a vehicle injection of saline, mice (n=6 mice) that were injected with a 30 mg/kg injection of morphine 30 minutes prior to a cough assay, have a reduced cough rate (p=0.0478; n=6 mice) whereas mice that were injected with a 1 mg/kg of fentanyl have an increased cough rate (p=0.0418; n=6 mice) (morphine to fentanyl p=0.0310; n=6 mice). One way ANOVA with Tukey's multiple comparisons test.

6.2 The development of MSPOTIT2

To understand how opioids interact with brain regions in the cough circuit, we first needed to develop a method to detect opioid molecules in vivo. State-of-the-art methods for detecting opioid molecules use microdialysis coupled with nanoflow liquid chromatography-mass spectrometry (Al-Hasani et al., 2018). However, this method has a typical spatial resolution on the order of 500 μm and is limited by the probe size. While this is sufficient for detecting opioids in certain brain regions, this method precludes microdialysis from more precise studies on cellular or subcellular levels.

To modulate the activity of endogenous opioid systems, microinjection of exogenous opioids can be used (Morgan et al., 2014). While this can reveal brain regions involved in opioid-dependent behaviors, it cannot differentiate cell types or neuronal circuits in close proximity. Therefore, the specific cells or circuits involved in the behavior will remain obscure.

The Wang Lab and, specifically, Dr. Kayla Kroning developed a G-protein-coupled receptor (GPCRs) agonist integrator that can determine the localization of neuromodulators, such as opioids, in cell cultures. This integrator, termed M-SPOTIT (MOR Single-chain Protein-based Opioid Transmission Indicator Tool), and its brighter version, M-SPOTIT2, can be used for detecting opioids at a cellular resolution (Kroning et al., 2021, 2022). By using M-SPOTIT2, sites of opioid binding within the central cough circuit can be detected at subcellular resolution.

In M-SPOTIT, the circularly permuted green fluorescent protein11 (cpGFP) is embedded between the C-terminus of the MOR and a Gαi-mimic nanobody, Nb3912 (**Figure 6-2 a**). When a MOR agonist is present, Nb39 is recruited to MOR, and the sensor undergoes a conformational change, inducing a change in the chromophore environment of cpGFP and a subsequent enhanced fluorescence (**Figure 6-2 b**). Once activated, the cpGFP undergoes chromophore maturation, resulting in a persistent signal. This process allows post-mortem image analysis of the location of opioids at high spatial resolution. Upon extensive optimization of MOR and the linkers, M-SPOTIT can respond to both morphine and fentanyl with excellent sensitivity (**Figure 6-2 c-d**). M-SPOTIT has been validated in both HEK293T and neuronal cell culture. The goal of this chapter is to optimize its use in animals.

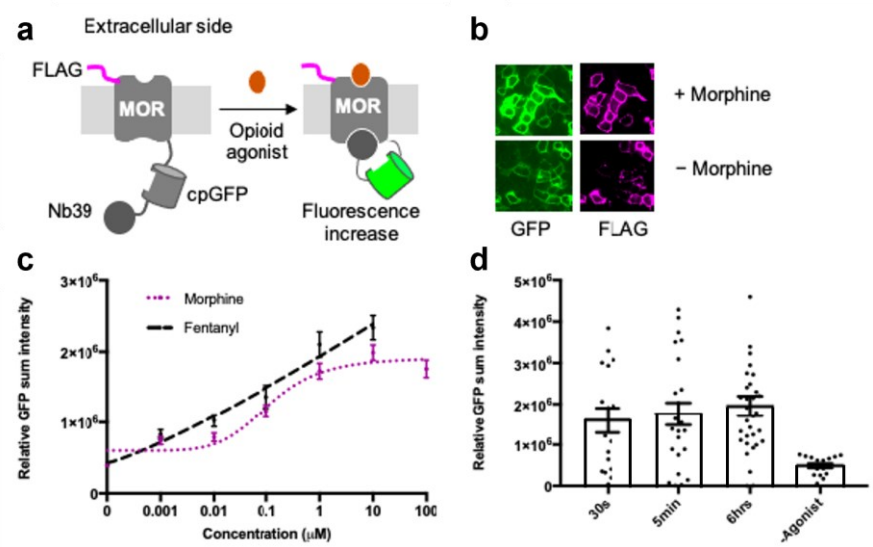

Figure 6-2 **Design and testing of M-SPOTIT**. **a,** Design of M-SPOTIT. An opioid's interaction with the sensor causes a conformational change in cpGFP, leading to an increase of fluorescence. cpGFP: circularly permutated green fluorescent protein. **b,** M-SPOTIT expressed in HEK 293T cells. GFP indicates sensor activation and FLAG indicates sensor expression. **c,** Titration of morphine and fentanyl. A 0.001μM concentration of fentanyl shows a signal change from baseline. **d,** M-SPOTIT's response to different fentanyl exposure times. As short as 30 seconds of fentanyl exposure provides a 3-fold signal change from baseline (-Agonist.)

6.3 Animal application of M-SPOTIT2

To evaluate the potential of this single-chain fluorescent integrator for detecting GPCR agonists in animal models, we tested M-SPOTIT2 in a mouse brain. We first tested M-SPOTIT2 (Kroning et al., 2021) by injecting adeno associated viruses (AAV) 1/2 mixed serotype encoding M-SPOTIT2 into the vicinity of the VRC, which is impacted by opioid signaling (Montandon et al., 2011). Six days after viral injection of M-SPOTIT2, we administered 100 mg/kg morphine or saline via IP injection to the mice (**Figure 6-3 a**). Twenty-four hours after morphine or saline administration, we sacrificed the mice for imaging. We observed a 4.9 times signal increase in the morphine administered group in comparison to the saline control group (**Figure 6-3 b-c**), validating the use of MSPOTIT2 in vivo.

To determine the sensitivity of M-SPOTIT2 to morphine in an animal brain, we also administered more dilute morphine amounts, 60 mg/kg or 30 mg/kg. We saw significant

fluorescence activation in the 60 mg/kg stimulated group and non-significant activation in the 30 mg/kg group (**Figure 6-3 c**).

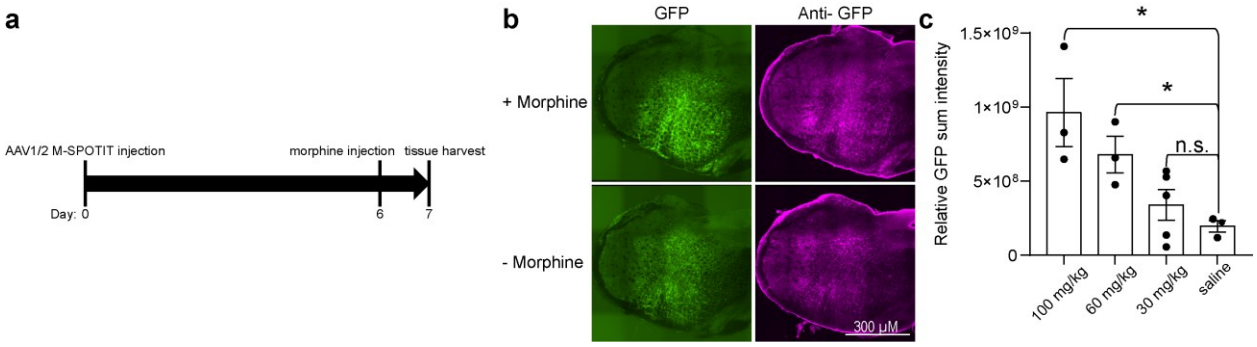

Figure 6-3 **Mouse testing of M-SPOTIT2 with AAV1/2 viral serotype**. **a**, Experimental protocol for M-SPOTIT2 mouse testing. **b**, Representative images of M-SPOTIT2 mouse testing. 100 mg/kg of morphine or saline was administered through intraperitoneal injection 6-days after viral delivery to the VRC. GFP, cpGFP fluorescence. Anti-GFP, protein expression levels. Scale bar, 300µm. **c**, Statistics of experiment described in b, as well as 60 mg/kg and 30 mg/kg morphine testing. Data is presented as Mean ± SEM. (100 mg/kg: p= 0.0303; n=3 mice, 60 mg/kg: p= 0.0201; n=3 mice, 30 mg/kg: n.s.= 0.3483; n=5 mice, saline: n=3 mice). One way ANOVA with Dunnett's multiple comparisons test.

It is important to note that lower M-SPOTIT2 protein levels were observed in the saline stimulated condition (**Figure 6-3 b,** "-Morphine"). Lower protein levels in the absence of drug have previously been observed for the SPOTIT sensors and is due to the instability of the inactive cpGFP-Nb39 complex (Kroning et al., 2021). Therefore, the higher signal in the morphine stimulated condition is due to both fluorophore maturation and higher sensor stability. Because of the lower protein levels and consequently lower anti-GFP signal in the saline conditions, we take the ratio of the morphine-stimulated fluorescence over the saline-stimulated fluorescence without normalizing to protein levels for quantification of M-SPOTIT2's signal to noise ratio.

6.4 Pre-administration of naloxone diminishes morphine-induced signal increase

Next, we performed an important sensor control in which we used the MOR antagonist, naloxone, to block M-SPOTIT2 prior to morphine injection. Naloxone binds opioid receptors

and can reverse and block the effects of opioids such as morphine. If full blockage by naloxone is achieved, morphine will not bind to and activate the M-SPOTIT2 sensor.

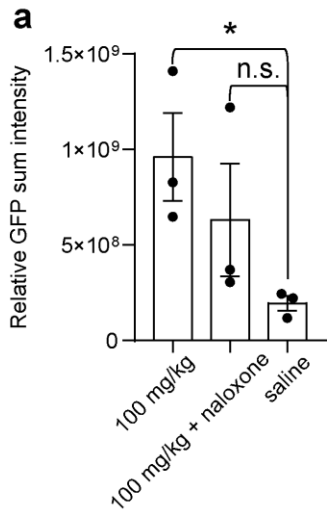

Figure 6-4 **Pre-administration of naloxone diminishes morphine-induced signal increase**. **a**, Quantification of the effects of naloxone on the relative GFP sum intensity. Data is presented as Mean ± SEM. (100 mg/kg: p= 0.0303; n=3 mice, 100 mg/kg + naloxone: n.s.= 0.2150; n= 3 mice). One way ANOVA with Dunnett's multiple comparisons test.

We administered morphine to mice expressing M-SPOTIT2 5 minutes after a 100mg/kg naloxone injection. Compared to the 100 mg/kg injection of morphine and saline-injected mouse cohorts shown in Figure 6-3, we saw that adding 100 mg/kg naloxone prior to 100 mg/kg morphine stimulation was sufficient to prevent significant sensor activation (**Figure 6-4**). Within this cohort, two-thirds of mice showed similar green fluorescence as the saline condition, thereby illustrating naloxone blockage. However, one mouse showed activation as high as 100 mg/kg morphine. Naloxone in this mouse might have been cleared away from its system too quickly where morphine lasted longer in the system resulting in M-SPOTIT2 activation. When considering all three mice, the green fluorescence was not significant over saline, indicating the effect of the naloxone blockage on M-SPOTIT2.

6.5 M-SPOTIT2 expression does not impact mouse breathing frequency

A concern with genetically encoded GPCR-based sensors is that they will affect the natural physiology of animals, resulting in biological artifacts. To evaluate how M-SPOTIT2 expression affects a mouse's physiology, we measured the breathing frequencies of mice prior to MSPOTIT2 viral injection and after in response to morphine and saline. We chose to measure breathing frequencies because of the endogenous opioid receptor's role in suppressing breathing (Montandon et al., 2011). In both the morphine- and saline-stimulated conditions, we saw no significant difference in the breathing frequencies of mice before and after M-SPOTIT2 expression. This experiment shows that the expression of M-SPOTIT2 does not impact the endogenous opioid receptor's role in suppressing breathing (**Figure 6-5**).

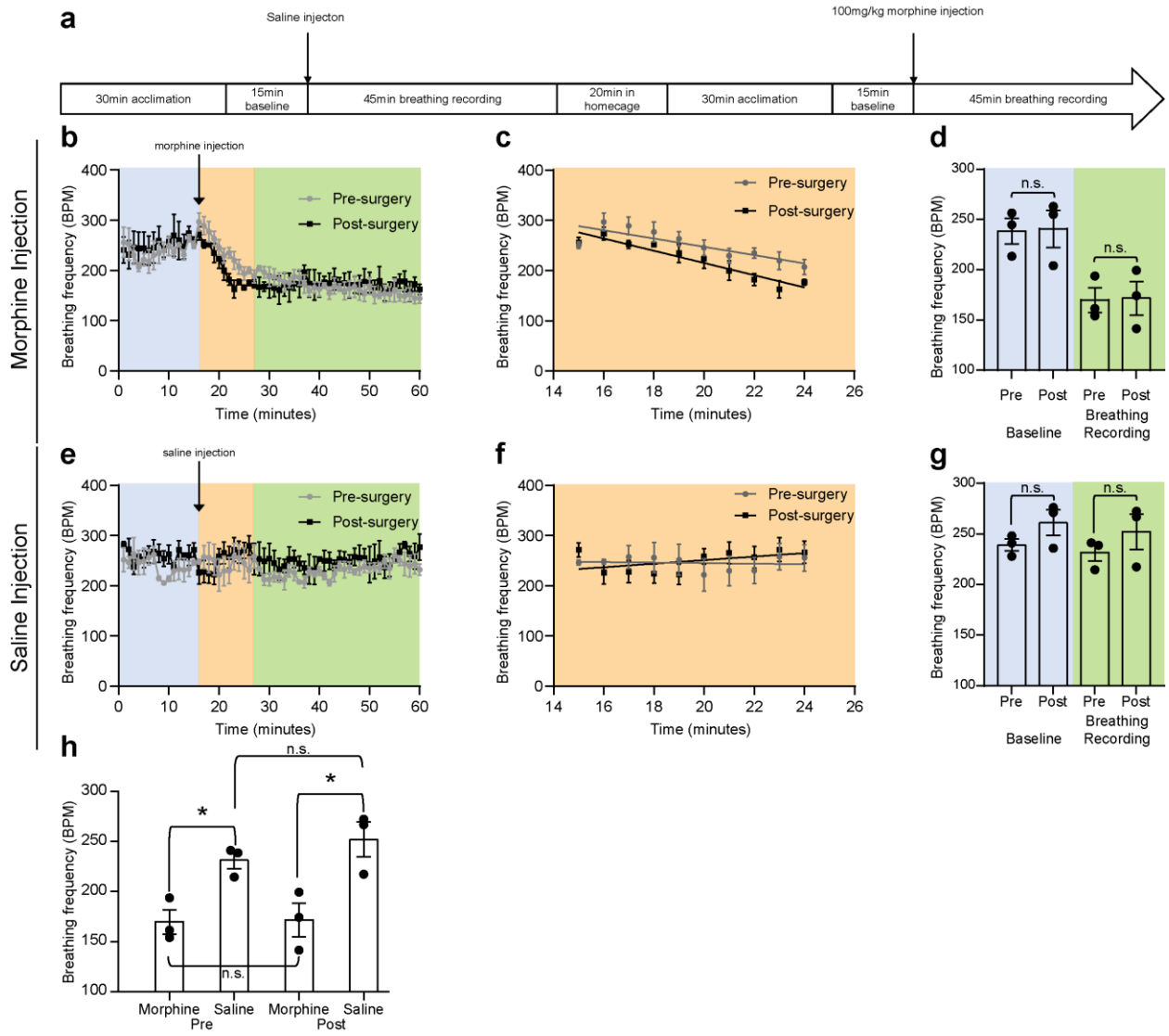

Figure 6-5 **The effect of M-SPOTIT2 expression on the breathing frequency of mice. a,** Experimental timeline of the breathing frequency recording. Mice were recorded in two different time points: (1) three days before surgery and (2) on day six following surgery (surgery is day 0). Breathing frequency was compared in these two recordings to observe the effects of MSPOTIT2 injection on opioid breathing depression. To test the respiratory depression of morphine, individual mice were placed in a 450mL WBP chamber at room temperature (22°C) with normoxia air continuously flushed through the chamber. The day before the respiratory recording, mice were placed in the WBP chamber for four hours for acclimation. **b**, Impact of MSPOTIT2 expression on morphine-induced breathing suppression. Mouse breathing frequency was recorded before (blue) and after (yellow and green) morphine administration. Pre-surgery is without MSPOTIT2 expression and post-surgery is with MSPOTIT2 expression in the same mice. **c**, Plotting only the yellow region of the plot shown in b to calculate the slope of the morphine-induced decrease on breathing frequency. The slopes are not significantly different, the pooled slope is -10.22. **d**, Plotting the averages of the blue and green regions of plot b. The blue region represents the baseline recording prior to morphine injection and the green region represents the breathing recording after morphine injection once the breathing frequency has plateaued. **e**, **f**, and **g** are similar to b, c, and d, respectively, except with an injection of saline as a vehicle. In f, the slopes are not significantly different, the pooled slope is 1.486. **h**, Comparing the pre- and post-surgeries morphine- or saline-stimulated plateaus (green region in b and e). The green regions of the plots shown in b and c were averaged and plotted. For d: baseline: n.s.= 0.9154; n=3 mice, breathing recording: n.s.= 0.9282; m=3 mice. For g: baseline: n.s.= 0.1902; n=3 mice, breathing recording: n.s.= 0.3464; n=3 mice. For h: morphine and

saline pre-surgery: p= 0.0141; n=3 mice, morphine and saline post-surgery: p= 0.0293; n=3 mice, saline pre-surgery and saline post-surgery: n.s.= 0.3464; n=3 mice, morphine pre-surgery and morphine post-surgery: n.s.= 0.9282; n=3 mice.

6.6 Discussion

Coughing is an important respiratory mechanism necessary for all mammalian life. However, there is no evidence that current treatments for cough are any better than placebo (Schroeder & Fahey, 2014). Effective anti-tussive medications are lacking due to the limited knowledge on the neural circuit controlling cough. This research gap is due to guinea pigs – the most commonly used animal in cough research – lacking genetic tools to precisely define the cough controlling neurons and circuits(Canning & Chou, 2008). In previous chapters, we characterized the cough-like behavior in the mouse model, allowing us to take advantage of the genetic tools available in mice to better understand the cough circuit. For example, we can utilize an opioid sensor to study the roles of opiates and their role in the cough circuit.

In cases of chronic cough, opiates are recommended as cough suppressors despite concerns with their use (Chung, 2005). Despite being used as a cough remedy since the 18th century (Mudge, 1778), the mechanism in which opiates suppress cough is poorly understood (Dickinson et al., 2014). Therefore, there is a critical need to unveil these mechanisms so that we can develop safer and more targeted antitussive medications.

Here, we used the cpGFP-Nb39 tool motif to engineer a series of opioid integrator sensors called SPOTIT. Then, we used the brighter version, MSPOTIT2, for morphine detection in the mouse brain. We showed that M-SPOTIT2 functions in vivo where its brighter signal can overcome the autofluorescence of animal tissue to give a robust morphine-induced fluorescence response. The brightness of MSPOTIT2 depends on the concentration of morphine and it is blocked by the administration of naloxone, a morphine antagonist. Importantly, we show that the injection of MSPOTIT2 has no effect on other respiratory responses.

Now that we have validated and optimized the use of M-SPOTIT2 in vivo, we can take advantage of this tool to determine the localization of opioids in the cough circuit and further elucidate the role of opioid signaling in inducing or silencing cough. We expect different exogenous opioids will have a different localization within these circuits, thereby influencing their biological effect.

Chapter 6 was largely adapted from the following manuscript in review:
Kroning, K.E.*, Gannot, N.*, Li, X.*, Zhou, G., Sescil, J., Putansu, A., Shen, J., Fiel, H., Wilson, A., Li, P., Wang, W. Single-chain fluorescent integrators for mapping G-protein-coupled receptor agonists. *PNAS*. (* co-first authors)

Noam Gannot and Minte Beyecha performed the experiment in 6-1, Dr. Kayla Kroning performed the experiments in 6-2, and Noam Gannot performed the experiments in 6-3, 6-4 and 6-5.

Chapter 7 Summary of Results and Future Directions

7.1 Summary of Results

In chapter two, we conducted a single cell RNA-seq analysis and show that the NTS contains molecularly heterogenous neuronal populations. With the use of optogenetics, we demonstrated that the activation of different neuronal populations within the NTS induces distinct functions in controlling diverse breathing patterns. Among them, we showed that activating a cluster of NTS neurons expressing Tac1 induces an expiratory defensive behavior.

In chapter three, we characterized different defensive behaviors in freely moving mice, including sneezes, coughs, and expiratory reflexes. To distinguish between coughs and sneezes, we facilitated an automated and unbiased categorization of respiratory responses with the use of a linear support vector machine (SVM) that establishes objective criteria based on identified differences in respiratory responses between coughs and sneezes. We verified the accuracy of this classifier and used it in future chapters, ensuring consistency with our findings. To the best of our knowledge, this is the first time that the application of machine learning has been used in this context, which contributed valuable insights to the challenging question of categorizing coughs and sneezes in animal studies. We also showed that mice exhibit cough-like responses to different tussive agents and we characterized the cough-like behavior in mice.

In chapter four we confirmed that the expiratory defensive behavior observed by the optogenetic activation of NTS Tac1 neurons is a cough-like behavior. We then further characterized the role of these neurons in the cough-like behavior. We showed that NTS Tac1

neurons are preferentially activated in the NTS by a tussive challenge and that the genetic ablation or chemogenetic silencing of them attenuates the cough-like response to tussive agents with little effect on other breathing patterns. Furthermore, we showed that these cough-like behaviors are mediated by glutamate release and not the Tac1 neuropeptides.

In chapter five we traced the downstream projections of NTS Tac1 neurons in the brainstem. We also showed that these NTS Tac1 neurons project to distinct medullary areas and the photoactivation of NTS Tac1 terminals in these sites evoked respectively partial, but complementary elements of the integrated cough-like behaviors.

In chapter six, after we characterized the cough-like behavior in mice and identified important nodes in the cough circuit, we optimized a tool to be used in vivo to help elucidate the role of opioids in the cough circuit.

7.2 A neural control circuit for cough-like defensive behaviors in mice

The NTS mediates the interoceptive signals from the visceral organs, including the airways, and also receives afferent inputs from the vagal sensory neurons with the cell bodies that reside in the vagal ganglion (Kupari et al., 2019; Prescott et al., 2020). NTS Tac1 neurons receive this synaptic input and project to regions such as the para-NA. The para-NA, along with other regions, such as the cVRG, project to the efferent musculature to produce the cough. Glutamatergic signaling is necessary to execute this behavior. We conclude that this neural circuit plays an essential role in controlling cough-like behaviors in mice (**Figure 7-1**).

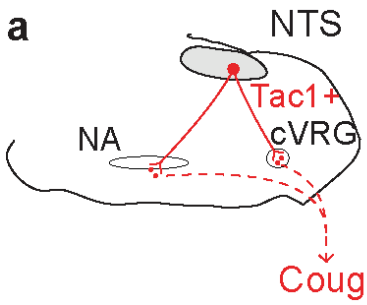

Figure 7-1 **A neural circuit for cough-like defensive behaviors in mice. a**, Model for the cough control circuit within the brain. Tac1+ neurons in the NTS project to the para-NA region and the cVRG region in the ventrolateral medulla to release glutamate to elicit a cough-like behavior.

7.3 Significance of results

An occasional cough is a normal and healthy function of the body that is crucial for clearing the airways of germs, mucus, and dust. At times, coughing can become a medical concern and lead to devastating and potentially dire consequences when the cough reflex is either excessive or deficient. A cough is the most common symptom of respiratory diseases and is the leading cause for patients to seek medical attention. Despite its prevalence, treatments for chronic coughing are lacking due to current anti-tussive medications being no more efficacious than a placebo and having significant negative side effects. This issue is largely because much is still unknown regarding how coughing is controlled in physiological and pathological conditions. Therefore, there is a critical need to identify the neuronal populations and pathways in the brain involved in cough, so that better targeted treatments for chronic cough can be developed.

Most animal studies on the cough reflex use guinea pigs as the model of choice. However, guinea pig models lack the extensive system of genetic tools that allow for the detailed identification of molecularly defined pathways. This barrier limits the discovery of endogenous cough pathways, as well as the development of a targeted anti-tussive medication. In contrast, the mouse is a premier mammalian model for the study of the genetic and molecular bases of physiology and behavior. The ability to manipulate the mouse genome makes them an attractive

target for cough research. Despite this ability, mice have not been used to study coughing since there has been debate in the field about whether they can even cough (Belvisi & Bolser, 2002). Here, we demonstrated that mice cough in response to a variety of different tussive agents and have characterized this behavior using breathing airflow waveform, intrapleural pressure changes, muscle activity, vocal cord closure, sharp sound, and body movement. The results presented here are reminiscent of the cough-like behaviors of other species (Korpas J, 1979; J. Widdicombe & Fontana, 2006; Xiang et al., 1998; Zhuang et al., 2019). Therefore, we took advantage of the genetic tools available in the mouse model and advanced the knowledge of the endogenous central neural circuits and pathways underlying cough. Furthermore, we can use the mouse model to identify drug targets for manipulating cough, thereby providing new opportunities for the development of novel therapeutics and better treatments for those suffering from excessive coughing.

While both the cough reflex and expiratory reflex involve the compressive and expulsive phases and often occur intermittently in clinical settings, the relationship between these two essential airway defensive functions is still not fully understood (Fontana & Widdicombe, 2007). Our results show that both responses require the shared neural circuit through the NTS Tac1 neurons as the silence or ablation of these neurons reduces both behaviors. Furthermore, activating the terminals of NTS Tac1 neurons in different ventral medullary regions induces distinct phases of these cough-like behaviors. This evokes a divergent modular circuit organization from these NTS Tac1 neurons in controlling the sequential motor pattern of the expiratory expulsive efforts.

The NTS, a key brain region that receives diverse interoceptive signals from visceral organs, has been thought to be the primary site that receives vagal afferents to mediate

respiratory reflexes (Canning et al., 2006, 2014; Lucanska et al., 2020). Our results demonstrate not only the diverse respiratory responses associated with NTS subpopulations, but also the critical role of NTS Tac1 neurons, a small population of the NTS neurons, as a key component of the central pattern generator for cough-like defensive behaviors in mice. Together with the recently identified neural circuits that specifically control sighing (P. Li et al., 2016, 2020; Yao et al., 2023), we propose that there are dedicated neural circuits for stereotyped breathing patterns and perhaps other respiratory-related functions. Thus, there are perhaps other segregated circuits connecting the visceral organs to the brain to control different interoceptive functions through NTS subpopulations with specific functions in mediating interoceptive processes.

An important component of the results presented here is that the neural circuit involving NTS Tac1 neurons is functionally specific in mediating coughing, as opposed to other breathing patterns. When these neurons are ablated or silenced, it only diminishes cough-like reflexes, but not other aspects of breathing, such as eupneic breathing, sighing, and hypoxic respiratory response. This result highlights the specificity of the NTS Tac1 neurons to cough-like behaviors in mice.

7.4 Future Directions

Our work here focuses on the NTS-ventral medulla circuit for cough-like behaviors in mice. However, cough is a defensive airway reflex subjected to a high degree of cortical control since the cough motor patterns can be mimicked voluntarily and reflex cough can be inhibited up to complete suppression. Understanding how other brain regions, including higher cortical regions, interface with the neural circuit identified here would shed light on the voluntary control mechanisms of coughing.

Leveraging mouse genetics, we investigated the role of various genes in mediating cough-like behaviors. For example, disrupting glutamate release in all Tac1 neurons abolished induced coughs, whereas deletion of tachykinin 1-encoded neuropeptides did not eliminate coughs. It is noteworthy that these experiments were conducted in tussive-induced coughs. Further exploration of the contribution of these neurotransmitters/neuropeptides, and how the cough neural circuit identified here malfunctions in pathological conditions, such as excessive coughing, holds promise for developing novel and effective antitussive medications.

Although mouse models offer genetic access to pinpoint the neural circuit and molecular pathways underlying a behavior, determining whether the identical neurons and neural circuitry are conserved for coughing in other species, including humans, necessitates further comparative studies across different species. Such investigations will yield valuable insights into the evolution of this vital respiratory function that safeguards the airways and its underlying neural circuitry.

Consistent with the studies in mouse models (Chen et al., 2013; Iwata et al., 2015; Kamei et al., 1993; C. Zhang et al., 2017), our results demonstrated that mice exhibit stereotypic behavioral responses to tussive challenges that trigger cough reflexes and expiratory reflexes in human and other species. These results together suggest that cough-like behaviors are evolutionarily conserved functions that protect the lungs and airways. While it makes sense that essential defensive functions like these are conserved across species, there might still be evolutionary differences. Although there may be differences in these cough-like behaviors between humans and other species that have yet to be discovered, the neural circuit identified here plays a crucial role in the primitive cough-like behaviors observed in mice. Further

investigation is needed to understand how these essential respiratory behaviors and their underlying neural circuits have evolved across different species.

An important aspect of this work is to characterize the cough-like behavior in mice and show that they can be used in future studies that investigate this behavior. For example, we can study the roles of opioids in suppressing cough. The novel sensor (M-SPOTIT) developed in the Wang Lab by Dr. Kayla Kroning will provide unprecedented precision in studying how opioids are integrated in the neuronal circuits of cough. By using M-SPOTIT, sites of opioid binding within the central cough circuit can be detected at subcellular resolution for the first time. By using M-SPOTIT in this context, we will have identified the action sites of opioid drugs in the neurons modulating cough and have identified the role of MOR in this circuit. This will contribute to better clinical treatment of cough.

Chapter 7 was largely adapted from the following manuscript in review:
Gannot N., Li X., Phillips C., Ozel A., Uchima Koecklin K., Lloyd J., Zhang L., Emery K., Stern T., Li J., Li. P. A vagal- brainstem interoceptive circuit for cough- like defensive behaviors in mice. *Nature Neuroscience.*

Appendix: Materials and Methods

Mouse Lines

All procedures were carried out in accordance with the animal care standards in National Institutes of Health (NIH) guidelines and approved by the University Committee on Use and Care of Animals at the University of Michigan. Animals were maintained on a 12 h light/dark cycle with ad libitum access to food and water. All mice strains utilized were C57BL/6J genetic background. Ai9 (Madisen et al., 2010), Grp-Cre (Gong et al., 2003), Tac1-Cre(Harris et al., 2014), Vglut2 flox (Tong et al., 2007), Vgat-Cre, Vglut2-Cre (Vong et al., 2011), Oprm1- Cre (Bailly et al., 2020), Gal- Cre, and Tac1-/- null (Cao et al., 1998) were previously reported.

Sample preparation of single cell RNA-seq

Five mice at postnatal day 5 were euthanized by isoflurane inhalation followed by decapitation. The brain was isolated and embedded in 4% agarose II in artificial cerebrospinal fluid (ACSF) and sectioned at 200um thickness on a VT 1000S vibratome (Leica). The caudal NTS tissue and adjacent regions in the dorsal vagal complex were manually dissected based on the morphology (the relative position to area postrema, 4^{th} ventricle, and central canal), and referred as the NTS. Tissue was pulled together in hibernate A solution (Gibco), followed by digestion with 20 u/ml papain (Worthington Biochemical Corporation) and serial trituration by Pasteur pipets to generate single cell suspension. The cells were stained with 0.2% DyeCycle Ruby (Invitrogen) at 37 degree for 15 minutes before passing through a 70um cell strainer (Falcon). The live cell suspensions were sorted and collected by a BD FACSAria III Cell Sorter

(BD Biosciences) with a nozzle diameter of 100 um. The FACS sample was loaded to the 10X Chromium platform for capturing. The following cDNA synthesis with PCR and library preparation were done according to the manufacturer's protocol. Sequencing was performed on a NovaSeq sequencer (Illumina).

Single cell RNA-seq data analysis

For alignment and digital gene expression matrix generation, 10X Genomics Cell Ranger v3.0.0 workflow was utilized in the preprocessing of the raw data. Specifically, the raw base call (BCL) files generated by Illumina NovaSeq were demultiplexed into fastq files using the CellRanger mkfastq function. Then, the Cell Ranger count function was used to align and filter reads, count the barcodes and UMIs, and generate Digital Gene Expression matrices. Mouse genome mm10 was used as the reference for alignment. R Package Seurat v.4.0.4 was used for subsequent steps of the analysis (Hao et al., 2021).

For cell filtering, normalization and data scaling, the starting pool of 9,578 cells and 20,902 genes was filtered by excluding cells with fewer than 1,000 or more than 8,100 detected genes, or with >8% of its transcripts corresponding to mitochondria-encoded genes, or fewer than 500 or more than 60,000 UMIs. These filters resulted in 5,523 cells, for which the average number of detected genes was 4,430 (IQR 3,120 - 5,824), and the average UMIs was 16,618 (IQR 7,450 - 24,231). Transcript counts were normalized across cells by using the global-scaling method called "LogNormalize" (Seurat function NormalizeData), which divided the UMI counts by the total UMI count per cell, multiplied with a scale factor of 10,000 (default), and log-transformed. Subsequently, normalized counts for each gene were centered and scaled across cells by using the Seurat function ScaleData, so that the mean and variance across cells are 0 and 1, respectively.

For dimensionality Reduction and Louvain-Jaccard Clustering, we performed principal component analysis (PCA) on the normalized, scaled expression data by using the top 2,000 highly variable genes selected by using the Seurat function RunPCA. We used the elbow point in the scree plot and chose the top 20 PC scores for downstream clustering. We obtained 8 clusters by using Louvain-Jaccard clustering with the Seurat functions FindNeighbors and FindClusters (with resolution 0.05). UMAP were utilized to visualize the clusters.

For cluster annotation to known cell types, we relied on the reference scRNAseq dataset for adult mouse nervous system (Zeisel et al., 2018). We annotated the 8 clusters in our own data against the 16 major cell types at the "Rank 3" level by calculating the 16-by-8 matrix of rank correlation coefficients between each of the 8 cluster centroids of our data and each of the 16 centroids from the reference data. The results were represented in a heatmap using the R package corrplot v0.9, which showed relatively strong correlations between Cluster 1 in our dataset and 7 of the 16 reference clusters corresponding to neuronal cells. Cluster 2 cells had a higher mitochondrial gene content and low number of UMIs, suggesting low quality, and ignored from annotation. Cluster 3 and Cluster 8 had high correlations with the "Astroependymal cells" in the reference. Similarly, we annotated Cluster 4 as "Neural crest-like glia"; Cluster 5 as "Oligodendrocytes", Cluster 6 as "Immune cells", and Cluster 7 as "Vascular cells". For the rest of the analysis, we focused on Cluster 1, the 'Neuronal Cell' cluster, which contains 1,960 cells.

For clustering for neuronal cells, we performed principal component analysis like before (Seurat function RunPCA) on the normalized, scaled data for the 1,960 neuronal cells, using the top 2,878 highly variable genes. We chose the top 20 PC scores and found 19 subclusters using Louvain-Jaccard clustering.

For marker selection for the 19 Neuronal Subclusters, the gene expression in each cluster was compared with all the other 18 clusters using the Wilcox test embedded in the Seurat function FindAllMarkers. Subsequent selection criteria are: (1) at least 0.25 log2 fold higher expression in the cluster than the other clusters, (2) detected in > 25% cells in either of the two comparison groups. The distribution of gene expression levels for the markers with biological interest was compared across clusters in violin plots using Seurat function ViolinPlot. It should be noted that some cells from nearby regions may have been included in our analysis.

Breathing monitoring and analysis

Individual mice were placed in a 450ml whole-body plethysmography chamber at room temperature (22°C) in 21% O_2 (for normoxia) or 10% O_2 (for hypoxic challenge) balanced with N_2. Mice were allowed to acclimate to the chamber for 30 minutes before the respiratory parameters were recorded by Emka IOX2 software (EMKA Technologies, Paris, France).

For the capsaicin tussive challenge (cough assay), individual animals were placed in a whole-body plethysmography chamber (Buxco) modified with a small microphone in the arm. Capsaicin (Sigma, CAS: 404-86-4) was initially dissolved in EtOH for a stock solution of 10mM. The stock solution was then further diluted in saline to achieve the necessary concentrations. For the internasal instillation of polyvinyl alcohol, polyvinyl alcohol (PVAL) (Aldrich, CAS: 9002-89-5) was dissolved in saline. Individual mice were injected with 10μL of a 20% PVAL solution (5 μL in each nostril) and were then placed in the WBP for a ten-minute recording. For the internasal instillation of compound 48/80, Compound 48/80 (Sigma, CAS: 94724-12-6) was dissolved in saline. Individual mice were injected with 15μL of a 1 μg/μL compound 48/80 solution (7.5 μL in each nostril) and were then placed in the WBP for a ten-minute recording. Room air was constantly flushed through the chamber. Respiratory defensive

behaviors were defined as events whose amplitude exceeded 150% of the preceding eupneic breath. Cough-like responses were identified via the plethysmograph traces, the intrapleural pressure, the audio generation, and the movement of the mouse. Sighs, sneezes, expiratory peaks, and other respiratory patterns and audio events were excluded from the cough reflexes and expiratory reflexes quantification. Please note that each of the defensive respiratory behaviors (e.g., coughs, sneezes and expiratory reflexes) were run through the classifier to ensure that these events were characterized correctly. Sighs were identified in plethysmography traces by their characteristic biphasic ramp, augmented flow in the second phase of the inspiratory effort, and prolongation of expiratory time following the event, as previously described (P. Li et al., 2016, 2020). Sneezes were defined using the predictor described in chapter three and as previously reported (Chen et al., 2013; Iwata et al., 2015; Xiang et al., 1998). Expiratory peaks were defined in plethysmography traces by a sharp expiratory peak without preceding inspiration. At least two experienced researchers performed the blind analysis on the behavioral recordings independently. Only the events that were confirmed by the two researchers were used for the final quantification. For the c-Fos experiment, mice were placed in the chamber with nebulization of 30 μM capsaicin for 5 minutes, and recovery for 5 minutes. Fifteen minutes after the tussive challenge, the brain tissue was harvested and immediately embedded into OCT followed by RNAscope assay.

For hypoxia challenge, mice were placed in a whole-body plethysmography chamber for a 30-minute habituation prior to recording. Animals underwent a 10-minute baseline under conditions of normoxia (21% O2). Following this baseline, animals were exposed to a 10-minute hypoxic challenge (10% O2) and then allowed a 10-minute recovery period in normoxia. The chamber was flushed with the new air condition for one minute at each switch.

Anterior ethmoidal nerve (AEN) transection

Adult mice were placed on a stereotaxic apparatus to maintain anesthetic state under 1.5% isoflurane. Shaved heads were disinfected by povidone followed by alcohol prior to surgery. A midline incision was made in the skin from bregma along posterior frontal suture direction to expose the medialis orbits. Anterior ethmoidal nerve (AEN) was separated from the connective tissue and a rhizotomy was performed on it.

Hierarchical clustering of breathing waveforms and automated classifier

The defensive respiratory events of mice undergoing the capsaicin nebulization assay and compound 48/80 assay, both before and after anterior ethmoidal nerve (AEN) denervation, were recorded. The raw data capturing these defensive respiratory events in the assays were then extracted, resulting in a dataset of 314 sequences. To discard minute recording artefacts, all sequences were smoothed using a smoothing spline. To prepare for cluster identification, we explored the distribution of sequence similarities by first applying Z-score normalization to all sequences, then constructing a hierarchical clustering tree of all sequences. We depended on Euclidean distances as a pairwise metric and applied the Weighted Pair Group Method with Arithmetic Mean (WPGMA) clustering approach. The WPGMA method is beneficial for our context because it attributes equal weight to each sequence within a cluster. This ensures that our analysis is not unduly influenced by any larger group.

To assign cough and sneeze to each cluster, we quantified the fraction of sequences that were recorded after the AEN denervation. In the case of sneeze clusters, a low fraction of post-manipulation events was anticipated, due to the essential role of the AEN in mediating sneezing stimuli. On the other hand, the denervation would not dramatically impact the frequency of coughs, leading to a fraction of post-manipulation likely to be around 50%. Accordingly, each

cluster was inferred as either a cough or as a sneeze, depending on the percentage of events that occurred after the AEN denervation in each cluster and the similarity between waveforms. Therefore, clusters #1, 2, 3, 4, and 7 were inferred as coughs, while clusters 5, 6, 8 were inferred as sneezes. Overall, the divergence of all sequences into two archetypal shapes solidly supports the fact that they represent two distinct physiological functions.

For future automated and unbiased categorizing of sequences, we conducted training on a linear support vector machine (SVM; 5-fold cross validation) for breath pattern classification. The Linear SVM classifier, possessing few assumptions inherent in its model, is particularly appealing for its adaptability across a variety of datasets and robustness against overfitting. The latter is especially significant given the high-dimensional nature of our data, thus making the SVM method an optimal choice in our case. Training the SMV on our data led to an impressive accuracy rate of 98.08%. Besides offering a dependable technique for future sample analysis, the high accuracy rate obtained from the relatively straightforward SVM classifier underscores the idea that the separated signal geometries are indicative of distinct physiological functionalities.

Intrapleural Recording

Adult mice were anesthetized with isoflurane (4 – 5% for induction, 1.5% for maintenance) for the implantation. The tip of a telemetry sensor (PA-C10) and the transmitter with an attached catheter were surgically implanted in the intrapleural space and under the lower back skin, respectively. Five days following surgery, mice underwent a cough assay while the intrapleural pressure, box flow, audio and video were recorded.

Characterization of Cough Reflex and Expiratory Reflexes

Coughs and expiratory reflexes are defined by combining the box flow detected by the WBP, intrapleural pressure, sound, and video. In brief, the cough-like behavior is composed of

three distinct phases: (1) the inspiratory phase, (2) the compressive phase and (3) the expulsive phase (also see Figure S3). During the inspiratory phase, the rib cage expands, and intrapleural pressure decreases, allowing air to be inhaled into the lungs. Meanwhile, owing to the elevated temperature and humidity within the animal's body, pressure increases within the chamber, causing air to flow out of the chamber, as evidenced by a negative box flow trace. In the compressive phase, immediately following inspiration, the glottis closes, and muscles compress the rib cage, leading to a rapid increase in intrapleural pressure. Due to the decreased pressure in the chamber, air is drawn into it, resulting in a positive box flow. The expulsive phase commences with the opening of the glottis, causing a sudden reduction in intrapleural pressure as the pressure in the lungs is released. The sound is generated during this phase due to air rushing past the glottis. During this phase, the box flow graph is negative because air is expelled from the chamber. The expiratory reflex contains only the compressive and expulsive phase of the cough and lacks the initial inspiratory phase. To classify an event as a cough, the amplitude of the inspiratory phase must constitute at least one-third of the inspiration of the previous eupneic breath. Any event exhibiting an inspiration with amplitude lower than one-third of the inspiration of the preceding eupneic breath is classified as an expiratory reflex.

Stereotactic injection

Adult mice were anesthetized with isoflurane (4 – 5% for induction, 1.5% for maintenance) for stereotactic injection. Animals received 5mg/kg of preemptive analgesic Rimadyl (carprofen) (Zoetis) prior to placement in the stereotactic frame (David Kopf Instruments) and body temperature was maintained at 35 – 37 °C using a feedback-controlled heating pad (Physitemp, TCAT-2LV). The following coordinates were used for injection: NTS, ± 0.4 mm from the midline; - 7.5 mm posterior to the bregma, −3.45 to -3.55 mm ventral from

the brain surface. PreBötC, ± 1.3 mm from the midline; - 6.7 mm posterior to the bregma, −6.1 mm ventral from bregma.

For tracing the postsynaptic terminals of the NTS Tac1 neurons, 400 nL of AAV-hSyn-FLEX-mGFP-2A-Synaptophysin-mRuby (titer: 2.7 X10e13, serotype: AAV1) was injected into the NTS of Tac1-Cre mice at a rate of 50 nL/min.

For MSPOTIT testing, 500nL of the AAV1/2-CAG-M-SPOTIT2 virus was injected into the PreBotC at a rate of 50nL/minute.

Vagotomy

Anesthetized mice were placed on a stereotaxic apparatus to maintain anesthetic state under 1.5% isoflurane. The neck was shaved and disinfected by povidone followed by alcohol prior to surgery. A 1 cm midline incision was made in the neck to expose the trachea and vagus nerve. Blunt forceps were used to carefully isolate nodose ganglia form the connective tissue, vagotomy was made unilaterally at the distal nerve of nodose ganglia. A unilateral vagotomy was previously used in other species because a bilateral vagotomy is detrimental to lung function (Canning & Mori, 2011; Hanáček et al., 1984).

SLN and AEN stimulation

Animals were anesthetized with intraperitoneal injections of urethane (1600-2000 mg/kg). To evoke the fictive cough, the superior laryngeal nerve (SLN) was exposed by a ventral approach, with an incision in the midline of the neck. The electrode was placed unilaterally around the SLN, and the nerve was electrically stimulated (pulse width, 0.2 ms; frequency, 2-10 Hz; intensity, 40-300 μA). To evoke the fictive sneeze, the anterior ethmoidal nerve (AEN) was exposed by a midline incision along posterior frontal suture direction to expose the medialis orbits. The electrode was placed unilaterally around the AEN, and the nerve was electrically

stimulated (pulse width, 0.2-0.7 ms; frequency, 10-20 Hz; intensity, 100-600 μA) (Satoh et al., 1998b). For both stimulations, a monopolar tungsten electrode (impedance 0.1-0.5 MΩ; Microprobes, Maryland, USA) was used for electrical stimulation, with a reference electrode placed on the peripheral skin close to the stimulation site. The stimulus was controlled using a stimulus isolator (FE-180; AD instruments).

The styloglossus muscle is the muscle at the back of the tongue, which is activated during sneeze, but not cough (Satoh et al., 1998b; Simera et al., 2015). To monitor its activity, the styloglossus muscle was accessed intraorally by using a custom mouth opener made by diameter stainless steel wire. After opening the mouth, the tongue was gently drawn forward to expose the muscle. A 3-4 mm incision was created on the lateral side of the posterior portion of the tongue to access the styloglossus muscle fibers. Two stainless steel wire electrodes (36 AWG size, Cat: 36744MHW, Phoenix Wire, Vermont, USA) were positioned 2mm apart from each other and then secured with a 7-0 polypropylene surgical suture (Prolene TM, Ethicon, Puerto Rico, USA). EMG signals were recorded using an amplifier (Quad Bio Amp; AD instruments) that is connected to PowerLab 8/35 (AD instruments). Signals were digitally filtered (high pass filter at 25 Hz) and integrated (time constant of 0.1 s) by software Labchart 8. The amplitude of the EMG recording was evaluated and compared to the baseline.

Histology and immunostaining

Mice were deeply anesthetized and transcardially perfused with 10mL PBS, followed by 10mL 4% paraformaldehyde (PFA). Tissues, including the brain, the nodose jugular ganglion complex, the trachea, and the lung, were removed and post-fixed overnight at 4 °C in 4 % PFA and then cryopreserved in 30% sucrose for 48 hr. The processed tissue was then embedded into optimum cutting temperature compound (OCT) and sectioned (brains and tracheas were

sectioned coronally while lungs and ganglia were sectioned sagittally) into serial slices through the relevant region at 16 – 40 microns with a Leica cryostat CM3050 S cryostat. For the quantification of NTS neurons, the brain tissue was sectioned at 35 μm and the cells were counted every fourth section. For the quantification of ganglion neurons, the tissue was sectioned at 16 μm and the cells were counted on every third section.

For immunostaining, sections were washed in 0.1% PBS Tween 20 and permeabilized with 0.3% PBS Triton X-100 for 30 min, followed by 2% bovine serum albumin (BSA) blocking solution at room temperature for 1 hr. Sections were then incubated with primary antibody in BSA overnight at 4 °C. the following primary antibodies were used: chicken anti-GFP (Abcam 13970; 1:1000 dilution), goat anti-phox2b (Santa Cruz, sc-13224; 1:150), rabbit anti-Dsred (Takara 632496; 1:1000 dilution), rabbit anti-Tyrosine Hydroxylase (Abcam ab112; 1:400 dilution), goat anti-Choline Acetyltransferase (Millipore AB144P; 1:500 dilution). After washing in 0.1% PBS Tween 20 three times (5 min each time), sections were incubated with secondary antibody for 1 hr. The following secondary antibodies were used: Alexa Fluor 488-conjugated donkey anti-chicken (Jackson Immuno Research; 1:400 dilution), Alexa Fluor 555-conjugated donkey anti-rabbit (Invitrogen A31572; 1:500 dilution), Alexa Fluor 555-conjugated donkey anti-goat (Life technologies A21432; 1:500) Alexa Fluor 647-conjugated donkey anti-goat (Invitrogen A21447; 1:500 dilution), Alexa Fluor 647-conjugated donkey anti-rabbit (Invitrogen A31573; 1:400 dilution). After washing in 0.1% PBS Tween 20 three times (5 min each time), sections were then stained with 4’,6 -diamidino-2-phenylindole, dihydrochloride (DAPI; Invitrogen; D1306) diluted 1:10000 in PBS. After washing in 0.1% PBS Tween 20 three times (5 min each time), sections were mounted on slides with prolong gold antifade reagent (Invitrogen;

P36930) and imaged on a confocal microscope. For MSPOTIT imaging, sections weren't mounted and instead were imaged on a confocal microscope with pH 11 buffer.

In situ hybridization

Brains were sectioned at 16 microns, fixed in 4% paraformaldehyde, dehydrated in an ethanol series, and treated with Pretreatment Reagent (Advanced Cell Diagnostics). Multiplex fluorescent *in situ* assay was then performed using proprietary RNAscope technology with their probes: *Cre*, *c-fos, and Tac1* (Advanced Cell Diagnostics).

Optogenetics

For optogenetic activation of the NTS neurons and the Tac1 projections, 400nL of adenoassociated viral (AAV) vector AAV-EF1a-DIO-hChR2(H134R)-EYFP (titer: 3.0 X10e13; serotype: AAV5) was stereotactically injected into the NTS of different mouse Cre lines (Tac1-Cre, Vglut2-Cre, Grp-Cre and Vgat-Cre). Control mice were injected with 400nL of AAV-Ef1a-DIO-EYFP (titer: 1.3 X10e13; serotype: AAV5). A fiber optic was implanted 200 microns above the injection site in the NTS for cell body activation or above NA ±1.35 mm from the midline; -6.7 mm posterior to the bregma, -6.1 mm ventral from the brain surface or above cVRG ±1.3 mm from the midline; -8 mm posterior to the bregma, -6.1 mm ventral from the brain surface for the projection activation. Four weeks later, the animals were placed in a modified whole-body plethysmography chamber for detecting respiratory and other behavioral responses, with the cannula connected to a 473 nm laser. Mice were optogenetically activated at 15ms pulses every 10 seconds, unless otherwise noted in the figure. Their breathing trace, video and audio were recorded throughout the experiments when laser pulses were administered.

Chemogenetics

For chemogenetic silencing of the NTS Tac1 neurons, 400nl of AAV-hSyn-DIO-hM4Di-mCherry (experimental) (titer: 5.3 X10e12; serotype: AAV2) or AAV-hSyn-DIO-mCherry (control) (titer: 3.9 X10e12; serotype: AAV2) (Krashes et al., 2011b) (University of North Carolina Viral Core) was stereotactically injected into the NTS of Tac-Cre mice. Four weeks later, clozapine-n-oxide (CNO) (1 mg/ml) was injected intraperitoneally (20g/ 100µL) 20 minutes prior to the behavior assay to activate the receptor hM4Di. Saline was injected as control. Then, the animals were placed in a whole-body plethysmography chamber for detecting the cough-like responses to nebulization of tussive challenge or for respiratory response to hypoxic air. For quantification, brains were harvested, sectioned and stained for DAPI, the number of mCherry-labeled cells were quantified in and around the NTS.

Genetic ablation

For genetic ablation of the NTS Tac1 neurons, 400nl AAV-Flex-taCasp3-TEVp (titer: 4.0 X10e12; serotype: AAV2) was stereotactically injected into the NTS of Tac1-Cre; Ai9 mice that underwent pre-operative tussive challenge and hypoxic challenge assays. Four weeks later, animals were placed in a whole-body plethysmography chamber for post-operative tussive challenge and hypoxic challenge assays. For quantification, brains from a subset of mice were harvested, sectioned and stained for DAPI, the number of Ai9 cells were quantified in and around the NTS.

NA and cVRG retrograde tracing

For the retrograde tracing, 200nL of AAVretro-DIO-eGFP (titer: 5.2 X10e12; serotype: AAV2Retro) was injected unilaterally into the cVRG and 200nL of AAVretro-DIO-mCherry (titer: 4 X10e12; serotype: AAV2Retro) was injected unilaterally into the ipsilateral NA of Tac1-

Cre mice. Three weeks later, animals were euthanized anf the brain was harvested and processed for cryosectioning. Cells labeled in the NTS were quantified.

Vocal Cord Visualization and Analysis

For vocal cord visualization of the terminal projections, mice with an optogenetic implant were anesthetized under isoflurane and kept at 1% during the visualization. The cannula was connected to a 473 nm laser. A portable ear endoscope cleaning camera (inskam model i98) was placed down the throat of the mouse until the vocal cords were visualized. Mice were optogenetically activated at 200ms laser pulses every ten seconds and the laser light was visualized in the video. The video was extracted into individual frames and saved as separate image files using a MATLAB code. The distance between the vocal cords was measured manually in each of the frames.

For analysis of the vocal cord visualization of SLN and AEN stimulation, the closure magnitude during respiration and during fictive cough/sneeze was measured and compared.

Opioid administration for MSPOTIT2 Testing

6 days after injection of the viral vectors into the mouse brain, 30mg/kg, 60mg/kg, or 100mg/kg of morphine or saline was administered through intraperitoneal injection. Twenty-four hours after drug or saline administration, the mice were deeply anesthetized and transcardially perfused with 10 mL PBS, followed by 10 mL 4% paraformaldehyde (PFA). The brain tissue was removed and post-fixed overnight at 4 °C in 4 % PFA and then cryopreserved in 30% sucrose for 48 hours. The processed tissue was then embedded into optimum cutting temperature compound (OCT) and sectioned into serial slices through the relevant region at 40 microns with a Leica cryostat CM3050 S cryostat.

Measuring the breathing frequency of mice expressing M-SPOTIT2

To test the respiratory depression of morphine, individual mice were placed in a 450mL whole-body plethysmography (WBP) chamber at room temperature (22°C) with normoxia air continuously flushed through the chamber. The day before the respiratory recording, mice were placed in the WBP chamber for four hours for acclimation. For testing the following day, mice were placed into the chamber and allowed to acclimate to the chamber for 30 minutes before the respiratory parameters were recorded by Emka IOX2 software (EMKA Technologies, Paris, France). Animals then underwent a 15-minute baseline recording before a 200 uL IP injection of sterile saline. Following the injection, mice underwent an additional 45-minute recording and then returned to their home cage for 20 minutes. Mice were then returned to the WBP for a 30-minute acclimation period, followed by a 15-minute baseline recording before an IP injection of 100 mg/kg of morphine. Following the injection, the mice were recorded for an additional 45 minutes. Mice were recorded in two different time points: (1) once, three days before M-SPOTIT2 AAV injection and (2) on day six following AAV injection (AAV injection is day 0). Breathing frequency was compared in these two recordings to observe the effects of MSPOTIT injection on opioid breathing depression.

Blockade by naloxone of M-SPOTIT2 morphine detection in a mouse brain. 6 days after M-SPOTIT2 AAV injection, mice were given an IP injection of 100mg/kg of naloxone. Five minutes after the initial injection, mice were injected with 100mg/kg of morphine. The following day, mice were sacrificed and processed for imaging following the aforementioned protocol.

Bibliography

Adcock, J. J., Douglas, G. J., Garabette, M., Gascoigne, M., Beatch, G., Walker, M., & Page, C. P. (2003). RSD931, a novel anti-tussive agent acting on airway sensory nerves. *British Journal of Pharmacology*, *138*(3), 407–416.

Al-Hasani, R., Wong, J. M. T., Mabrouk, O. S., McCall, J. G., Schmitz, G. P., Porter-Stransky, K. A., Aragona, B. J., Kennedy, R. T., & Bruchas, M. R. (2018). In vivo detection of optically-evoked opioid peptide release. *ELife*, *7*, 1–13.

Alheid, G. F., Gray, P. A., Jiang, M. C., Feldman, J. L., & McCrimmon, D. R. (2002). Parvalbumin in respiratory neurons of the ventrolateral medulla of the adult rat. *Journal of Neurocytology*, *31*(8–9), 693–717.

Andrews, T. S., Kiselev, V. Y., McCarthy, D., & Hemberg, M. (2020). Tutorial: guidelines for the computational analysis of single-cell RNA sequencing data. *Nature Protocols 2020 16:1*, *16*(1), 1–9.

Armbruster, B. N., Li, X., Pausch, M. H., Herlitze, S., & Roth, B. L. (2007). Evolving the lock to fit the key to create a family of G protein-coupled receptors potently activated by an inert ligand. *Proceedings of the National Academy of Sciences of the United States of America*, *104*(12), 5163–5168.

Arthurs, J. W., Bowen, A. J., Palmiter, R. D., & Baertsch, N. A. (2023). Parabrachial tachykinin1-expressing neurons involved in state-dependent breathing control. *Nature Communications*, *14*(1), 1–16.

Bailly, J., Rossi, N. Del, Runtz, L., Li, J., Park, D., Scherrer, G., Tanti, A., Birling, M., Darcq, E., Kieffer, L. (2020). Targeting morphine-responsive neurons: Generation of a knock-in mouse line expressing Cre recombinase from the Mu-opioid receptor gene locus. *Eneuro.Org*, *7*(3).

Banner, A. S. (1986). Cough: physiology, evaluation, and treatment. *Lung*, *164*(2), 79–92.

Baraniuk, J. N., & Kim, D. (2007). Nasonasal Reflexes, the Nasal Cycle, and Sneeze. *Current Allergy and Asthma Reports*, *7*, 105–111.

Barik, A., Thompson, J. H., Seltzer, M., Ghitani, N., Correspondence, A. T. C., & Chesler, A. T. (2018). A Brainstem-Spinal Circuit Controlling Nocifensive Behavior Article A Brainstem-Spinal Circuit Controlling Nocifensive Behavior. *Neuron*, *100*.

Bautista, T. G., Pitts, T. E., Pilowsky, P. M., & Morris, K. F. (2014). The Brainstem Respiratory Network . In *Neuronal Networks in Brain Function, CNS Disorders, and Therapeutics* (pp. 235–245).

Belvisi, M. G., & Bolser, D. C. (2002). Summary: Animal models for cough. *Pulmonary Pharmacology and Therapeutics*, *15*(3), 249–250.

Belvisi, M. G., & Hele, D. J. (2008). Animal Models of Cough. *Cough: Causes, Mechanisms and Therapy*, 217–222.

Benarroch, E., Freeman, R., & Kaufmann, H. (2007). Autonomic Nervous System. *Textbook of Clinical Neurology: Third Edition*, 383–404.

Bianchi, A. L., Denavit-Saubié, M., & Champagnat, J. (1995). Central control of breathing in mammals: neuronal circuitry, membrane properties, and neurotransmitters. *Physiological Reviews*, *75*(1), 1–45.

Bolser, D. C., & Davenport, P. W. (2002). Functional Organization of the Central Cough Generation Mechanism. *Pulmonary Pharmacology & Therapeutics*, *15*, 221–225.

Bolser, D. C., Reier, P. J., & Davenport, P. W. (2000). Responses of the anterolateral abdominal muscles during cough and expiratory threshold loading in the cat. *Journal of Applied Physiology*, *88*(4), 1207–1214.

Bongianni, F., Mutolo, D., Nardone, F., & Pantaleo, T. (2005). Ionotropic glutamate receptors mediate excitatory drive to caudal medullary expiratory neurons in the rabbit. *Brain Research*, *1056*(2), 145–157.

Boyden, E. S., Zhang, F., Bamberg, E., Nagel, G., & Deisseroth, K. (2005). *Millisecond-timescale, genetically targeted optical control of neural activity*.

Burke, W. (2012). Why do we sneeze? *Medical Hypotheses*, *78*, 502–504.

Burt, C. W., & Schappert, S. M. (2004). Ambulatory care visits to physician offices, hospital outpatient departments, and emergency departments: United States, 1999-2000. *Vital and Health Statistics, Series 13: Data on Health Resources Utilization*, *13*(157).

Byrd, R. B., & Burns, J. R. (1975). Cough dynamics in the post thoracotomy state. *Chest*, *67*(6), 654–657.

Canning, B. J. (2009). Central Regulation of the Cough Reflex: Therapeutic Implications. *Pulmonary Pharmacology & Therapeutics*, *22*(2), 75.

Canning, B. J., Chang, A. B., Bolser, D. C., Smith, J. A., Mazzone, S. B., & McGarvey, L. (2014). Anatomy and Neurophysiology of Cough: CHEST Guideline and Expert Panel Report. *Chest*, *146*(6), 1633–1648.

Canning, B. J., & Chou, Y. (2008). Using guinea pigs in studies relevant to asthma and COPD. *Pulmonary Pharmacology and Therapeutics*, *21*(5), 702–720.

Canning, B. J., Mazzone, S. B., Meeker, S. N., Mori, N., Reynolds, S. M., & Undem, B. J. (2004). Identification of the tracheal and laryngeal afferent neurones mediating cough in anaesthetized guinea-pigs. *The Journal of Physiology*, *557*(Pt 2), 543–558.

Canning, B. J., & Mori, N. (2010). An essential component to brainstem cough gating identified in anesthetized guinea pigs. *The FASEB Journal*, *24*(10), 3916.

Canning, B. J., & Mori, N. (2011). Encoding of the cough reflex in anesthetized guinea pigs. *American Journal of Physiology - Regulatory Integrative and Comparative Physiology*, *300*(2), 369–377.

Canning, B. J., Mori, N., & Mazzone, S. B. (2006). Vagal afferent nerves regulating the cough reflex. *Respiratory Physiology and Neurobiology*, *152*(3), 223–242.

Cao, Y. Q., Mantyh, P. W., Carlson, E. J., Gillespie, A. M., Epstein, C. J., & Basbaum, A. I. (1998). Primary afferent tachykinins are required to experience moderate to intense pain. *Nature*, *392*(6674), 390–394.

Chang, A. B. (2006). The physiology of cough. *Paediatric Respiratory Reviews*, *7*(1), 2–8.

Chang, R. B., Strochlic, D. E., Williams, E. K., Umans, B. D., & Liberles, S. D. (2015). Vagal sensory neuron subtypes that differentially control breathing. *Cell*, *161*(3), 622–633.

Chen, L., Lai, K., Lomask, J. M., Jiang, B., & Zhong, N. (2013). Detection of Mouse Cough Based on Sound Monitoring and Respiratory Airflow Waveforms. *PLoS ONE*, *8*(3).

Chou, Y. L., Mori, N., & Canning, B. J. (2018). Opposing effects of bronchopulmonary C-fiber subtypes on cough in guinea pigs. *American Journal of Physiology - Regulatory Integrative and Comparative Physiology*, *314*(3), R489–R498. https://doi.org/10.1152/AJPREGU.00313.2017

Chung, K. F. (2005). Drugs to suppress cough. *Expert Opinion on Investigational Drugs*, *14*(1), 19–27.

Chung, K. F., McGarvey, L., Song, W. J., Chang, A. B., Lai, K., Canning, B. J., Birring, S. S., Smith, J. A., & Mazzone, S. B. (2022). Cough hypersensitivity and chronic cough. *Nature Reviews. Disease Primers*, *8*(1).

Chung, K. F., & Widdicombe, J. G. (2004). Cough as a symptom. *Pulmonary Pharmacology & Therapeutics*, *17*(6), 329–332.

Cough Reflex Induced by Microinjection of Citric Acid Into the Larynx of Guinea Pigs: New Coughing Model. (2003). *Journal of Pharmacological Sciences*, *93*(4), 465–470.

Cronin, M. (2016). *Plasmids 101: FLEx Vectors*. Addgene Blog. https://blog.addgene.org/plasmids-101-flex-vectors

Cutsforth-Gregory, J. K., & Benarroch, E. E. (2017). Nucleus of the solitary tract, medullary reflexes, and clinical implications. *Neurology*, *88*(12), 1187–1196.

Daller, J. R., Wong, J., Brooks, B. D., & McKee, J. S. (2012). An inexpensive system for evaluating the tussive and anti-tussive properties of chemicals in conscious, unrestrained guinea pigs. *Journal of Pharmacological and Toxicological Methods*, *66*(3), 232–237.

Dampney, R. A. L. (1994). Functional organization of central pathways regulating the cardiovascular system. *Physiological Reviews*, *74*(2), 323–364.

Data Sciences International. (2021). The Cough and the Whole Body Plethusmograph. In *Cough Site Application Manual* (pp. 3–7).

Davenport, P. W., Bolser, D. C., Vickroy, T., Berry, R. B., Martin, A. D., Hey, J. A., & Danzig, M. (2007). The effect of codeine on the urge-to-cough response to inhaled capsaicin. *Pulmonary Pharmacology & Therapeutics*.

Davenport, P. W., & Vovk, A. (2009). Cortical and subcortical central neural pathways in respiratory sensations. *Respiratory Physiology & Neurobiology*, *167*(1), 72–86.

Deisseroth, K., & Hegemann, P. (2017). The form and function of channelrhodopsin. *Science (New York, N.Y.)*, *357*(6356).

Del Negro, C. A., Funk, G. D., & Feldman, J. L. (2018). Breathing matters. *Nature Reviews Neuroscience 2018 19:6*, *19*(6), 351–367.

Dhand, R., & Li, J. (2020). Coughs and Sneezes: Their Role in Transmission of Respiratory Viral Infections, including SARS-CoV-2. *American Journal of Respiratory and Critical Care Medicine*, *202*(5), 651–659.

Dickinson, R. S., Morjaria, J. B., Wright, C. E., & Morice, A. H. (2014). Is opiate action in cough due to sedation? *Therapeutic Advances in Chronic Disease*, *5*(5), 200.

Dicpinigaitis, P. (2020). Understanding the foundations of chronic cough. *Am. J. Manag. Care*, *26*, S232–S238.

Dicpinigaitis, P. V, Morice, A. H., Birring, S. S., Mcgarvey, L., Smith, J. A., Canning, B. J., & Page, C. P. (2014). *Antitussive Drugs — Past, Present, and Future*. *April*, 468–512.

DiMarco, A. F., Kowalski, K. E., Geertman, R. T., & Hromyak, D. R. (2006). Spinal cord stimulation: A new method to produce an effective cough in patients with spinal cord injury. *American Journal of Respiratory and Critical Care Medicine*, *173*(12), 1386–1389.

Do, J., Chang, Z., Sekerková, G., Mccrimmon, D. R., & Martina, M. (2020). *A Leptin-Mediated Neural Mechanism Linking Breathing to Metabolism*.

Dotiwala, A. K., & Samra, N. S. (2023). Anatomy, Head and Neck, Tongue. *StatPearls*.

Dowsett, G. K. C., Lam, B. Y. H., Tadross, J. A., Cimino, I., Rimmington, D., Coll, A. P., Polex-Wolf, J., Knudsen, L. B., Pyke, C., & Yeo, G. S. H. (2021). A survey of the mouse hindbrain in the fed and fasted states using single-nucleus RNA sequencing. *Molecular Metabolism*, *53*(May), 101240.

Dutschmann, M., Jones, S. E., Subramanian, H. H., Stanic, D., & Bautista, T. G. (2014). The physiological significance of postinspiration in respiratory control. *Progress in Brain Research*, *212*(C), 113–130.

El-Hashim, A. Z., & Amine, S. A. (2005). The role of substance P and bradykinin in the cough reflex and bronchoconstriction in guinea-pigs. *European Journal of Pharmacology*, *513*(1–2), 125–133.

Estis, G., Ezri, T., & Tomori, Z. (2014). Cough, expiration and aspiration reflexes: possible anesthetic implications – a brief review. *Romanian Journal of Anaesthesia and Intensive Care*, *21*(2), 113.

Feldman, J. L., McCrimmon, D. R., & Speck, D. F. (1984). Effect of synchronous activation of medullary inspiratory bulbo-spinal neurones on phrenic nerve discharge in cat. *The Journal of Physiology*, *347*(1), 241–254.

Fontana, G. A., & Widdicombe, J. (2007). What is cough and what should be measured? *Pulmonary Pharmacology and Therapeutics*, *20*(4), 307–312.

French, C. L., Irwin, R. S., Curley, F. J., & Krikorian, C. J. (1998). Impact of chronic cough on quality of life. *Archives of Internal Medicine*, *158*(15), 1657–1661.

Fu, X. C., Shi, L., Wei, Z., Yu, H., Hao, Y., Tian, Y., Liu, Y., Zhang, Y., Zhang, X., Yuan, F., & Wang, X. S. (2019). Activation of Phox2b-Expressing Neurons in the Nucleus Tractus Solitarii Drives Breathing in Mice. *The Journal of Neuroscience*.

Galli, V., & Barbas, C. (2004). High-performance liquid chromatographic analysis of dextromethorphan, guaifenesin and benzoate in a cough syrup for stability testing. *Journal of Chromatography A*, *1048*(2), 207–211.

Gatti, R., Pedretti, P., Nassini, R., & Trevisani, M. (2012). Enhanced Cough, Animal Models. *Methods in Pharmacology and Toxicology*, *I*, 343–360.

Geddes, J. F., & Talbert, D. G. (2006). Paroxysmal coughing, subdural and retinal bleeding: a computer modelling approach. *Neuropathology and Applied Neurobiology*, *32*(6), 625–634.

Generali, J., & Cada, D. (2014). Lidocaine: Cough (fentanyl induced). *Hospital Pharmacy*, *49*(1), 23–25.

Godson Akunna, G., & Ed, A. (2023). Deciphering the Nucleus Ambiguus: Anatomy, Functions and Clinical Implications Explored. *J Clin Med*, *7*(6), 1000264.

Gong, S., Zheng, C., Doughty, M. L., Losos, K., Didkovsky, N., Schambra, U. B., Nowak, N. J., Joyner, A., Leblanc, G., Hatten, M. E., & Heintz, N. (2003). A gene expression atlas of the central nervous system based on bacterial artificial chromosomes. *Nature*, *425*(6961), 917–925.

Grant, M. C., Geoghegan, L., Arbyn, M., Mohammed, Z., McGuinness, L., Clarke, E. L., & Wade, R. G. (2020). The prevalence of symptoms in 24,410 adults infected by the novel coronavirus (SARS-CoV-2; COVID-19): A systematic review and meta-analysis of 148 studies from 9 countries. *PLoS ONE*, *15*(6 June).

Gray, P. A., Janczewski, W. A., Mellen, N., Mccrimmon, D. R., & Feldman, J. L. (2001). *Normal breathing requires preBötzinger complex neurokinin-1 receptor-expressing neurons*.

Han, W., & de Araujo, I. E. (2021). Dissection and surgical approaches to the mouse jugular-nodose ganglia. *STAR Protocols*, *2*(2).

Hanáček, J., Davies, A., & Widdicombe, J. G. (1984). Influence of lung stretch receptors on the cough reflex in rabbits. *Respiration*, *45*(3), 161–168.

Hao, Y., Hao, S., Andersen-Nissen, E., Mauck III, W. M., Zheng, S., Butler, A., Lee, M. J., Wilk, A. J., Darby, C., Zager, M., Hoffman, P., Stoeckius, M., Papalexi, E., Mimitou, E. P., Jain, J., Srivastava, A., Stuart, T., Fleming, L. M., Yeung, B., … Satija, R. (2021). Integrated analysis of

multimodal single-cell data. *Cell.ComY Hao, S Hao, E Andersen-Nissen, WM Mauck, S Zheng, A Butler, MJ Lee, AJ Wilk, C DarbyCell, 2021•cell.Com*, *184*(13), 3573-3587.e29.

Harris, J. A., Hirokawa, K. E., Sorensen, S. A., Gu, H., Mills, M., Ng, L. L., Bohn, P., Mortrud, M., Ouellette, B., Kidney, J., Smith, K. A., Dang, C., Sunkin, S., Bernard, A., Oh, S. W., Madisen, L., & Zeng, H. (2014). Anatomical characterization of Cre driver mice for neural circuit mapping and manipulation. *Frontiers in Neural Circuits*, *8*.

Hashimoto, Y., Murata, A., Mikami, M., Nakamura, S., Yamanaka, E., & Kudoh, S. (2003). Influence of the rheological properties of airway mucus on cough sound generation. *Respirology (Carlton, Vic.)*, *8*(1), 45–51.

He, Z. X., Xi, K., Liu, K. J., Yue, M. H., Wang, Y., Yin, Y. Y., Liu, L., He, X. X., Yu, H. L., Xing, Z. K., & Zhu, X. J. (2023). A Nucleus Accumbens Tac1 Neural Circuit Regulates Avoidance Responses to Aversive Stimuli. *International Journal of Molecular Sciences*, *24*(5).

Hegland, K. W., Bolser, D. C., & Davenport, P. W. (2012). Volitional control of reflex cough. *Journal of Applied Physiology (Bethesda, Md. : 1985)*, *113*(1), 39–46.

Hewitt, M. M., Adams, G., Mazzone, S. B., Mori, N., Yu, L., & Canning, B. J. (2016). Pharmacology of Bradykinin-Evoked Coughing in Guinea Pigs. *Journal of Pharmacology and Experimental Therapeutics*, *357*(3), 620–628.

Hoffman, G. E., Smith, M. S., & Verbalis, J. G. (1993). c-Fos and related immediate early gene products as markers of activity in neuroendocrine systems. *Frontiers in Neuroendocrinology*, *14*(3), 173–213.

Holstege, G. (1989). Anatomical study of the final common pathway for vocalization in the cat. *Journal of Comparative Neurology*, *284*(2), 242–252.

Irwin, R. S., Rosen, M. J., & Braman, S. S. (1977). Cough. A comprehensive review. *Archives of Internal Medicine*, *137*(9), 1186–1191.

Iwata, T., Ito, I., Niimi, A., Ikegami, K., Marumo, S., Tanabe, N., Nakaji, H., Kanemitsu, Y., Matsumoto, H., Kamei, J., Setou, M., & Mishima, M. (2015). Mechanical stimulation by postnasal drip evokes cough. *PLoS ONE*, *10*(11), 1–23.

Juniper, E. F., Ståhl, E., Doty, R. L., Simons, F. E. R., Allen, D. B., & Howarth, P. H. (2005). Clinical outcomes and adverse effect monitoring in allergic rhinitis. *Journal of Allergy and Clinical Immunology*, *40*(1).

Kamei, J., Iwamoto, Y., Kawashima, N., Suzuki, T., Nagase, H., Misawa, M., Kasuya, Y., & Kamei, J. (1993). Possible involvement of/t2-mediated mechanisms in fl-mediated antitussive activity in the mouse. *Neuroscience Letters*, *149*, 169–172.

Korpas, J., & Jakus, J. (2000). The expiration reflex from the vocal folds. *Acta Physiologica Hungarica*, *87*(3), 201–215.

Korpas, J., & Kalocsayova, G. (1973). Mechanoreception of the cat respiratory tract on the first days of postnatal life. *Physiologia Bohemoslovaca*, *22*(4), 365–373.

Korpas, J., Sadlonova, J., Salat, D., & Masarova, E. (1987). The origin of cough sounds. *Bulletin Europeen de Physiopathologie Respiratoire*, *23 Suppl 10*, 47s–50s.

Korpas J, T. Z. (1979). Cough and other respiratory reflexes. In *Progress in Respiratory Research* (pp. 15–188).

Korpáš, J., & Tatar, M. (1975). The expiration reflex during ontogenesis in the rat. *Physiologia Bohemoslovaca*.

Krashes, M. J., Koda, S., Ye, C. P., Rogan, S. C., Adams, A. C., Cusher, D. S., Maratos-Flier, E., Roth, B. L., & Lowell, B. B. (2011). Rapid, reversible activation of AgRP neurons drives feeding behavior in mice. *Journal of Clinical Investigation*, *121*(4), 1424–1428.

Kroning, K. E., Li, M., Petrescu, D. I., & Wang, W. (2021). A genetically encoded sensor with improved fluorescence intensity for opioid detection at cellular resolution. In *Chemical Communications* (Vol. 57, Issue 81, pp. 10560–10563).

Kroning, K. E., Li, M., Shen, J., Fiel, H., Nassar, M., & Wang, W. (2022). A Modular Fluorescent Sensor Motif Used to Detect Opioids, Protein-Protein Interactions, and Protease Activity. *ACS Chemical Biology*, *17*(8), 2212–2220.

Kubin, L., Alheid, G. F., Zuperku, E. J., & McCrimmon, D. R. (2006). Central pathways of pulmonary and lower airway vagal afferents. *Journal of Applied Physiology (Bethesda, Md. : 1985)*, *101*(2), 618–627.

Kumada, M., Terui, N., & Kuwaki, T. (1990). Arterial baroreceptor reflex: its central and peripheral neural mechanisms. *Progress in Neurobiology*, *35*(5), 331–361.

Kupari, J., Hä Ring, M., Agirre, E., Alo Castelo-Branco, G., & Ernfors, P. (2019). An atlas of vagal sensory neurons and their molecular specialization. *Cell Reports*.

Laude, E. A., Higgins, K. S., & Morice, A. H. (1993). A Comparative Study of the Effects of Citric Acid, Capsaicin and Resiniferatoxin on the Cough Challenge in Guinea-pig and Man. *Pulmonary Pharmacology*, *6*(3), 171–175.

Lee, P., & Eccles, R. (2004). Cough induced by mechanical stimulation of the upper airway in humans. *Acta Oto-Laryngologica*, *124*(6), 720–725.

Li, F., Jiang, H., Shen, X., Yang, W., Guo, C., Wang, Z., Xiao, M., Cui, L., Luo, W., Kim, B. S., Chen, Z., Huang, A. J. W., & Liu, Q. (2021). Sneezing reflex is mediated by a peptidergic pathway from nose to brainstem. *Cell*, *184*(14), 3762-3773.

Li, P., Janczewski, W. A., Yackle, K., Kam, K., Pagliardini, S., Krasnow, M. A., & Feldman, J. L. (2016). The peptidergic control circuit for sighing. *Nature*, *530*(7590), 293–297.

Li, P., Li, S. Bin, Wang, X., Phillips, C. D., Schwarz, L. A., Luo, L., de Lecea, L., & Krasnow, M. A. (2020). Brain Circuit of Claustrophobia-like Behavior in Mice Identified by Upstream Tracing of Sighing. *Cell Reports*, *31*(11).

Loudon, R. G., & Shaw, G. B. (1967). Mechanics of cough in normal subjects and in patients with obstructive respiratory disease. *American Review of Respiratory Disease*, *96*(4), 666–677.

Lu, H., & Cao, · Peng. (2023). *Neural Mechanisms Underlying the Coughing Reflex*. *39*(12), 1823–1839.

Lucanska, M., Hajtman, A., Calkovsky, V., Kunc, P., & Pecova, R. (2020). Upper Airway Cough Syndrome in Pathogenesis of Chronic Cough. *Physiological Research*, *69*(Suppl 1), S35–S42.

Ludwig, M. Q., Cheng, W., Gordian, D., Lee, J., Paulsen, S. J., Hansen, S. N., Egerod, K. L., Barkholt, P., Rhodes, C. J., Secher, A., Knudsen, L. B., Pyke, C., Myers, M. G., & Pers, T. H. (2021). A genetic map of the mouse dorsal vagal complex and its role in obesity. *Nature Metabolism*, *3*(4), 530–545.

Machado, B. H. (2001). Neurotransmission of the cardiovascular reflexes in the nucleus tractus solitarii of awake rats. *Annals of the New York Academy of Sciences*, *940*, 179–196.

Mackenzie, A. J., Spina, D., & Page, C. P. (2004). Models used in the development of antitussive drugs. *Drug Discovery Today: Disease Models*, *1*(3), 297–302.

Madisen, L., Zwingman, T. A., Sunkin, S. M., Wook Oh, S., Zariwala, H. A., Gu, H., Ng, L. L., Palmiter, R. D., Hawrylycz, M. J., Jones, A. R., Lein, E. S., & Zeng, H. (2010). A robust and high-throughput Cre reporting and characterization system for the whole mouse brain. *Nature.ComL Madisen, TA Zwingman, SM Sunkin, SW Oh, HA Zariwala, H Gu, LL Ng, RD PalmiterNature Neuroscience, 2010•nature.Com*, *13*(1), 133–140.

Manvich, D. F., Webster, K. A., Foster, S. L., Farrell, M. S., Ritchie, J. C., Porter, J. H., & Weinshenker, D. (2018). *The DREADD agonist clozapine N-oxide (CNO) is reverse-metabolized to clozapine and produces clozapine-like interoceptive stimulus effects in rats and mice OPEN*. *8*, 3840.

Mazzone, S. B., Cole, L. J., Ando, A., Egan, G. F., & Farrell, M. J. (2011). Investigation of the neural control of cough and cough suppression in humans using functional brain imaging. *The Journal of Neuroscience : The Official Journal of the Society for Neuroscience*, *31*(8), 2948–2958.

Mazzone, S. B., Mori, N., & Canning, B. J. (2005). Synergistic interactions between airway afferent nerve subtypes regulating the cough reflex in guinea-pigs. *Journal of Physiology*, *569*(2), 559–573.

Mazzone, S. B., & Undem, B. J. (2016). Vagal Afferent Innervation of the Airways in Health and Disease. *Physiological Reviews*, *96*(3), 975–1024.

Mcgarvey, L. P. A., & Nishino, T. (2004). Acute and chronic cough. *Pulmonary Pharmacology & Therapeutics*, *17*, 351–354.

McGovern, A. E., Davis-Poynter, N., Farrell, M. J., & Mazzone, S. B. (2012). Transneuronal tracing of airways-related sensory circuitry using herpes simplex virus 1, strain H129. *Neuroscience*, *207*, 148–166.

McGovern, A. E., Davis-Poynter, N., Rakoczy, J., Phipps, S., Simmons, D. G., & Mazzone, S. B. (2012). Anterograde neuronal circuit tracing using a genetically modified herpes simplex virus expressing EGFP. *Journal of Neuroscience Methods*, *209*(1), 158–167.

McRitchie, D. (1993). The internal organization of the human solitary nucleus. *Elsevier*.

Medicine, M., & Bryda, E. C. (2013). The Mighty Mouse: The Impact of Rodents on Advances in Biomedical Research. *Missouri Medicine*, *110*(3), 207.

Midgren, B., Hansson, L., Karlsson, J.A., Simonsson, B.G., and Persson, C. G. (1992). Capsaicin-induced cough in humans. *Am Rev Respir Dis*, *146*, 347–351.

Mifflin, S. W. (1992). Arterial chemoreceptor input to nucleus tractus solitarius. *The American Journal of Physiology*, *263*(2 Pt 2).

Mifflin, S. W., Spyer, K. M., & Withington-Wray, D. J. (1988). Baroreceptor inputs to the nucleus tractus solitarius in the cat: modulation by the hypothalamus. *The Journal of Physiology*, *399*(1), 369.

Mills, C., Jones, R., & Huckabee, M.-L. (2017). Measuring voluntary and reflexive cough strength in healthy individuals. *Respiratory Medicine*, *132*.

Monica, N., McGovern, A. E., Yang, S.-K., Farrell, M. J., & Mazzone, S. B. (2014). Afferent neural pathways mediating cough in animals and humans. *Journal of Thoracic Disease* , *6*.

Monnier, A., Alheid, G. F., & McCrimmon, D. R. (2003). Defining ventral medullary respiratory compartments with a glutamate receptor agonist in the rat. *Journal of Physiology*, *548*(3), 859–874.

Montandon, G., Qin, W., Liu, H., Ren, J., Greer, J. J., & Horner, R. L. (2011). PreBötzinger complex neurokinin-1 receptor-expressing neurons mediate opioid-induced respiratory depression. *Journal of Neuroscience*, *31*(4), 1292–1301.

Morgan, M. M., Reid, R. A., Stormann, T. M., & Lautermilch, N. J. (2014). Opioid selective antinociception following microinjection into he periaqueductal gray of the rat. *Journal of Pain*, *15*(11), 1102–1109.

Morice, A. H. (2004). Post-nasal drip syndrome-a symptom to be sniffed at? *Pulmonary Pharmacology & Therapeutics*, *17*, 343–345.

Morice, A. H. (2015). Over-the-counter cough medicines: New approaches. *Pulmonary Pharmacology & Therapeutics*, *35*, 149–151.

Morice, A. H., Fontana, G. A., Belvisi, M. G., Birring, S. S., Chung, K. F., Dicpinigaitis, P. V., Kastelik, J. A., McGarvey, L. P., Smith, J. A., Tatar, M., & Widdicombe, J. (2007). ERS guidelines on the assessment of cough. *European Respiratory Journal*, *29*(6), 1256–1276.

Morice, A. H., McGarvey, L., & Pavord, I. (2006). Recommendations for the management of cough in adults. *Thorax*, *61*(Suppl 1), i1.

Mudge, J. (1778). *A radical and expeditious cure for a recent catarrhous cough*.

Mutolo, D., Bongianni, F., Fontana, G. A., & Pantaleo, T. (2007). The role of excitatory amino acids and substance P in the mediation of the cough reflex within the nucleus tractus solitarii of the rabbit. *Brain Research Bulletin*, *74*(4), 284–293.

Nemati, E., Rahman, M. M., Nathan, V., Vatanparvar, K., & Kuang, J. (2020). A comprehensive approach for classification of the cough type. *2020 42nd Annual International Conference of the IEEE Engineering in Medicine & Biology Society (EMBC)*, 208–212.

Neubauer, J. A. (2006). Neuroanatomy. In *Encyclopedia of Respiratory Medicine, Four-Volume Set* (pp. 145–149). Academic Press.

Ohi, Y., Yamazaki, H., Takeda, R., & Haji, A. (2005). Functional and morphological organization of the nucleus tractus solitarius in the fictive cough reflex of guinea pigs. *Neuroscience Research*, *53*(2), 201–209.

Otsuka, K., Niimi, A., Matsumoto, H., Ito, I., Yamaguchi, M., Matsuoka, H., Jinnai, M., Oguma, T., Takeda, T., Nakaji, H., Chin, K., Sasaki, K., Aoyama, N., & Mishima, M. (2011). Plasma substance P levels in patients with persistent cough. *Respiration; International Review of Thoracic Diseases*, *82*(5), 431–438.

Pandey, C. K., Raza, M., Ranjan, R., Singhal, V., Kumar, M., Lakra, A., Navkar, D. V., Agarwal, A., Singh, R. B., Singh, U., & Singh, P. K. (2005). *Intravenous lidocaine 0.5 mg·kg –1 effectively sup- presses fentanyl-induced cough*. 172–175.

Pennefather, J. N., Lecci, A., Candenas, M. L., Patak, E., Pinto, F. M., & Maggi, C. A. (2004). Tachykinins and tachykinin receptors: a growing family. *Life Sciences*, *74*, 1445–1463.

Petko, B., & Tadi, P. (2023). Neuroanatomy, Nucleus Ambiguus. In *StatPearls*. StatPearls Publishing.

Plevkova, J., Brozmanova, M., Matloobi, A., Poliacek, I., Honetschlager, J., & Buday, T. (2021). Animal models of cough. *Respiratory Physiology & Neurobiology*, *290*.

Poliacek, I., Corrie, L. W. C., Wang, C., Rose, M. J., & Bolser, D. C. (2007). Microinjection of DLH into the region of the caudal ventral respiratory column in the cat: Evidence for an endogenous cough-suppressant mechanism. *Journal of Applied Physiology*, *102*(3), 1014–1021.

Ponder, K. G., & Boise, L. H. (2019). The prodomain of caspase-3 regulates its own removal and caspase activation. *Cell Death Discovery 2019 5:1*, *5*(1), 1–10.

Pratter, M. R. (2006). Chronic upper airway cough syndrome secondary to rhinosinus diseases (previously referred to as postnasal drip syndrome): ACCP evidence-based clinical practice guidelines. *Chest*, *129*(1 Suppl), 63S-71S.

Prescott, S. L., Umans, B. D., Williams, E. K., Brust, R. D., & Liberles, S. D. (2020). An airway protection program revealed by sweeping genetic control of vagal afferents. *Cell.ComSL Prescott, BD Umans, EK Williams, RD Brust, SD LiberlesCell, 2020•cell.Com*, *181*(3), 574-589.

Qu, J.-M., Cao, B., & Chen, R.-C. (2021). Clinical features of COVID-19. *COVID-19*, 13.

Reiner, B. C., Crist, R. C., Borner, T., Doyle, R. P., Hayes, M. R., & De Jonghe, B. C. (2022). Single nuclei RNA sequencing of the rat AP and NTS following GDF15 treatment. *Molecular Metabolism*, *56*(December 2021), 101422.

Rhee, M. H., Lee, D. R., & Kim, L. J. (2016). Differences in abdominal muscle activation during coughing between smokers and nonsmokers. *Journal of Physical Therapy Science*, *28*(4), 1147.

Roth, B. L. (2016). DREADDs for Neuroscientists. *Neuron*, *89*(4), 683.

Rothschild, A. M. (1970). Mechanisms of histamine release by compound 48/80. *Br. J. Pharmac*, *38*, 253–262.

Rousseau, J.-P., Furdui, A., Scarpellini, C. da S., Horner, R. L., & Montandon, G. (2023). Medullary tachykinin precursor 1 neurons promote rhythmic breathing. *ELife*.

Saji, M., & Miura, M. (1990). Thoracic expiratory motor neurons of the rat: localization and sites of origin of their premotor neurons. *Brain Research*, *507*(2), 247–253.

Sandhu, G. S., & Kuchai, R. (2013). The larynx in cough. *Cough (London, England)*, *9*(1), 16.

Satoh, I., Shiba, K., Kobayashi, N., Nakajima, Y., & Konno, A. (1998). Upper airway motor outputs during sneezing and coughing in decerebrate cats. *Neuroscience Research*, *32*(2), 131–135.

Schreiber, A. F., Bertoni, M., Coiffard, B., Fard, S., Wong, J., Reid, W. D., Brochard, L. J., Piva, S., & Goligher, E. C. (2021). Abdominal Muscle Use During Spontaneous Breathing and Cough in Patients Who Are Mechanically Ventilated: A Bi-center Ultrasound Study. *Chest*, *160*(4), 1316–1325.

Schroeder, K., & Fahey, T. (2002). Systematic review of randomised controlled trials of over the counter cough medicines for acute cough in adults. *British Medical Journal*, *324*(February), 1–6.

Sekizawa, K., Jia, Y. X., Ebihara, T., Hirose, Y., Hirayama, Y., & Sasaki, H. (1996). Role of Substance P in Cough. *Pulmonary Pharmacology*, *9*(5–6), 323–328.

Shevtsova, N. A., Marchenko, V., & Bezdudnaya, T. (2019). Modulation of Respiratory System by Limb Muscle Afferents in Intact and Injured Spinal Cord. *Frontiers in Neuroscience*, *13*.

Simera, M., Poliacek, I., Dobrolubov, B., Veternik, M., Plevkova, J., & Jakus, J. (2015). Interactions of mechanically induced coughing and sneezing in cat. *Respiratory Physiology and Neurobiology*, *205*, 21–27.

Singh, S. (2022). *What is a paroxysmal cough?* Top Doctors. https://www.topdoctors.co.uk/medical-articles/what-is-a-paroxysmal-cough#

Smith, J. A., Aliverti, A., Quaranta, M., Mcguinness, K., Kelsall, A., Earis, J., & Calverley, P. M. (2012). Chest wall dynamics during voluntary and induced cough in healthy volunteers. *The Journal of Physiology*, *590*(3), 563–574.

Smith, J. A., & Woodcock, A. (2016). Chronic Cough. *New England Journal of Medicine*, *375*(16), 1544–1551.

Smith, J. C., Abdala, A. P. L., Koizumi, H., Rybak, I. A., & Paton, J. F. R. (2007). Spatial and functional architecture of the mammalian brain stem respiratory network: A hierarchy of three oscillatory mechanisms. *Journal of Neurophysiology*, *98*(6), 3370–3387.

Smith, J. C., Ellenberger, H. H., Ballanyi, K., Richter, D. W., & Feldman, J. L. (1991). Pre-Bötzinger Complex: a Brainstem Region that May Generate Respiratory Rhythm in Mammals. *Science*, *254*(5032), 726–729.

Smith, J., Owen, E., Earis, J., & Woodcock, A. (2006). Effect of codeine on objective measurement of cough in chronic obstructive pulmonary disease. *Journal of Allergy and Clinical Immunology*, *117*(4), 831–835.

Smith, S. M., Schroeder, K., & Fahey, T. (2014). Over-the-counter (OTC) medications for acute cough in children and adults in community settings. *Cochrane Database of Systematic Reviews*.

Song, G., Li, Q., & Lü, M. (2001). Roles of the Bötzinger complex in the formation of respiratory rhythm. *Advances in Experimental Medicine and Biology*, *499*, 153–157.

Songu, M., & Cingi, C. (2009). Sneeze reflex: Facts and fiction. *Therapeutic Advances in Respiratory Disease*, *3*(3), 131–141.

Steinhoff, M. S., von Mentzer, B., Geppetti, P., Pothoulakis, C., & Bunnett, N. W. (2014). Tachykinins and their receptors: Contributions to physiological control and the mechanisms of disease. In *Physiological Reviews* (Vol. 94, Issue 1, pp. 265–301).

Suárez-Quintanilla, J., Cabrera, A. F., & Sharma, S. (2023). *Anatomy, Head and Neck: Larynx*. StatPearls Publishing.

Surdyka, M. M., & Figiel, M. (2021). Retrograde capabilities of adeno-associated virus vectors in the central nervous system. *BioTechnologia*, *102*(4), 473.

Symanowicz, P. T., Gianutsos, G., & Morris, J. B. (2004). Lack of role for the vanilloid receptor in response to several inspired irritant air pollutants in the C57Bl/6J mouse. *Neuroscience Letters*, *362*(2), 150–153.

Tanaka, M., & Maruyama, K. (2005). Mechanisms of capsaicin- and citric-acid-induced cough reflexes in guinea pigs. *Journal of Pharmacological Sciences*, *99*(1), 77–82.

Tatar, M., Hanacek, J., & Widdicombe, J. (2008). The expiration reflex from the trachea and bronchi. *The European Respiratory Journal*, *31*(2), 385–390.

Taylor-Clark, T. E. (2015). Peripheral Neural Circuitry in Cough. *Current Opinion in Pharmacology*, *22*, 9.

Terlep, S., & Abbott, B. (2022). Why You Might Be Having Trouble Buying Children's Flu and Cold Medicine. *The Wall Street Journal*. https://www.wsj.com/articles/cold-cough-drugs-in-short-supply-in-some-areas-as-families-fight-flu-rsv-and-covid-11671075522

The Jackson Laboratory. (n.d.). *What is a mouse model?* Retrieved March 2, 2024, from https://www.jax.org/why-the-mouse/model

Tomori, Z., Donic, V., Benacka, R., Gresova, S., Peregrim, I., Kundrik, M., Pallayova, M., & Jakus, J. (2012). Reversal of functional disorders by aspiration, expiration, and cough reflexes and their voluntary counterparts. *Frontiers in Physiology*.

Tong, Q., Ye, C., McCrimmon, R. J., Dhillon, H., Choi, B., Kramer, M. D., Yu, J., Yang, Z., Christiansen, L. M., Lee, C. E., Soo Choi, C., Zigman, J. M., Shulman, G. I., Sherwin, R. S., Elmquist, J. K., & Lowell, B. B. (2007). Synaptic glutamate release by ventromedial hypothalamic neurons is part of the neurocircuitry that prevents hypoglycemia. *Cell.ComQ Tong, CP Ye, RJ McCrimmon, H Dhillon, B Choi, MD Kramer, J Yu, Z YangCell Metabolism, 2007•cell.Com*, *5*(5), 383–393.

Ujie, Y., Sekizawa, K., Aikawa, T., & Sasaki, H. (1993). Evidence for substance P as an endogenous substance causing cough in guinea pigs. *The American Review of Respiratory Disease*, *148*(6 Pt 1), 1628–1632.

Umezaki, T., Zheng, Y., Shiba, K., & Miller, A. D. (1997). Role of nucleus retroambigualis in respiratory reflexes evoked by superior laryngeal and vestibular nerve afferents and in emesis. *Brain Research*, *769*(2), 347–356.

Venkatasamy, R., Mckenzie, A., Page, C. P., Walker, M. J., & Spina, D. (2010). Use of within-group designs to test anti-tussive drugs in conscious guinea-pigs. *Journal of Pharmacological and Toxicological Methods*, *61*, 157–162.

Vong, L., Ye, C., Yang, Z., Choi, B., Chua, S., & Lowell, B. B. (2011). Leptin Action on GABAergic Neurons Prevents Obesity and Reduces Inhibitory Tone to POMC Neurons. *Neuron*, *71*(1), 142–154.

Whole Body Plethysmography - PrimeBioscience. (2017). https://primebioscience.com/pb-applications/whole-body-plethysmography/

Widdicombe, J., & Fontana, G. (2006). Cough: What's in a name? *European Respiratory Journal*, *28*(1), 10–15.

Widdicombe, J. G. (1998). Afferent receptors in the airways and cough. *Respiration Physiology*, *114*(1), 5–15.

Williams, C. B. J. (1841). Report of experiments on the physiology of the lungs and air-tubes. *Rep Br Assn Adv Sci*, 411–420.

Woo, T. (2008). Pharmacology of Cough and Cold Medicines. *Journal of Pediatric Health Care*, *22*(2), 73–79.

Xiang, A., Uchida, Y., Nomura, A., Iijima, H., Dong, F., Zhang, M. J., & Hasegawa, S. (1998). Effects of airway inflammation on cough response in the guinea pig. *Journal of Applied Physiology*, *85*(5), 1847–1854.

Yang, C. F., Chiang, M. C., Gray, D. C., Prabhakaran, M., Alvarado, M., Juntti, S. A., Unger, E. K., Wells, J. A., & Shah, N. M. (2013). Sexually dimorphic neurons in the ventromedial hypothalamus govern mating in both sexes and aggression in males. *Cell*, *153*(4), 896–909.

Yao, Y., Chen, J., Li, X., Chen, Z. F., & Li, P. (2023). A carotid body-brainstem neural circuit mediates sighing in hypoxia. *Current Biology*, *33*(5), 827-837.e4.

Yu, H., Shi, L., Chen, J., Shirui Jun, Hao, Y., Wang, S., Fu, Congrui, Zhang, Xiang, Lu, H., Wang, S., & Fang Yuan. (2022). A Neural Circuit Mechanism Controlling Breathing by Leptin in the Nucleus Tractus Solitarii. *Neuroscience Bulletin*, *38*.

Zeisel, A., Hochgerner, H., Lönnerberg, P., Johnsson, A., Memic, F., van der Zwan, J., Häring, M., Braun, E., Borm, L. E., La Manno, G., Codeluppi, S., Furlan, A., Lee, K., Skene, N., Harris, K. D., Hjerling-Leffler, J., Arenas, E., Ernfors, P., Marklund, U., & Linnarsson, S. (2018). Molecular Architecture of the Mouse Nervous System. *Cell*, *174*(4), 999-1014.e22.

Zhang, C., Lin, R. L., Hong, J., Khosravi, M., & Lee, L. Y. (2017). Cough and expiration reflexes elicited by inhaled irritant gases are intensified in ovalbumin-sensitized mice. *American Journal of Physiology - Regulatory Integrative and Comparative Physiology*, *312*(5),

Zhang, J. W., Walker, J. F., Guardiola, J., & Yu, J. (2006). Pulmonary sensory and reflex responses in the mouse. *Journal of Applied Physiology*, *101*(3), 986–992.

Zhou, W., Zhang, D., Tian, S., Yang, Y., Xing, Z., Ma, R., Zhou, T., Bao, T., Sun, J., & Zhang, Z. (2019). Optimal dose of pretreated-dexmedetomidine in fentanyl-induced cough suppression: A prospective randomized controlled trial. *BMC Anesthesiology*, *19*(1), 1–7.

Zhuang, J., Zhao, L., Gao, X., & Xu, F. (2019). An advanced recording and analysis system for the differentiation of guinea pig cough responses to citric acid and prostaglandin E 2 in real time.

Zoccal, D. B., Furuya, W. I., Bassi, M., Colombari, D. S. A., & Colombari, E. (2014). The nucleus of the solitary tract and the coordination of respiratory and sympathetic activities. *Frontiers in Physiology*, *5 JUN*.

Zoorob, R., Sidani, M., & Murray, J. (2011). Croup: An Overview. *American Family Physician*, *83*(9), 1067–1073.